Calcium Signalling during Primary Angiogenic Sprouting in Zebrafish

Inaugural-Dissertation
to obtain the academic degree
Doctor rerum naturalium (Dr. rer. nat.)

submitted to the Department of Biology,
Chemistry, Pharmacy
of Freie Universität Berlin

by
Laura Bartolini

2019

I herewith declare that I have produced this paper without the prohibited assistance of third parties and without making use of aids other than those specified; notions taken over directly or indirectly from other sources have been identified as such. This paper has not previously been presented in identical or similar form to any other German or foreign examination board.

I completed my doctorate studies from April 1, 2013 to October, 2018 under the supervision of Dr. Daniela Panáková at the Max Delbrück Center for Molecular Medicine in the Helmholtz Association, Berlin-Buch.

Primary Reviewer: Dr. Daniela Panáková
Secondary Reviewer: Prof. Dr. Petra Knaus

Date of Disputation: 04.06.2019

Abstract

Angiogenesis, the formation of new blood vessels from pre-existing ones, is a critical step for the formation of a functional vascular system during embryonic development. Furthermore, dysregulation of the vascular patterning is associated with more than 70 different diseases, including cancer, myocardial infarction, stroke and ocular disorders, such as macular degeneration. Studies of endothelial cells (ECs) *in vitro* and *in vivo*, have revealed the importance of vascular endothelial growth factor (VEGF) signalling together with the activation of the Dll4/Notch pathway to regulate EC's differentiation into tip vs stalk cells as well as EC migration and proliferation during angiogenesis.

Similarities between the endothelial tip cell and the axonal growth cone are well established. The two cell types share not only a similar anatomical structure, but also common molecular pathways and respond to the same molecular cues. Ca^{2+} signalling especially through the L-type Ca^{2+} channel (LTCC) is crucial to regulate the axonal turning in order to promote attraction or repulsion in response to a molecular cue. In ECs, increase in cytosolic Ca^{2+} concentration ($[Ca^{2+}]_i$) is a key regulator of migration, proliferation, contraction, gene expression and other biological aspects. Despite the similarities between neuronal and vascular systems, the role of Ca^{2+} signalling through the LTCC during vascular formation and angiogenesis is still poorly understood.

This study provides evidence that the LTCC regulates EC migration during the primary angiogenic sprouting of the intersegmental vessels (ISV) in zebrafish embryos. The stimulation of the LTCC strongly increased EC migration from the dorsal aorta (DA), resulting in an overbranching phenotype, while the downregulation of the channel reduced the EC migration and proliferation compromising the ISV formation. Additionally, I observed that LTCC synergistically interacts with the canonical transient receptor potential-1 (TRPC1) Ca^{2+} channel to promote ISV development, suggesting the importance of Ca^{2+} fluxes through the plasma membrane during angiogenesis. Furthermore, mRNA-expression analysis of VEGF signalling and Dll4/Notch-pathway components revealed the importance of the LTCC during angiogenesis: perturbation of LTCC conductance, but not TRPC1, increased the mRNA-expression level of the VEGF and Dll4/Notch pathway components, compromising the angiogenic behaviour of ECs. Taken together, this study demonstrates that Ca^{2+} fluxes through plasma membrane of endothelial cells represent an integral part of angiogenic process. Moreover, like axon growth cone, the endothelial migration requires a tight regulation of Ca^{2+} signaling.

Zusammenfassung

Die Angiogenese, die Entstehung neuer Blutgefäße aus vorbestehenden Blutgefäßen, stellt einen wichtigen Schritt bei der Formation eines funktionalen vaskulären Systems während der embryonalen Entwicklung dar. Fehlregulierungen bei der Entstehung des vaskulären Geflechts sind außerdem mit einer Vielzahl von Krankheiten, wie Krebs, Herzinfarkt und Schlaganfällen und Augenerkrankungen wie Makuladegeneration und mehr als 70 anderen Krankheiten assoziiert. Sowohl *in vitro* als auch *in vivo* Studien an Endothelzellen (EZ) zeigten einen wichtigen Einfluss des *Vascular endothelial growth factor* - (VEGF) Signalweges sowie der Aktivierung des Dll4/Notch-Signalweges auf die Regulierung der Differenzierung von EZ zu Spitzen- oder Stielzellen, auf die Migration von EZ sowie deren Proliferation während der Angiogenese.

Gemeinsamkeiten zwischen der endothelialen Spitzenzelle und dem axonalen Wachstumskegel sind seit langem bekannt. Die beiden Zelltypen weisen nicht nur eine ähnliche anatomische Struktur, sondern auch gemeinsame molekulare Signalwege auf und reagieren auf dieselben Botenstoffe.

Die Signaltransduktion durch Calciumionen, vorallem über den L-Typ Calciumkanal (LTCC), spielt eine wichtige Rolle bei der axonalen Wegfindung und beeinflusst entweder die Anziehung oder die Abstoßung der axonalen Zelle als Antwort auf Botenstoffe. In EZ ist ein Anstieg der zytosolischen Calcium-Konzentration ($[Ca^{2+}]_i$) unter anderem ein Schlüsselreiz für die Migration, Proliferation und Kontraktion der EZ sowie die Expression bestimmter Gene. Trotz der Gemeinsamkeiten zwischen dem neuronalen und vaskulären System, ist vor allem über die Rolle der Ca2+-Signaltransduktion über den LTCC bei der Formation des vaskulären Systems und der Angiogenese wenig bekannt.

Die hier vorliegende Studie zeigt, dass der LTCC die Migration von EZ während der ersten angiogenetischen Aussprossung intersegmentaler Blutgefäße (ISV) in Zebrafisch-Embryonen reguliert. Eine Stimulation des LTCC führte zu einem starken Anstieg der Migration von EZ aus der dorsalen Aorta (DA) und resultierte in einer erhöhten Verzweigung entstehender Blutgefäße. Die Herunterregulation des Kanals reduzierte die Migration und Proliferation von EZ und führte zu einer Beeinträchtigung der Ausbildung von ISV. Des Weiteren konnte nachgewiesen werden, dass der LTCC bei der Entstehung von ISV synergistisch mit dem kanonischen *transient receptor potential-1* (TRPC1) Ca^{2+}-Kanal wechselwirkt, was die entscheidende Rolle des Ca^{2+}-Fluxes durch die Plasmamembran während der Angiogenese beweist.

Insgesamt zeigt die hier vorliegende Arbeit, dass Ca^{2+} - Ströme durch die Plasmamembran von Endothelzellen einen wichtigen Bestandteil des angiogenetischen Prozesses darstellen. Desweiteren ist für die Migration von Endothelzellen, wie beim axonalen Wachstumskegel, eine engmaschige Regulation von Calcium - Signalwegen vonnöten.

1 Introduction

The proper functioning of the animal body is maintained by the coordination of different organs. The cardiovascular system, which controls the blood circulation, is responsible for bringing nutrient supplies, metabolites and oxygen to distant organs, while eliminating waste material from them, ensuring the body's survival. Due to this central function, it is not surprising that proper vascular formation is a crucial step during embryonic development (Coultas et al. 2005; Carmeliet 2005; Fraisl et al. 2009). Moreover, dysregulation of blood vessel formation is associated with more than 70 different diseases, along with cancer, myocardial infarction, stroke and ocular disorders, such as macular degeneration (Carmeliet 2005). For these reasons much effort has been focused on the development of therapeutic approaches targeting the molecular mechanisms that control vascular maturation (Ferrara & Kerbel 2005; Potente et al. 2011). The therapeutic techniques currently available, however, have not led to the desired results, revealing drug resistance and limited efficiency (Carmeliet 2005; Potente et al. 2011). Therefore, understanding the molecular processes regulating vascular growth, with a focus on the interaction of endothelial cells (ECs) with each other and with their environment, will contribute to the generation of new targets for therapeutic applications.

1.1 Blood vessel formation: vasculogenesis and angiogenesis

The maturation of the circulatory system is one of the earliest events during embryogenesis. After the specification of the three germ layers during gastrulation, ECs, which will form the vascular walls, differentiate from the mesoderm, more precisely from lateral plate mesoderm (LPM) (Amali et al. 2013; Mosimann et al. 2015). The hemangioblast, a group of multipotent progenitors derived from the LPM, gives rise to two different cell lines: the hematopoietic stem cells, which differentiate into the bloods cellular components; and the angioblast, from which ECs arise (Vogeli et al. 2006). Through a process known as *vasculogenesis* the angioblasts rearrange and generate a primitive vascular plexus, which allows the formation of the early blood vessels (Griendling et al. 2007). The primitive vascular plexus then undergoes a series of complex remodelling processes called *angiogenesis,* which involves migration, growth, sprouting and pruning of ECs, guiding the development of a functional circulatory

system. Two different kinds of angiogenic processes have been identified: sprouting angiogenesis and non-sprouting or intussusceptive angiogenesis (Burri & Tarek 1990).
Sprouting angiogenesis is the best characterised and was first to be identified more than 30 years ago (Marin-Padilla 1985). As the name suggests, it is defined by the sprouting of ECs from pre-existing vessels under the stimulation of angiogenic factors, such as Vascular endothelial growth factor A (VEGF-A) (Shalaby et al. 1995; Fong et al. 1995; Carmeliet et al. 1996; Gerhardt et al. 2003). In this process, the activated ECs start an enzymatic degradation of the basement membrane to promote the sprouting of the vessel (Blasi & Carmeliet 2002; Dao Thi et al. 2012). The highly polarised endothelial cell at the forefront of the sprouting vessel, called the tip cell, is characterised by the presence of many filopodia, which sense the environment and guide the vessel growth following the gradient of angiogenic stimuli (Dorrell et al. 2002; Ruhrberg et al. 2002; Gerhardt et al. 2003). The tip cell is then followed by other cells, called stalk cells, which actively migrate and proliferate from the pre-existing vessel, forming a solid and elongated structure (Gerhardt et al. 2003) (Fig. 1 A). The new branch can then connect with other sprouting branches through fusion of the tip cells to form loops (Carmeliet et al. 2009). Only after the shape of the new vessel is established, with tip and stalk cells forming the trunk of the new vessel, the lumen is formed allowing blood to circulate (Gerhardt et al. 2003; Kamei et al. 2006; Davis et al. 2007). The maturation of the vessels continues with the recruitment of pericytes, deposition of extracellular matrix, tightening of cellular junctions and induction of quiescence (Hellstrom et al. 1999; Saunders et al. 2006; Santoro et al. 2009; Dejana et al. 2009).
Non-sprouting angiogenesis is characterized by the intussusception mechanism in which the ECs forming the wall of the vessels invaginate into the lumen forming intraluminal endothelial pillar and thus divide the existing vessel in two (Djonov et al. 2003) (Fig. 1 B). This form of angiogenesis is considered faster than sprouting angiogenesis, since it does not require endothelial proliferation and migration. Non-sprouting angiogenesis occurs throughout life but plays a remarkable function during embryogenesis, where the vasculature development is fast and the resources are limited (Burri et al. 2004; Cahill et al. 2018). However, the molecular mechanisms that oversee non-sprouting angiogenesis are still poorly understood compared to sprouting angiogenesis (Karthik et al. 2018).

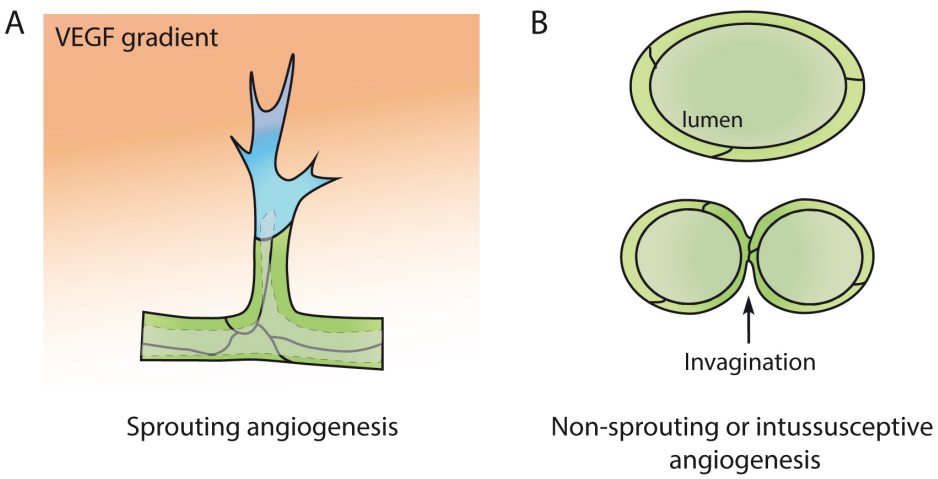

Figure 1: Schematic representation of sprouting and splitting angiogenesis. (A) In response to a VEGF gradient the tip cell (blue) migrates out from the existing vessel and promotes sprouting. Only after the vessel is established the lumen is formed. **(B)** Representation of non-sprouting angiogenesis: opposing endothelial cells forming the vessel wall invaginate into the vessel lumen forming endothelial pillar and divide the vessel in two.

1.2 Angiogenesis in pathological conditions

While angiogenesis plays a crucial role in embryonic development, most of the blood vessels remain quiescent during adulthood. Adult angiogenesis, however, still occurs in cycling ovaries and during pregnancy in the placenta (Tamanini & De Ambrogi 2004; Nezu et al. 2017). Moreover, ECs maintain their capability to activate, migrate, and proliferate in response to certain physiological stimuli, such as hypoxia or inflammation (Fraisl et al. 2009; Majmundar et al. 2010).

Vascular remodelling has been associated with the development of several disorders included tumorigenesis, ocular conditions (Gariano & Gardner 2005), myocardial infarction and stroke (Carmeliet 2005; Folkman 2007).

Angiogenesis is not causative in tumor formation, but participates in its advancement and metastasis (Carmeliet 2005). Once a developing tumor reaches a few millimetres in diameter, oxygen and nutrients are not able to reach the tumor centre by simple diffusion. In this condition the tumor creates an acidic and hypoxic micro-environment that stimulates the angiogenic switch allowing the formation of blood vessels and the consequent arrival of nutrients (Pouysségur et al. 2006). The tumor cells release cytokines and growth factors to activate the quiescent ECs triggering a cascade of events, which soon goes uncontrolled (Goel et al. 2011). Due to this uncontrolled

activation the structure and the function of tumor vessels are abnormal: areas with high vessel density are close to poorly perfused ones; vessels are irregular, chaotic and tortuous, being thin with a compressed lumen or abnormally wide. The basal membrane is discontinuous in thickness and composition. ECs forming the vessel's wall are weakly connected, sometimes in multi-layers or partially detached, often lacking the mural cell coverage with loosely associated pericytes (Fukumura et al. 1995; Carmeliet & Jain 2000; Brown et al. 2001; Jain et al. 2002). Moreover, the typical arterio-venous hierarchy is compromised with a damaged perfusion affecting the oxygen, nutrients, and drug distribution (Fukumura et al. 1997; Jain 2005; Goel et al. 2011). Due to the disassembled vessel walls, tumor cell intravasation and dissemination are facilitated (Mazzone et al. 2009).

Angiogenesis is associated with a several forms of ocular conditions (Gariano & Gardner 2005). It has to be noted that the retinal vascular anatomy is an attractive model for studying angiogenesis due to its high-ordered organization and the easy visualization (Stone et al. 1995; Dorrell et al. 2002; Stahl et al. 2010). The retinal vascularization begins in the most superficial (or inner) retinal layer at the optic nerve head and radiates outwards from this central point, reaching the retinal periphery just before birth in humans and during the first weeks of life in mice (Dorrell et al. 2002). The maturation proceeds through angiogenesis by capillary sprouting from the nascent inner vessels, adding a vascular network in the deeper retinal layers (Hughes et al. 2000). It has been shown that retinal vascularization is regulated by oxygen levels and the hypoxia-inducible VEGF (Stone et al. 1995). The regulation of oxygen levels has many implications, not only in the normal retinal vasculature development, but also on the progression of ocular disorders. Indeed, many types of retinopathies are characterized by excess of angiogenesis that may result in blindness or severe vision loss (Saint-Geniez & D'Amore 2004). For instance, diabetic retinopathy, the most common cause of vision impairment occurring in up to 20% of diabetes patients is, as other retinopathies, characterized by the loss of pericytes and active abnormal angiogenesis (Cooke et al. 2012). Nowadays, surgery is the most efficient treatment to reduce the risk of severe vision loss, however, the surgical therapy is applied only in late stages of neovascularization and does not target the basic biological irregularities that lead to this disease (Gariano & Gardner 2005; Powers et al. 2017). More investigation on retinal angiogenesis as well as on anti-angiogenic therapies is required to develop non-surgical alternatives and improve prognosis of patients suffering from these conditions.

Regulation and control of angiogenesis is of high therapeutic value. On the one hand, inhibition of angiogenesis would contribute to the suppression of tumor growth and would

inhibit the development of retinopathy in ocular conditions (Goel et al. 2011; Powers et al. 2017). On the other hand, angiogenic stimulation would be critical in improving the functional recovery after myocardial infarction, stroke, or in peripheral vascular diseases, as the stimulation of new blood vessel formation may partially restore the perfusion of the ischemic tissue (Brevetti et al. 2010; Seiler et al. 2013; Ruan et al. 2015). Due to this therapeutic role, angiogenic stimulation has been intensively explored in cardiovascular research, and animal studies have been encouraging (Sato et al. 2000; Venna et al. 2014; Khan et al. 2015). However, so far, results obtained during clinical trials are not satisfying due to several reasons, such as the short half-live of the pro-angiogenic factor *in vivo,* the insufficient uptake of the target tissue, and the de-sensitization of the chronically ischemic tissue to angiogenic factors treatments (Rissanen & Ylä-Herttuala 2007; Giacca & Zacchigna 2012; Rubanyi 2013). Moreover the animals used in pre-clinical studies are usually young and healthy, whereas patients are typically older and often infirm (Rajanayagam et al. 2000; Eagle et al. 2004).

1.3 Angiogenesis in Zebrafish

Despite their anatomical differences, the development of the cardiovascular system is evolutionary conserved in all vertebrates. Due to its crucial role during embryogenesis several model systems have been established to study angiogenesis *in vivo*, including mouse, quail, chicken, and zebrafish embryos. Each of them have specific advantages and/or disadvantages, nevertheless, the zebrafish model has been considered an excellent system to study angiogenesis *in vivo* (Chávez et al. 2016).

1.3.1 The Zebrafish model

Zebrafish (*Danio rerio*) is a small freshwater fish native to the Himalayan region. In the early 1980s it was proposed as animal model for developmental genetics by George Streisinger (Streisinger et al. 1981; Chakrabarti et al. 1983; Walker & Streisinger 1983). Nowadays zebrafish has become one of the most powerful vertebrate model systems for studying diverse biological processes *in vivo*. This success is due to the many advantages of this model that makes it a valuable research tool for embryonic development, genetics, physiology and disease; and due to the constant development

of new techniques to improve genetic manipulation and microscopic visualization (Chávez et al. 2016).

The strength of the zebrafish model lies in the concomitance of being a vertebrate organism, while maintaining some characteristics typical of simpler animals, such as *ex utero* development, large number of offspring (200-300 per mating), and short generation time (2-3 years). During the first 48 hours post fertilization (hpf) the embryos are completely transparent, allowing the possibility to follow organ development. In this short period of time most of the organs are formed and at five days post fertilization (dpf) the maturation is complete and the larvae start feeding (Westerfield 2007). The sexual maturity is reached after three months and a zebrafish adult is able to produce a high number of eggs, making this model suitable for large-scale experimental studies.

A peculiar advantage of zebrafish embryos is their ability to survive for about five days in the absence of blood flow (Sehnert et al. 2002) due to the intake of oxygen from water by passive diffusion (Pelster & Burggren 1996). This allows the observation of the effects of functional blood circulation and blood pressure on angiogenic processes, particularly on lumen formation, which is deeply connected with blood pressure (Gebala et al. 2016); as well as the phenotypic analysis of embryos with severe cardiovascular defects during embryogenesis (Bournele & Beis 2016). Furthermore, the establishment of several transgenic reporter lines, and the improvement of microscopy technology allowing for non-invasive *in vivo* imaging to follow organ morphology, make zebrafish ideal for vascular development investigations (Chávez et al. 2016). Moreover, the full zebrafish genome sequencing revealed large blocks of chromosomal synteny and homology with the human genome, with a significant homology at the protein level (Postlethwait et al. 1998), allowing the establishment of genetic models for human diseases (Lam et al. 2005; Fisher et al. 2006). Consequently, zebrafish can be used as an efficient drug screening model as the homology between the two genomes indicates a conservation of their drug response (MacRae & Peterson 2003; Kaufman et al. 2009). In addition, one advantage of the zebrafish model for drug screening applications is the simplicity of drug administration, as most of the compounds can be directly diluted into the fish water and will then readily diffuse into the animal (MacRae & Peterson 2003; Kaufman et al. 2009). Thus, the genetic homology and the conserved molecular pathways make zebrafish an ideal model to investigate complex developmental processes and test new therapeutic approaches for cardiovascular and other human diseases (Bournele & Beis 2016).

1.3.2 Morphogenesis of the intersegmental vessels

In vivo imaging studies of zebrafish transgenic lines expressing EGFP specifically in endothelial cells revealed much information on the angiogenic processes during embryogenesis. As in other vertebrates during vasculogenesis, the zebrafish angioblast differentiates from the mesoderm, rearranges and gives rise to the primitive vascular plexus (Isogai et al. 2003; Schuermann et al. 2014; Gore et al. 2012). Vasculogenesis forms the longitudinal major axial vessels, the dorsal aorta (DA), the cardinal and posterior cardinal vein (CV and PCV, respectively). Shortly after, around 24 hpf, the heart starts beating and blood circulation is initiated in the DA and the PCV. At the same time, the first angiogenic process is observed as endothelial tip cells sprout bilaterally from the dorsal part of the DA, alongside the vertical myotome boundaries. These primary angiogenic sprouts extend dorsally and give rise to the intersegmental vessels (ISVs) (Fig. 2 I). Through elongation the ISVs reach the dorsolateral roof of the neuronal tube and divide into two branches along the caudal/rostral axis (Fig. 2 I, II). Branches from neighbouring vessels then fuse between each other forming the dorsal longitudinal anastomotic vessel (DLAV) (Fig. 2 III). After the lumen forms the blood circulation starts in the new vessels. Around the same time, at 30 hpf, the secondary sprouting phase begins - the tip cells emerge and elongate from the CV and the PCV localized underneath the DA (Fig. 2 III, IV). The secondary sprouts elongate alongside the ISVs that originated during the primary sprout, and approximately half of the newly formed vessels fuse through anastomosis with the primary segment, connecting the PCV with the primary vascular network (Fig. 2 B). When the connection is established the portion of the original vessel still joined to the DA prunes and regresses, thus segmental veins (vISVs) stabilize and diversify from the segmental arteries (aISVs) formed in the first sprouting phase (Isogai et al. 2003; Schuermann et al. 2014; Gore et al. 2012) (Fig. 2 V). Not all the vessels from the secondary sprout connect with the ISVs, some simply regress, while many contribute to the formation of the parachordal vessels, located along the horizontal myoseptum on either side of the notochord, which give rise to the lymphatic system around 3 dpf. (Mulligan & Weinstein 2014; Kim et al. 2014).

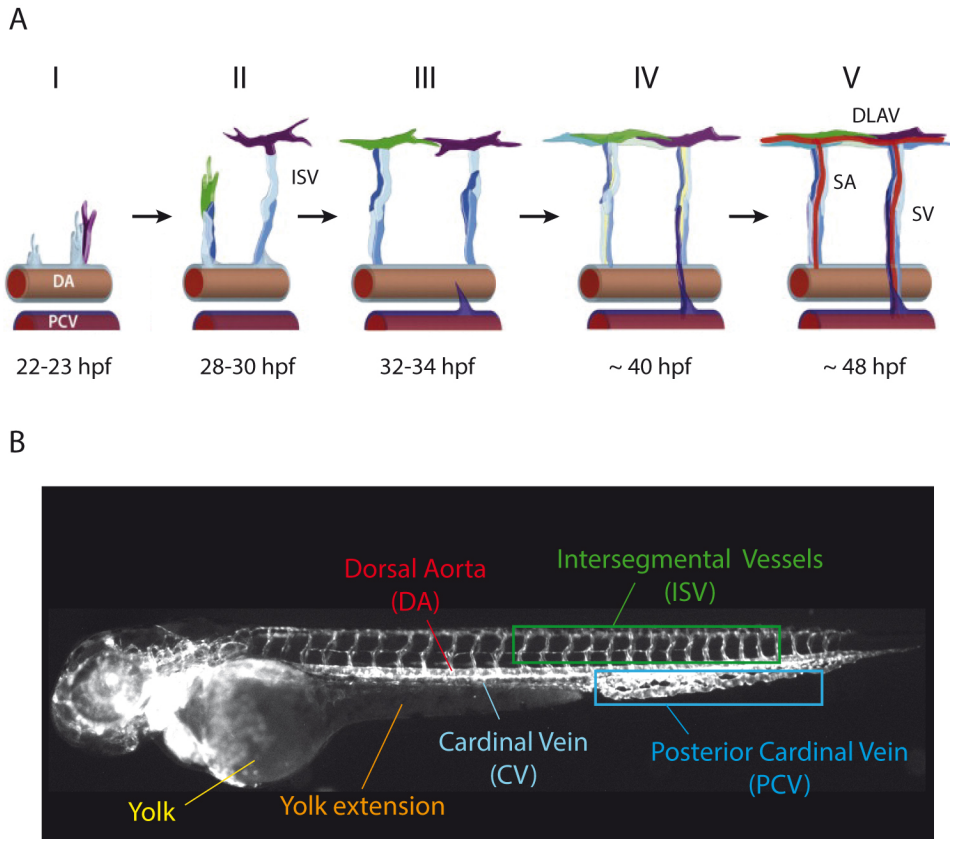

Figure 2: Schematic representation of zebrafish vascular network formation. (A I, II) Primary sprouts emerge only from the dorsal aorta (DA), newly formed intersegmental vessels (ISVs) grow dorsally to the dorsolateral roof of the neural tube and divide into two branches along the caudal/rostral axis. Branches from neighbouring vessels then fuse between each other forming the dorsal longitudinal anastomotic vessel (DLAV). **(A III)** Around the same time the secondary sprouts emerge from the posterior cardinal vein (PCV). **(A IV, V)** Some of the newly formed vessels fuse by anastomosis with the base of primary segments and become intersegmental veins (SV), while primary segments connected only to the DA become arteries (SA). Secondary sprouts that do not connect with the primary contribute to the formation of the parachordal vessels, located along the horizontal myoseptum. Adapted from (Ellertsdottir et al. 2010). **(B)** Fluorescent image in *Tg(kdrl:EGFP)* zebrafish embryo, expressing EGFP specifically in EC, at 48hpf. Yolk, yolk extension, dorsal aorta (DA) , intersegmental vessels (ISVs), cardinal vein (CV), and posterior cardinal vein (PCV) are indicated.

1.4 Signalling in angiogenesis

The formation of a functional vascular network is ensured by the fine regulation of EC migration and proliferation, which is controlled by the coordination of different signalling pathways. Sprouting angiogenesis is guided by attractive signals, like VEGF-A, and repulsive signals, like Semaphorin3a (*sema3a*) and can be considered a multistep process starting with the differentiation of the tip and stalk cells upon VEGF-A stimulation

(Wälchli et al. 2015). The second most important player for sprouting angiogenesis is the Dll4/Notch pathway. The interplay between the VEGF and Notch pathways regulates not only the tip/stalk cell differentiation, but also EC migration, proliferation and survival (Hellstrom et al. 2007; Siekmann et al. 2008; Phng & Gerhardt 2009).

1.4.1 The VEGF pathway in endothelial cells

Currently, the VEGF ligand family includes five members - VEGF-A, B, C, D and the placenta growth factor (PLGF) - which bind to three different tyrosine kinase receptors VEGFR-1, VEGFR-2, and VEGFR-3 (homologous to *flt1*, *kdr*/*kdrl*, and *flt4* in zebrafish, respectively) (Fig. 3). Not all the ligands can bind to every receptor and the binding occurs with different affinity.

The regulation of VEGF-A and VEGFR expression is crucial to vascular development. It has been shown that homozygous as well as heterozygous VEGF-A knockout (*vegf-a*$^{-/-}$, *vegf-a*$^{+/-}$) or homozygous VEGFR-1 knockout (*vegfr-1*$^{-/-}$) result in embryonic lethality in mice (Shalaby et al. 1995; Carmeliet et al. 1996; Ferrara et al. 1996). VEGF-A, commonly called just VEGF, binding to VEGFR-2 is the most important signal for vascular development, while VEGF-C binding to VEGFR-3 is implicated in embryonic angiogenesis (Dumont et al. 1998) and in lymphatic vessel formation (McColl et al. 2003). Due to its high affinity for the ligand and low kinase activity, VEGFR-1 is considered to be a decoy for VEGF-A ligand. Indeed, in zebrafish *flt1* alternative splicing produces a soluble form (*sflt1*) carrying only the extracellular domain, able to trap VEGF-A and reduce VEGF signalling (Krueger et al. 2011). In addition to VEGF-A, VEGFR-2 binds proteolytically processed VEGF-C and VEGF-D (McColl et al. 2003).

The VEGF pathway is activated by the binding of the ligand to the VEGF receptor leading to the formation of homo- or heterodimers (Fig. 3). The consequent VEGFR conformational changes activate the intracellular kinase domain promoting the auto- or trans-phosphorylation of tyrosine residues on the receptor itself or on downstream target components (Lemmon & Schlessinger 2010). This, directly or indirectly, activates the mitogen-activated protein kinase (MAPKs)/extracellular-signal-regulated kinase-1/2 (ERK1/2) cascade, phosphatidylinositol-3 kinase (PI3K) and AKT/protein kinase B (PKB) (Tchaikovski et al. 2008). The VEGF pathway can also be modulated by co-receptors such as heparan sulfate (HS) proteoglycans and Neuropilin-1 and -2 (NRP) (Koch & Claesson-Welsh 2012) (Fig. 3). In particular, NRP-1 supports VEGFR-1/2 activation (Kawamura, et al. 2008), whereas NRP-2 cooperates with VEGFR-3 (Fuh et al. 2000;

Gluzman-Poltorak et al. 2001). The fine regulation of different VEGF downstream signals leads to endothelial cell migration, proliferation, and survival (Olsson et al. 2006).

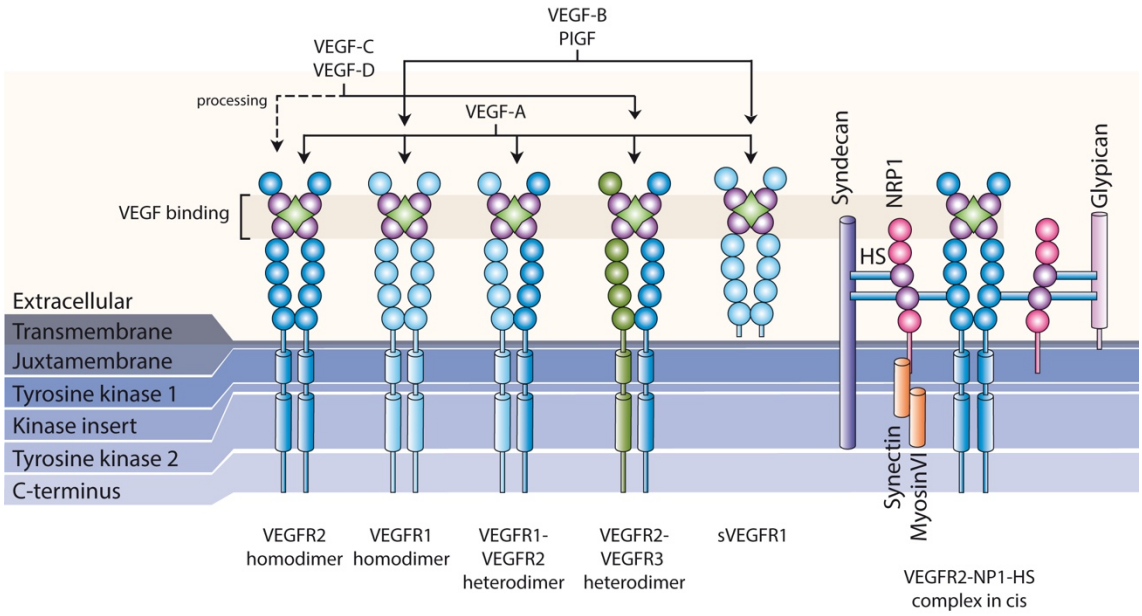

Figure 3: Schematic representation of binding specificities of VEGF family members to VEGFRs. Five vascular endothelial growth factors (VEGF-A, VEGF-B, VEGF-C, VEGF-D, and the placental growth factor (PlGF)) bind with different affinities to three VEGF receptors tyrosine kinases (VEGFR) and two Neuropilin (NRP) co-receptors, stimulating homo- and heterodimer formation. VEGFR-2 homodimer signalling is modulated not only by NRPs but also by the VEGF-binding co-receptor heparin sulfate (HS) proteoglycans (Sydecan or Glypican). Upon proteolytic processing (dotted line) VEGF-C and -D can bind to VEGFR-2. VEGFR-1 and -2 activity guides vasculogenesis and angiogenesis, while VEGFR-3 activity modulates embryonic angiogenesis and lymphangiogenesis.

1.4.2 The Notch pathway in endothelial cells

The Notch pathway is an evolutionary conserved signalling pathway crucial for embryonic development, responsible for cell fate regulation, as well as tissue homeostasis and stem cell maintenance during adulthood (Phng & Gerhardt 2009; Kopan & Ilagan 2009). It was originally discovered in *Drosophila*, where the mutated Notch allele generated a notched wing phenotype. Most of the Notch ligands are type I transmembrane proteins characterized by epidermal growth factor (EGF)-like repeats in the extracellular portion and classified through the presence, in Jagged, or absence, in Delta, of the cysteine-rich domain. In mammals, there are five canonical ligands: Delta-

like 1 (Dll1); Delta-like 3 (Dll3); Delta-like 4 (Dll4); Jagged-1 (Jag1); and Jagged-2 (Jag2) and four Notch receptors: Notch1 to Notch4. The Notch receptors are large (300 kDa) single-pass type I transmembrane proteins, carrying 29–36 tandem EGF-like repeats in the extracellular domain, some of which interact with the Notch ligands.

The binding of a Notch ligand to its receptor triggers a cascade of proteolytic cleavages of the Notch receptor itself. The first cleavage occurs in the extracellular region of the Notch receptor by a disintegrin and metalloprotease (ADAM) family member. This is followed by a second cleavage within the transmembrane domain, performed by the γ-secretase complex, releasing the Notch intracellular domain (NICD) from the cell membrane, which is then able to translocate into the nucleus (Kume 2009). In the absence of the NICD, the promoter region of Notch target genes is occupied by a co-repressor complex containing the transcription factor CSL (named after mammalian CBF1, Drosophila Su(H), and *Caenorhabditis elegans* LAG1; also known as Rbpsuh or RBP-Jκ). When NICD translocates to the nucleus, it interacts with the CSL and the co-repressor is replaced by a transcriptional activator complex formed by NICD, Mastermind-like proteins (MAML) and histone acetyltransferases, such as p300 (Fig. 4) (Kume 2009). This activates the expression of Notch target genes including helix-loop-helix proteins Hairy/Enhancer of Split (Hes), Hes-related proteins (Hey) and Notch-regulated ankyrin repeat protein (Nrarp) (Liu et al. 2006; Phng et al. 2009). Hey and Hes gene families encode transcriptional repressors acting on their own genes and on different downstream targets (Kume 2009).

The expression of Notch ligands is dynamic during development and can differ temporally and spatially. Notch3 is specific to smooth muscle cells (SMC), which also express Notch1. Notch1 is additionally expressed in ECs, together with Notch4. (Hofmann and Iruela-Arispe 2007; Villa et al. 2001). Dll1, Dll4, Jag1 and Jag2 are expressed in ECs, in contrast to Dll3 that has not been observed in the vasculature. Knockout studies on mice and zebrafish and biochemical analysis in cultured ECs, have shown the essential role of Dll4/Notch signalling to guide the vasculature formation (Villa et al. 2001; Claxton & Fruttiger 2004; Phng & Gerhardt 2009).

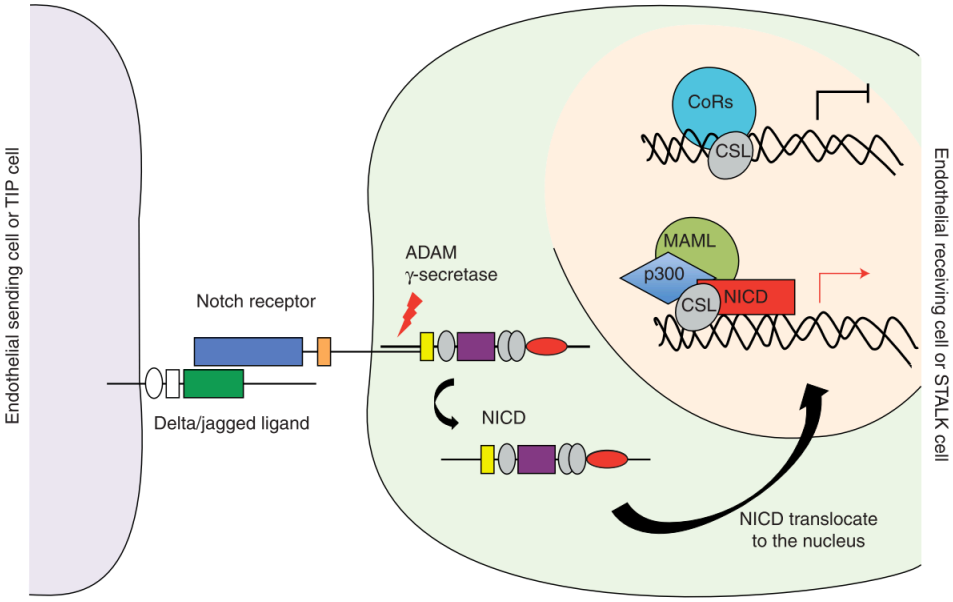

Figure 4: Schematic overview of the canonical Notch pathway. Notch signalling is activated upon ligand/receptor interaction, which are located on juxtaposing membranes of neighbouring cells. The Notch ligand binding triggers a series of proteolytic cleavages of the Notch receptor, this is catalysed by a member of the disintegrin and metalloproteases (ADAMS) family and the γ-secretase complex, thus culminating in the release of the Notch intracellular domain (NICD). The NICD translocates to the nucleus and interacts with the transcriptional activator CSL and the co-repressors (CoRs) are displaced by an activator complex formed by NICD, Mastermind-like proteins (MAML) and histone acetyltransferases (as p300). Hence, the transcription of Notch target genes such as Hairy/enhancer of split (HES) and HES-related proteins (HEY/HRT/HERP) family is induced. Adapted from (Blanco & Gerhardt 2013).

1.4.3 Integration of VEGF and Notch signalling

The first phase of sprouting angiogenesis is characterised by VEGF-stimulated tip cell differentiation and migration from the vascular wall of the existing vessel. Recent data and computational modelling indicate that endothelial tip and stalk cell differentiation is coordinated by the dynamic feedback loop between the VEGF and Notch pathways (Chappell et al. 2013). In particular, the tip cell, expressing VEGFR-1, 2 and 3, as well as the co-receptor Neuropilin-1 (Nrp1-1), upon VEGF-A stimulation, dynamically compete for the tip position with the neighbouring cells (Gerhardt et al. 2003; Hellstrom et al. 2007; Leslie et al. 2007; Lobov et al. 2007; Siekmann & Lawson 2007; Suchting et al. 2007; Suchting & Eichmann 2009). The competition occurs through the lateral inhibition of the tip cell phenotype by upregulating the Dll4 ligand expression level (Jakobsson et al. 2010). Dll4 on the tip cell surface activates the Notch-1 receptor in

adjacent stalk cells, in which the Notch signalling suppresses the tip cell phenotype, reducing the VEGF-A cell response, downregulating VEGFR-2, 3 and Nrp-1 expression level and upregulating VEGFR-1 (Lobov et al. 2007; Siekmann & Lawson 2007; Jakobsson et al. 2010; Blanco & Gerhardt 2013) (Fig. 5). Indeed, VEGFR-1 inhibits the angiogenic cell response to VEGF signalling forming inactive heterodimers with VEGFR-2 and increasing the level of the soluble isoform sVEGFR-1, which is able to trap VEGF-A and restrict its downstream signalling cascade (Funahashi et al. 2010). Moreover, downregulation of VEGFR-2 in the stalk cell reduces Dll4 expression levels, and consequently the potential activation of Notch signalling in the tip cell (Williams et al. 2006; Suchting et al. 2007; Phng & Gerhardt 2009) (Fig. 5).

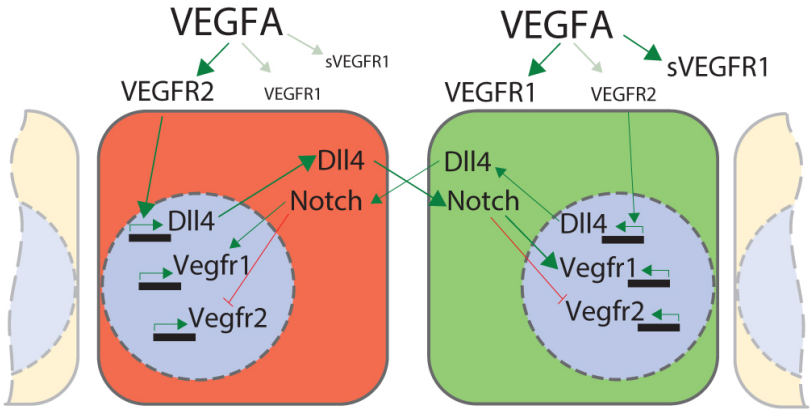

Figure 5: Tip/Stalk cell specification by VEGF/Notch coordinated signalling. VEGFR-2 stimulation on the tip cell (orange) by VEGF-A activates *Dll4* expression, which stimulates the Notch receptor in the adjacent stalk cell (green). Activation of Notch pathways suppresses the tip phenotype inhibiting *Vegfr-2* expression level and stimulating *Vegfr-1*, which is able to form inactive heterodimers with VEGFR-2 and increases its soluble form sVEGFR-1 acting as a VEGF-A trap. Adapted from (Jakobsson et al. 2010).

Different studies in mouse and zebrafish models have shown the critical role of VEGFR2-Dll4-Notch1 signalling during angiogenic development. Such experiments showed that genetic or pharmacological disruption of Dll4-Notch1 signalling leads to excess of the tip cell formation and overbranching phenotype, increasing cell proliferation and migration (Leslie et al. 2007; Siekmann & Lawson 2007). Conversely, stimulation of Notch signalling in endothelial cells *in vitro* and in both mouse (Liu et al. 2006; Harrington et al. 2008) and zebrafish (Leslie et al. 2007; Siekmann & Lawson 2007) models decreases EC migration and proliferation.

Collectively, these findings show the importance of a fine-regulated interaction between VEGF and Notch signalling not only to promote tip/stalk differentiation, but also to coordinate EC migration and proliferation (Siekmann et al. 2008; Phng & Gerhardt 2009).

1.4.4 Signalling in the migrating endothelial cells

In order to initiate and form new vessels, ECs need to migrate, proliferate and organise in a three dimensional structure. The first signal that initiates EC migration during angiogenesis is VEGF stimulation (Gerhardt et al. 2003; Olsson et al. 2006; Siekmann et al. 2008; Jakobsson et al. 2010). In addition to VEGF signalling, other pathways such as Semaphorin/PlexinD1 and chemokine signalling regulate EC migration and place the angiogenic sprout in the correct position and direction (Siekmann et al. 2009; Zygmunt et al. 2011).

1.4.4.1 VEGFR-2 and endothelial cell migration

During angiogenesis, VEGF signalling is responsible to initiate the first sprout of the new vessel and stimulates the first EC migration (Gerhardt et al. 2003; Olsson et al. 2006; Siekmann et al. 2008; Jakobsson et al. 2010). The binding of VEGF-A to VEGFR-2 triggers receptor dimerization and allow trans- or auto-phosphorylation of intracellular tyrosine residues (Dougher-Vermazen et al. 1994; Mac Gabhann & Popel 2007). Over the years, through studies of ECs *in vitro* and *in vivo*, several key phosphorylation sites on VEGFR-2 were identified and different signal transductions were associated with specific phosphorylated residues (Fantl et al. 1992; Dougher-Vermazen et al. 1994; Cunningham et al. 1997; Lemmon & Schlessinger 2010; Simons et al. 2016). Moreover, several studies have shown the implication of different VEGF-A isoforms in promoting distinguished signal transductions and cellular outcomes (Kawamura, et al. 2008; Zhang et al. 2000; Fearnley et al. 2015).

The major phosphorylation sites implicated in VEGF-induced EC migration are tyrosine Y951 in the kinase insert domain, Y1054 and Y1059 within the kinase domain, and Y1175 and Y1214 in the carboxy-terminal domain (Takahashi et al. 2001; Matsumoto et al. 2005) (Fig. 6). In particular, phosphorylated Y951 (pY951) is found only in a subset of vessels, and seems to be important in pathological angiogenesis. Indeed, pY951 serves as a binding site for the TSAd (T cell–specific adapter molecule, also known as

VEGF receptor-associated protein (VRAP)), which is expressed in tumor ECs (Matsumoto et al. 2005; Kaplun et al. 2012). Disruption of the TSAd/VEGFR-2 interaction prevents the VEGF-A dependent actin reorganization and EC migration, but not proliferation (Matsumoto et al. 2005). Moreover, VEGF-A induces the formation of a complex between TSAd and the cytosolic tyrosine kinase SRC, which is involved in vascular permeability and focal adhesion (Abu-Ghazaleh et al. 2001) (Fig. 6). The complex formation mediated by TSAd indicates that SRC and the vascular permeability activation are downstream of VEGFR-2 activity (Matsumoto et al. 2005). Additional important phosphorylation sites are located in the kinase domain. The phosphorylation of Y1054 and Y1059 are required to maximize the kinase activity (Kendall et al. 1999) and they seem to occur before the auto-phosphorylation of Y801 (Solowiej et al. 2009).
EC motility is tightly connected to the adhesion between neighbouring cells and to the ability to control it. It was shown that VEGFR-2 regulates EC attachment and migration through the control of focal adhesions (Parsons 2003). Indeed, the phosphorylation of Y1175 on VEGFR-2 is required for SHB (SH2 Domain Containing Adaptor Protein B) binding. SHB can bind to FAK (focal adhesion kinase) (Holmqvist et al. 2003), which is involved in focal adhesion turnover and is phosphorylated via VEGF signalling in a SRC-dependent manner (Abu-Ghazaleh et al. 2001) (Fig. 6).
EC migration and angiogenesis require the control of the cell rearrangement, specifically achieved through the activation of different pathways. In particular VEGFR-2 is able to bind and directly stimulate phospholipase-Cγ (PLCγ), and consequently protein kinase C (PKC), via pY1175-dependent phosphorylation of PLCγ (Takahashi et al. 2001) (Fig. 6). The stimulated PKC activates the MAPK/ERK1/2 cascade (RAF/MEK/ERK pathway), which is implicated in EC proliferation (Takahashi et al. 2001). Moreover, the activated PLCγ hydrolyses the membrane phospholipid, phosphatidylinositol 4,5-bisphosphate (PIP_2) resulting in accumulation of diacylglycerol (DAG) and inositol 1,4,5-trisphosphate (IP_3). Thus, the IP_3 accumulation stimulates Ca^{2+} release from the endoplasmic reticulum (ER) via IP_3-receptor (IP_3R) activation and the increase of intracellular calcium concentration, which is implicated in the angiogenic cell behaviour (Yokota et al. 2015; Fearnley et al. 2015) (Fig. 6). The drop in the Ca^{2+} pool in the ER upon IP_3 stimulation, can activate the store-operated Ca^{2+} channels (SOCs) and slowly restore the calcium level in the ER (Prakriya 2013; Dragoni et al. 2015). Furthermore, DAG accumulation, together with increased calcium concentration, activates PKC family members, which have been shown to regulate VEGF-mediated proliferation (Koch & Claesson-Welsh 2012) (Fig. 6).

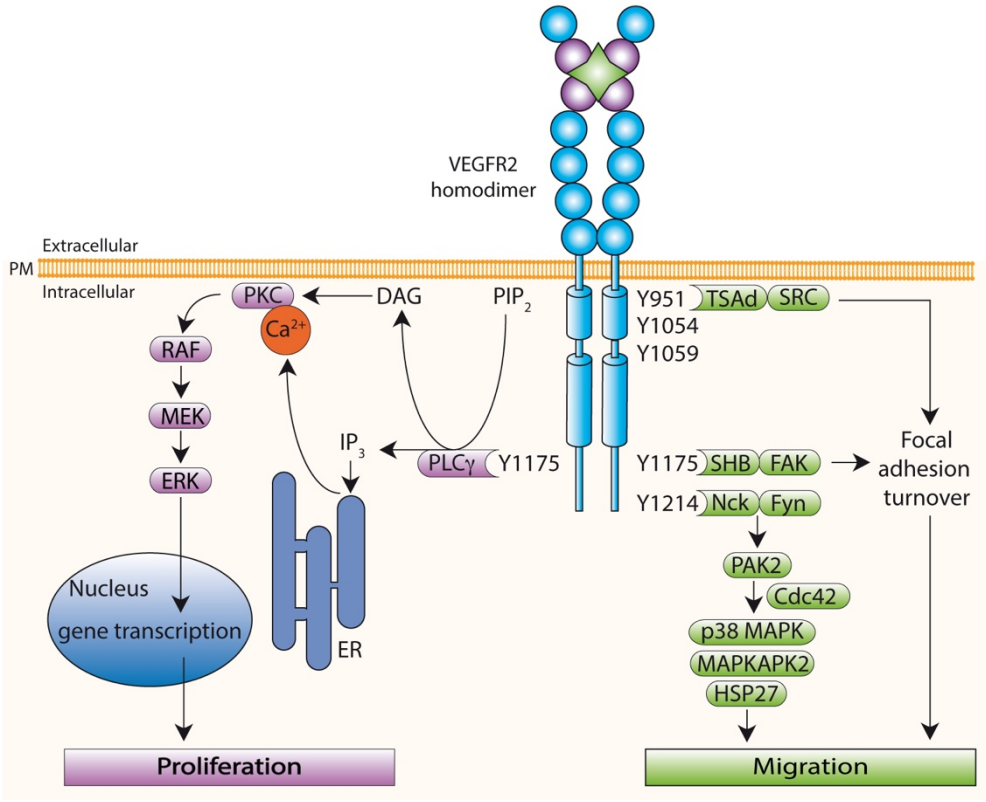

Figure 6: Schematic representation of VEGFR-2 signal transduction. Binding of VEGF-A to the extracellular Ig-like domains 2 and 3 of the VEGFR-2 (purple circles) triggers receptor dimerization and trans- or auto-phosphorylation. Specific phosphorylated residues are associated with different signal transductions. Signalling molecules (rocket shapes) bind to respective tyrosine (Y) phosphorylated sites (indicated by number) and activate downstream mediators (ovals) to modulate endothelial cell proliferation, migration, and survival. See main text for details. TSAd (T cell–specific adapter molecule); SRC (cytosolic tyrosine kinase); SHB (SH2 Domain Containing Adaptor Protein B); FAK (focal adhesion kinase); Nck (adapter protein); Fyn (cytoplasmic tyrosine kinase); MAPKs (mitogen-activated protein kinase); Cdc42 (cell division cycle 42); PAK2 (p21-activated protein kinase-2); p38MAPK (p38 mitogen-activated protein kinase); MAPKAPK2 (MAPK-activated protein kinase 2); Hsp27 (heat-shock protein-27); PLC (phospholipase C); PKC (protein kinase C); DAG (diacylglycerol); RAF (MAP3K), the Ras-activated serine/threonine kinase; MEK (MAP2K), mitogen-activated protein kinase kinase; ERK (MAPK), extracellular signal-regulated kinase; ER (endoplasmic reticulum).

Cytoskeletal reorganizations are essential to allow cell migration. In ECs the VEGFR-2 activity indirectly regulates cytoskeletal adaptation. In particular, VEGFR-2 phosphorylation on Y1214 is involved in actin remodelling through the recruitment of the adapter protein Nck and the cytoplasmic tyrosine kinase Fyn (Lamalice et al. 2006). The Nck/Fyn complex promotes the phosphorylation of the p21-activated protein kinase-2 (PAK-2) and the subsequent activation of cell division cycle 42 (Cdc42) and p38 mitogen-activated protein kinase (p38 MAPK) (Lamalice et al. 2004) (Fig. 6). Phosphorylation on Y1214 is also responsible for the heat-shock protein-27 (Hsp27) activating

phosphorylation via p38 MAPK and MAPK-activated protein kinase 2 (MAPKAPK2) (Lamalice et al. 2004): Hsp27 is a molecular chaperone implicated in VEGF-induced actin reorganization and migration (McMullen et al. 2005; Fearnley et al. 2015) (Fig.6).

1.4.4.2 Semaphorin/PlexinD1 signalling

The stereotypical well-characterised ISV development in zebrafish is guided by the fine regulation of pro- and anti-angiogenic factors. VEGF-A, secreted by the somitic tissue, together with the Notch pathway are the most important regulating signals. However, the mRNA distribution of their components does not correlate with ISV location. VEGF-A is expressed dorsally to the DA at the centre of both flanking somites and Notch pathway genes are expressed along the whole aorta, in the notochord, in the ISVs, and largely through the whole body (Leslie et al. 2007). The contribution of Semaphorin-Plexin signalling is indispensable for correct ISVs distribution. Initially discovered as neuronal repulsive cues for axon guidance, Semaphorins are transmembrane proteins that can bind different Plexin receptors, which occur in various combinations with the Neuropilin co-receptor (Tamagnone et al. 1999).

The implication of Semaphorin-Plexin signal on vascular development was shown through the study of the “out of boundaries” mutant (*obd*), which carries a mutation in the PlexinD1 receptor. Normally, ECs express the PlexinD1 receptor, while the Semaphorin ligands *sema3aa* and *sema3ab* are expressed in the somitic tissue, limiting vessel growth into the muscle. Indeed, the PlexinD1 loss of function in the *obd* mutant triggers ectopic sprouting from the DA at the level of somitic tissue. Downregulation of Semaphorin ligands also produces a similar but less severe effect revealing the redundancy of the different ligands (Torres-Vázquez et al. 2004; Zygmunt et al. 2011). Sema3a/PlexinD1 signalling limits the proangiogenic behaviour of ECs by maintaining a proper *sflt1* expression level. Thus sFlt1 acting as a trap for VEGF-A antagonizes the VEGF pathway, limiting VEGF-A pro-angiogenic action to the somitic boundaries. Upon blocking Sema3a/PlexinD1 signalling, ECs activated by ectopic VEGF differentiate as tip cells, migrate and form abnormal sprouts (Torres-Vázquez et al. 2004; Zygmunt et al. 2011; Tamagnone and Mazzone 2011).

1.4.4.3 Chemokine signalling

Besides VEGF, Notch and Sema3a/PlexinD1 signalling, other ligands and their receptors play a role in EC migration and proliferation. In particular, chemokines have received a considerable attention for their effect on both ECs and immune system cells. Chemokines are small (8-14 kDa) vertebrate specific proteins categorized into four subgroups according to the presence and position of conserved cysteine residues (C, CC, CXC and CX3C); so far more than 47 members have been identified in humans. Chemokines bind to a number of chemokine receptors (at least 18 receptors in human), which are members of the seven transmembrane G-protein coupled receptor family (GPCR). The receptors are classified based on the type of chemokines they bind to and their name includes a number signifying the chronological order of their identification (DeVries et al. 2005; Zlotnik et al. 2006).

The Cxcl12b/Cxcr4a ligand receptor pair has an important role during vascular development. Indeed, mice deficient for the chemokine receptor 4a (*cxcr4a*) or its ligand *cxcl12* (also known as *sdf1*), show disturbed vascular development, haematopoiesis, and cardiogenesis (Nagasawa et al. 1996; Tachibana et al. 1998). The expression of the *cxcr4a* ortholog or its ligand *cxcl12/sdf1* in zebrafish is specifically localized in the arterial ECs derived from anterior and not posterior lateral mesoderm (Siekmann et al. 2009). Deletion of *cxcr4a* or *cxcl12/sdf1* in zebrafish results in anterior lateral DA defects, whereas the DA formation in the trunk is not affected, revealing endothelial diversity within the aorta underlain by different local cues (Siekmann et al. 2009). Moreover, it was shown that *cxcr4a* expression is negatively regulated by blood flow and down regulation of Cxcl12b/Cxcr4a signalling results in arterial hindbrain capillary defects. These capillaries fail to establish proper connections with the arterial vessel and have an increased number of disconnected branches that remain angiogenic (Bussmann et al. 2011). Furthermore, the Cxcl12b/Cxcr4b ligand receptor pair plays an important role in vascular patterning, regulating endothelial migration within the caudal vein plexus (Torregroza et al. 2012). All together the data indicate the relevance of chemokine signalling during vascular development, although rather than stimulating sprouting or growth, chemokines regulate the guidance of EC migration.

1.5 Calcium signalling in ECs

Changes in cytosolic Ca^{2+} concentration ($[Ca^{2+}]_i$) serve as ubiquitous intracellular signals in several transduction pathways, involved in the control of diverse biological processes. The capability of this unique signal to modulate many distinct processes is connected to its high versatility in amplitude, speed, and spatiotemporal organization (Berridge et al. 2000). In ECs increases in $[Ca^{2+}]_i$ are a key regulator for migration, proliferation, segregation, contraction, adhesion, gene expression, and other biological aspects (Tran et al. 2000; Munaron 2006). The $[Ca^{2+}]_i$ increase can be generated by Ca^{2+} release from the cellular stores or through influx from the extracellular space by the activation of different types of calcium channels.

1.5.1 The L-type voltage gated calcium channel

Ion fluxes can be stimulated in response to changes in plasma membrane potentials through channels known as voltage-gated ion channels (VGCCs), commonly found in excitable cells such as neurons and muscle cells. The voltage gated ion channels share a basic transmembrane topology with an α-subunit composed of six membrane spanning segments (6-TM). This class includes monomeric ion channels with four domain repeats (I-IV) such as voltage-gated calcium and sodium channels; and tetrameric ion channels composed of four 6-TM monomers (Catterall 2011; Morera et al. 2015).

The voltage gated calcium channels are key components of the signal transduction, able to convert the electrical signal of action potential into chemical signals through the generation of calcium transients. Progressively, several VGCCs identified in neurons, skeletal, cardiac and smooth muscle cells, were classified based on physiological and pharmacological criteria of their calcium currents (Catterall 2011). Among the calcium channels present in vascular cells, the L-type and the T-type are the best characterized. The L-type calcium current is characterized by high voltage of activation, large single channel conductance and slow voltage-dependent inactivation (hence the name, L-type from the “long lasting” conductance when the calcium-dependent inactivation is inhibited) (Catterall 2011). Calcium current through the L-type calcium channel (LTCC), expressed in cardiac and smooth muscle cells, is required for the initiation of the excitation-contraction coupling (Navedo & Santana 2013). On the other hand, T-type calcium currents are characterized by lower voltage activation, smaller amplitude single channel conductance and faster voltage-dependent inactivation, compared to the L-type calcium

channel (therefore the name T-type from “tiny” or “transient” activation) (Tyson & Snutch 2013). T-type calcium channels are responsible for vasorelaxation in coronary and cerebral smooth muscle cells (Kuo et al. 2011), and vasoconstriction in smooth muscle cells from pulmonary, uterine and cerebral arteries (Chevalier et al. 2014). Although ECs are normally considered non-excitable cells, several studies revealed the expression of VGCCs in ECs from capillaries but not from large vessels (Bossu et al. 1992; Vinet & Vargas 1999; Moccia et al. 2012). The expression of VGCC in ECs is still disputed. While VGCCs are activated at depolarizing voltages, the depolarization of the EC membrane abolishes the Ca^{2+} influx into the cell (Dora and Garland 2013). Moreover, it is difficult to obtain accurate measurements of increasing calcium concentration, specifically through the plasma membrane and in particular trigged by membrane depolarization (Dora and Garland 2013). On the other hand LTCC expression was observed in human vascular endothelial cells (HUVEC) (Kim et al. 2016).

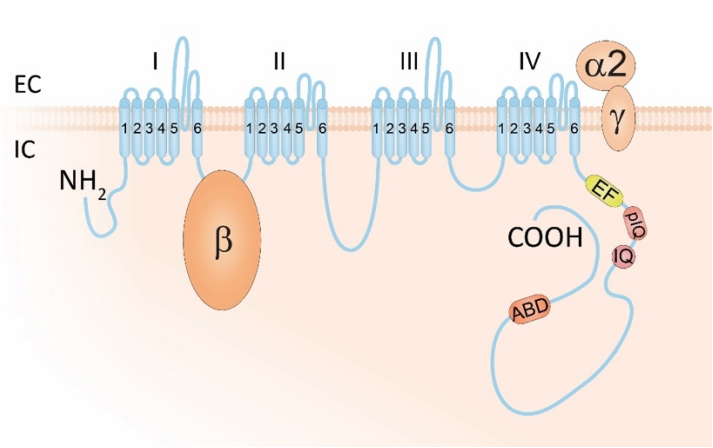

Figure 7: Schematic representation of the L-type Ca^{2+} channel. The L-type Ca^{2+} channel main pore forming subunit is composed of four homologous motifs (I, IV) each one containing six transmembrane α-helices (S1-S6), an intracellular N-terminal domain and C-terminal domain carrying the binding site for different regulators, the calcium binding EF domain, the calmodulin binding pre-IQ and IQ motif and an A-kinase anchoring protein (AKAP) binding domain (ABD). The α1c subunit interacts with α2/δ, β and in some tissues γ subunits to form a heteromultimeric protein complex.

The L-type calcium channels are heteromultimeric protein complexes consisting of α1, α2/δ, β and in some tissues γ. The α1 main pore forming subunit, encoded by the *cacna1c* gene, is composed by cytosolic N- and C-terminal tails and four homologous motifs (I-IV), each one formed by six transmembrane segments (S1-S6) (Morera et al. 2015) (Fig. 7). This subunit was the first one to be isolated and purified from cardiac myocytes; it is 1,4-dihydropyridine (DHP) sensitive and contains the channel voltage

sensing components, the gating machinery, and the binding sites for channel regulators (Carafoli et al. 2001; Catterall 2011). The C-terminal tail is responsible for the channel regulation, harbouring the calcium binding EF domain, the calmodulin binding pre-IQ and IQ motif, and the binding sites for different kinases and phosphatases through the A-kinase anchoring protein (AKAP) binding domain (ABD) (Takahashi et al. 1987; Christel and Lee 2012; Weiss et al. 2013) (Fig. 7).

According to the cell type, action potential stimulation of the LTCC triggers several intracellular events promoting excitation-contraction, excitation-secretion and excitation-transcription coupling (Carafoli et al. 2001). In cardiomyocytes, upon action potential stimulation, calcium fluxes through the LTCC induce Ca^{2+} release from the sarcoplasmic reticulum (SR), via the activation of ryanodine receptor-2 (RyR2) localized on the SR membrane; a process called calcium-induced calcium release (CICR). The rapid increase in $[Ca^{2+}]_i$ activates troponin-T and induces contraction (Bodi et al. 2005).

Together with the action potential stimulation, the β-adrenergic pathway is the most studied in the context of LTCC regulation. Indeed, it was shown that the β-adrenergic receptor (β-AR) expressed in many cells, indirectly activates the LTCC via phosphorylation of serine 1928 located in the C-terminus of the α1 subunit (Hulme et al. 2006). In particular, the stimulated β-AR, coupled to heterotrimeric G proteins, activates the adenylate cyclase (AC), which leads to an increase of cellular cyclic adenosine monophosphate (cAMP) levels, thus activating cAMP-dependent protein kinase (PKA), triggering the catalytic subunits to phosphorylate their substrates, including the LTCC, on specific threonine or serine residues (Kamp & Hell 2000) (Fig. 8A). Often cAMP-dependent proteins maintain their specific subcellular localization or association with specific kinase substrates, thanks to A-kinase anchoring proteins (AKAPs) (Sculptoreanu et al. 1993; Hulme et al. 2002; Weiss et al. 2013). AKAPs are formed by a targeting domain, which guides the protein to a specific subcellular location and a kinase-anchoring domain carrying an amphipathic α-helix that binds the regulatory subunit dimer of PKA. The voltage-dependent LTCC potentiation in cardiac and skeletal muscle requires PKA phosphorylation via anchoring through AKAP-15 (Sculptoreanu et al. 1993; Johnson et al. 1997; Hulme et al. 2003). Indeed, it was shown that AKAP-15 directly interacts with the distal C-terminus of the LTCC α1 subunit via a leucine zipper-like motif. Moreover, blocking this association by competing peptides inhibited PKA regulation of LTCC conductance (Fig. 8A) (Hulme et al. 2002; Hulme et al. 2003; Hulme et al. 2006). The enhancing effect of C-terminus phosphorylation is counterbalanced by the decrease in LTCC activity upon its dephosphorylation (Weiss et al. 2013). Indeed in mouse cardiomyocytes, it was shown that protein phosphatase-2-A (PP2A) modulates

LTCC conductance by dephosphorylating serine 1866 located at the C-terminus of the α1 subunit and promoting channel closure (Shi et al. 2012). LTCC conductance can also be modulated by protein kinase C (PKC).

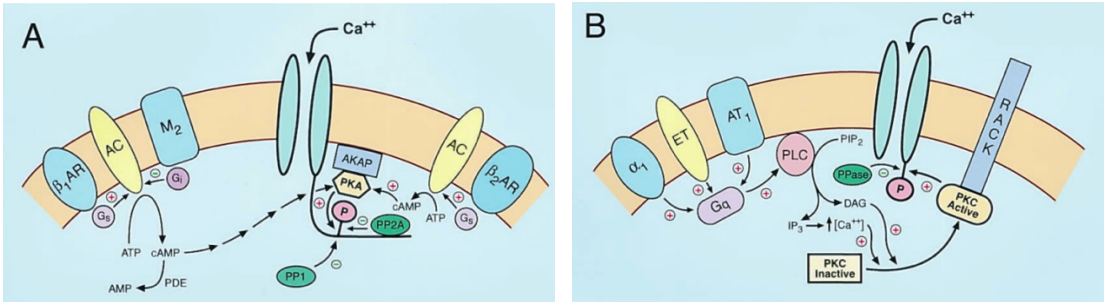

Figure 8: The L-Type Ca^{2+} channel regulation cascade. (A) Stimulation of the β-adrenergic receptor, coupled with the G-protein, activates the AC increasing the cytosolic cAMP level, which activates PKA. PKA enhances LTCC activity by promoting C-terminus phosphorylation and its localization is maintained by the AKAP. LTCC conductance is inhibited by PP1 and PP2A dephosphorylation. **(B)** Stimulation of α1, ET or AT_1 receptor contributes to PLC activation via G_q-protein. PLC-mediated hydrolysis of phosphatidylinositol PIP_2, generates PIP_3 and DAG. DAG then activates PKC which phosphorylates the N-terminus of the LTCC α1 subunit and inhibits Ca^{2+} conductance. β-AR (β-adrenergic receptor); AC (adenylate cyclase); cAMP (cyclic adenosine monophosphate); PKA (protein kinase A); PKC (protein kinase C); AKAP (A kinase anchoring protein); PP2A (protein phosphatase 2-A); α1 (α1 adrenergic receptor); ET (endothelin); AT1 (angiotensin II receptor); PIP_2 (phosphatidylinositol 4,5-bisphosphate); IP_3 (inositol trisphosphate); DAG (diacylglycerol) (Kamp & Hell 2000).

It was observed that PKC-mediated phosphorylation on two target sites located at the N-terminus of the LTCC α1 subunit, inhibits channel conductance (Fig. 8B) (McHugh et al. 2000). Several G_q-protein coupled receptors, including endothelin (ET), α1-adrenergic, and angiotensin II, can initiate the cascade promoting the activation of PKC. Receptor activation stimulates PLC, which generates PIP_3 and DAG via PIP_2 hydrolysis (Kamp & Hell 2000).

In neurons, the calcium fluxes through the LTCC are preferentially associated with the regulation of gene transcription, in comparison to calcium current via other ion channels (Flavell & Greenberg 2008). The molecular mechanism, by which calcium entering specifically through the LTCC, regulates gene transcription can be achieved in three distinct manners: the specific localization of the channel, the preferential interaction with binding partners or the nuclear translocation of a channel domain itself (Catterall 2011). Likely, all these aspects are implicated. It was shown that LTCCs are mainly localized in the cell body and proximal dendrites of central neurons, compared to other calcium channels (Hell et al. 1993). This could facilitate transcriptional regulation due to the

proximity to the nucleus (Hell et al. 1993). However, this condition is not sufficient to explain the LTCC preference, over other channels, to regulate gene transcription (Wheeler et al. 2008). Supporting studies revealed that calcium entering through the LTCC binds to Ca^{2+}-dependent regulatory proteins such as calmodulin or calcineurin. It was shown that calmodulin binding to the proximal carboxy-terminal domain of the LTCC is required for gene transcription in neurons (Dolmetsch 2001). However, pools of free calmodulin or Ca^{2+}/calmodulin complexes are present overall the cell, therefore further mechanisms are required to specifically link the LTCC- dependent calmodulin activation and translocation to the nucleus to regulate gene transcription in this context (Catterall 2011). Also calcineurin binding to the distal carboxy-terminal domain of the LTCC can regulate gene transcription (Oliveria et al. 2007). In addition, it was shown that the distal carboxy-terminus domain of the channel itself is involved in the regulation of transcription (Gomez-Ospina et al. 2006). Several studies revealed the existence of at least two forms of the α1 subunit: the full length and the truncated version of the distal carboxy-terminus, also called dCt. This shorter form can be produced by calpain-mediated proteolysis (Schroder et al. 2009) or by activation of a cryptic promoter located in exon 46 of the murine α1 subunit gene (*Cacna1c*) (Gomez-Ospina et al. 2013). The processed dCt can remain non-covalently associated with the main pore forming subunit regulating the channel conductance (Hulme et al. 2006). The dCt can translocate to the nucleus and regulate the transcription of several genes in neurons (Gomez-Ospina et al. 2006), including the α1 main pore forming subunit of the LTCC itself in cardiac myocytes (Schroder et al. 2009). Even though many aspects of the gene expression regulation by LTCC are known, the coordination of the distal carboxyl-terminus dual function between regulating channel activity and gene transcription remains to be elucidated (Gomez-Ospina et al. 2006).

1.5.2 The transient receptor potential channels

The transient receptor potential (TRP) superfamily channels represent an important component of calcium signalling in ECs. The TRP family was first discovered in *Drosophila* and the 33 members were divided in seven subfamilies: TRPC (for classical or canonical), TRPM (for the founding member called melastatin), TRPV (for the first cloned vanilloid receptor), TRPA (for a member with high numbers of ankyrin repeats), TRPP (for polycystins), TRPML (for mucolipins), and TRPN (for nomPC-like proteins). Studies in mammals revealed that among the 28 identified and unique members of the

TRP superfamily channels at least 19 are expressed in vascular ECs (Dietrich et al. 2014). The specific TRP channel identification and correlation with the detectable ion current generation in EC remains difficult. This is due to the intrinsic complexity of this family, the difficulties in detecting the small current produced and the absence of compounds to specifically inhibit or stimulate different channel isoforms (Beech 2013). Research on the structure of TRP channels had predicted that all the family members form tetramers, as the voltage-gated calcium channels, with a common pore in the middle. Among the different subfamilies the TRPC is the most promiscuous in forming hetero-tetramers (Hofmann et al. 2002; Abramowitz & Birnbaumer 2009), not only between the members of the subfamily, but also with TRPV4 and TRPP2 (Ma et al. 2010). Moreover, all the TRPC subfamily members are reported to be expressed in ECs and smooth muscle cells (Nilius & Droogmans 2001). Thus far, all of the known TRPC channels are non-selective cation channels, and may be potentially involved in mechanosensing (Nilius & Droogmans 2001). The TRPC1 is the founding member of the subfamily and the first TRP channel to be discovered in mammals. Despite extensive studies on TRPC1, its function as a cation channel in a physiological setting is still cryptic (Beech 2013). The potential role as a mechanosensor of TRPC channels, including TRPC1, is still a matter of debate in the scientific community (Dietrich et al. 2014). This member of the subfamily seems to be activated by other mechanosensitive receptors (as was shown for TRPC6 (Mederos y Schnitzler et al. 2008)) rather than having mechanosentivity abilities per se (Eijkelkamp et al. 2013). The TRPC, in some conditions, seem to be involved in regulating vascular smooth muscle contraction contributing to membrane depolarization and the increase in $[Ca^{2+}]_i$ (Kumar et al. 2006). However, the function of the TRPC in vascular smooth muscle cells is still disputed and studies on mice disproved any TRPC1 roles in this cell line (Dietrich et al. 2007; Dietrich et al. 2014). It was shown that in ECs TRPC1 is required for VEGF-induced $[Ca^{2+}]_i$ increase (Jho et al. 2005), regulating vascular functions, thus positively contributing to angiogenesis (Yu et al. 2010), and vascular tone and permeability (Ahmmed et al. 2004; Jho et al. 2005). Other researchers have identified TRPC6 as a regulator of VEGF-mediated angiogenesis (Cheng et al. 2006; Ge et al. 2009). Moreover, it is well accepted that the activation of TRPC1 is associated with store depletion of calcium (Prakriya 2013; Qu et al. 2017), although the mechanisms coupling store depletion with channel activation are still disputed. Typically, upon ER Ca^{2+} depletion, the luminal calcium sensor stromal interacting molecule 1 (STIM1) undergoes oligomerization and relocates towards ER-plasma membrane junctions, where it interacts directly with the pore forming subunit of Orai1, activating the calcium release-activated channels (CRACs) (Prakriya et

al. 2006; Li et al. 2011). Although the link between store depletion and TRPC1 activation is still missing, increasing evidence supports STIM1 as the interacting molecule activating TRPC1-based store operated Ca^{2+} channels.
More research is still required to completely understand TRPC function and the interplay with the VEGF pathway in ECs. The overall emerging picture shows an intricate TRPC response, which can be trigged by different conditions in relation to different cell types to stimulate and contribute to angiogenic cell behaviour (Moccia & Guerra 2016).

1.6 Calcium fluxes from intracellular stores

In resting or non-stimulated conditions the $[Ca^{2+}]_i$ is very low due to the activity of various channels to confine Ca^{2+} to the extracellular space or cytosolic intracellular stores. In particular, the plasma membrane Ca^{2+}-ATPase (PMCA) and the sarco-endoplasmic reticulum Ca^{2+}-ATPase (SERCA) extrude Ca^{2+} by direct ATP hydrolysis, while the Na^+/Ca^{2+} exchanger (NCX) expels Ca^{2+} by exploiting the Na^+ gradient across the plasma membrane (Moccia & Guerra 2016).
The ECs respond to various stimuli with the increase of $[Ca^{2+}]_i$ by activating calcium channels at the intracellular stores or plasma membrane. The main Ca^{2+} intracellular reservoir in ECs is the endoplasmic reticulum (ER). Due to the high electrochemical gradient between the cytosol and the ER compartment, the Ca^{2+} release is very rapid. The widespread tubular structure of this organelle is often located in the proximity of the plasma membrane, suggesting that the cytosolic calcium entry may be regulated by the physical interaction between channels located at the ER membrane (i.e. Ca-sensor) and plasma membrane channels (i.e. Ca-permeable). The proximity of the two membranes would then maximize the reaction speed. The fast calcium release occurs upon stimulation of two main receptors on the ER membrane: the ryanodine receptors (RyRs) and the inositol 1,4,5-triphosphate receptor (IP_3R) (Moccia et al. 2012).
The calcium release through the RyR may be stimulated by local Ca^{2+} increase via CICR or by another second messenger, the cyclic ADP-ribose (Wood & Gillespie 1998; Zhang 2006). Activated plasma membrane Ca^{2+} channels can locally increase the Ca^{2+} concentration, which then stimulate the proximal RyR, triggering a stronger calcium response. The CICR often occurs upon activation of mechanosensitive Ca^{2+} receptors to regulate the shear stress reaction in ECs (Wong & Klassen 1995; Berridge et al. 2003). On the other hand, IP_3R is activated by the highly diffusible hydrophilic messenger IP_3, produced by the cleavage of PIP_2. In ECs the cleavage is mediated by the VEGFR-2-

dependent activation of phospholipase-Cγ (PLCγ) (see chapter 1.4.4.1) (Takahashi et al. 2001). Indeed PLCγ activation and Ca^{2+} increase are associated with VEGFR-2-mediated angiogenic EC behaviour (Yokota et al. 2015; Fearnley et al. 2015). DAG, the second product of the PIP_2 hydrolysis reaction, activate PKC, which regulates a variety of physiological processes including EC migration via direct phosphorylation or indirectly through transcriptional activation (Tsai et al. 2015). DAG also activates the transient receptor potential canonical subfamily TRPC3/6/7 independently of store depletion (Albert 2011; Villalta & Townsley 2014). On the other hand, depletion of Ca^{2+} stores is associated with the activation of the store operated Ca^{2+} channels, such as the TRPC1/4 (Villalta & Townsley 2014).

Besides the ER compartment, Ca^{2+} can be stored in the mitochondria and in lysosomes. In particular, the mitochondria can contribute to agonist-induced Ca^{2+} signalling by cooperating either with Ca^{2+} release channels in the ER or store operated Ca^{2+} channels on the plasma membrane (Malli et al. 2005). Lysosomes contain a limited amount of Ca^{2+}, which can be released upon stimulation by the Ca^{2+}-mobilizer nicotinic acid adenine dinucleotide phosphate (NAADP) (Brailoiu et al. 2010). Due to the lysosomes proximity to the ER, the discrete low amount of Ca^{2+} released from lysosomes can be amplified to a global Ca^{2+} wave by the activation of the RyR through the CICR mechanism (Zhu et al. 2010).

1.7 Shear stress mediated calcium fluxes

ECs covering the inner surface of blood vessels are continuously exposed to mechanic stimuli due to the haemodynamic forces generated by the blood circulation. It has been shown that ECs are able to sense and transduce biomechanical stimuli as shear stress in biological responses by the activation of multiple intracellular signalling pathways mediated by a variety of mechanosensors. The response of ECs to shear stress is mediated by an increase of $[Ca^{2+}]_i$, which can be generated through several routes (Ando & Yamamoto 2013). The different signalling pathways activated by shear stress can regulate the Ca^{2+}-mediated EC polarity (Miyazaki et al. 2007; Lafaurie-janvore et al. 2016), vascular smooth muscle contractile state (tone) (Taylor et al. 2012), vessel remodelling (Nicoli et al. 2010) or stabilization according to the vessel type (Potente et al. 2011).

Shear stress was shown to activate the hyperpolarization of the EC plasma membrane stimulating the K^+-selective ionic current (Olesen et al. 1988). The cell membrane

hyperpolarization operates as a driving force which triggers the Ca^{2+} entrance from the extracellular space through the transient receptor vanilloid channel 4 (TRPV-4), thus stimulating the EC response (Moccia et al. 2012). Indeed, studies on the specific stretch activated channel have shown that the TRPV-4 is highly expressed in ECs and is responsible for the stretch activated calcium fluxes (Dunn et al. 2013). The shear stress-dependent $[Ca^{2+}]_i$ increase can also occur after the stimulation of the TRPC channel. However, the direct TRPC activation and its capability as a mechanosensor remain to be determined (Dietrich et al. 2014).

In addition, the P2X4 receptor, a subtype of ATP-operated cation channels, is constitutively expressed on EC plasma membranes and indirectly activated by shear stress to stimulate the $[Ca^{2+}]_i$ increase-mediated EC response. It has been shown that the exposing ECs to shear stress induces the dose-dependent release of ATP, which then activates the P2X4 receptor stimulating Ca^{2+} entrance through the channel (Yamamoto et al. 2003; Ando & Yamamoto 2013).

Several *in vitro* and *in vivo* studies have demonstrated that ECs can sense and transduce biomechanical stimuli, such as shear stress, through primary cilia (Hierck et al. 2008; Nauli et al. 2008; Goetz et al. 2014). One proposed mechanism, by which cilia are able to sense shear stress, suggests changes in cytoskeletal organization triggered by cilium bending. Further, cilium bending can activate the calcium signalling response, stimulating the extracellular Ca^{2+} influx through cation channels localised on the cilia (Ando & Yamamoto 2013). Indeed, mechanodetection and calcium signalling were associated with the cation channel polycystin-2 (PC2), a member of the TRP family (also known as PKD2 or TRPP2). PC2 is required for proper cilia localization and to transduce shear stress, leading to an increase in calcium concentration and nitric oxide (NO) production in several ciliated structures, such as the left-right organizer (McGrath et al. 2003; Yoshiba et al. 2012), kidney epithelial cells (Nauli et al. 2003) and cultured ECs (AbouAlaiwi et al. 2009). Moreover, studies in zebrafish revealed that ECs from the dorsal aorta and from ISVs are ciliated (Kallakuri et al. 2015), and are able to respond to shear stress from the blood flow by increasing calcium concentrations mediated by PDK2. Defects in this response were associated with impaired vascular morphogenesis (Goetz et al. 2014).

1.8 Endothelial cell-mediated regulation of vascular tone

Blood vessels are formed by organized layers of cells capable of responding to chemical and mechanical stimuli due to the haemodynamic forces generated by the blood circulation. ECs, covering the inner surface of the mature vessels, transduce biomechanical stimuli into molecular signals and regulate the response of the adjacent smooth muscle cells (SMCs) in order to maintain vascular tone homeostasis. Dysfunction of EC response in this context was associated with the development of several vascular diseases such as hypertension, thrombosis, aneurysm, and arteriosclerosis (Félétou et al. 2010). The EC-mediated regulation of vascular tone is associated with calcium signalling. Increase of $[Ca^{2+}]_i$ activates pathways leading to the production of soluble vasoconstrictors (or vasodilators) in ECs, or initiates the hyperpolarization of SMCs, and thus stimulates the vasodilatation. In particular, the calcium dependent vasodilatation of ECs occurs in three distinct modes. Vasodilatation can be mediated by the production of NO, a tissue-permeable gas generated as a by-product of the oxidation of arginine to citrulline and catalysed by the calcium-calmodulin dependent endothelial nitric oxide synthase (eNOS) (Busse & Mülsch 1990). ECs also produce other kind of vasodilators, such as prostacyclin derived from the arachidonic acid metabolism (Jaffe et al. 1987). The third vasodilatation mechanism involve the endothelial-derived hyperpolarizing factor (EDHF) activation, characterized by its EC small- and intermediate- conductance Ca^{2+}-activated potassium (K+) channels, KCa2.3 and KCa3.1 (Crane et al. 2003; Dora et al. 2008), which elicit hyperpolarization of underlying vascular SMC (Bychkov et al. 2002; Taylor et al. 2003; Taylor et al. 2012). Although several factors have been suggested to be associated with the EDHF response, accumulating evidence highlights the importance of heterocellular electrical coupling through gap junctions facilitating the EC-mediated hyperpolarizing current to SMCs (Coleman et al. 2001; Sonkusare et al. 2012).

The EC is able to mediate not just vasorelaxation, but also vasoconstriction. Indeed, ECs produce prostacyclin as well as the vasoconstrictor thromboxane, both derived from the arachidonic acid metabolism (Sandoo et al. 2010). Thromboxane is responsible for platelet aggregation mediated by the activation of its thromboxane prostanoid (TP) receptors located on platelets. TP receptors are also located on SMCs, where their stimulation triggers the increase of $[Ca^{2+}]_i$, which leads to vasoconstriction. Moreover, ECs produce and release the vasoconstrictor endothelin-1 (ET-1) (Yanagisawa et al. 1989) in response to stimulation by pro-inflammatory signals such as interleukins, whereas the release is inhibited by NO and prostacyclin (Alonso & Radomski 2003). ET-

1 receptors were identified in both ECs and SMCs (Davenport et al. 1995; Bacon et al. 1995). The activation of ET-1 receptors on SMCs triggers the increase of $[Ca^{2+}]_i$ and consequent vasoconstriction. On the other hand, stimulation of ET-1 receptors on ECs induce vasodilation through NO and prostacyclin production (Pollock et al. 1995). In the presence of endothelial dysfunction, ET-1 receptor expression is downregulated on ECs and upregulated on SMCs, thus reinforcing the vasoconstriction (Böhm et al. 2002; Sandoo et al. 2010).

As aforementioned, the increase of $[Ca^{2+}]_i$ is required for SMC contraction. The excitation-contraction mechanism, in skeletal, cardiac and SMCs, is initiated by the activation of voltage gated LTCC (Navedo & Santana 2013). Even though the LTCCs are responsible for the initiation of excitation-contraction coupling, the precise mechanisms by which they increase the $[Ca^{2+}]_i$ is specific to the type of muscle cell (Navedo & Santana 2013). In skeletal muscle the calcium fluxes through the LTCC are not required for the initiation of contraction (Franzini-Armstrong et al. 1999; Rebbeck et al. 2014). Accumulated research supports the idea that LTCCs located in the transverse tubules physically interact with the ryanodine receptor (RyR) on the sarcoplasmic reticulum; the voltage driven conformational changes of the LTCC would then directly activate calcium fluxes through the RyR (Rebbeck et al. 2014). In contrast to skeletal muscle, calcium entry through the LTCC is required for the initiation of the contraction in cardiac myocytes. Action potential stimulates the LTCC, and calcium fluxes through the channel trigger the activation of RyR and initiate the CICR from the sarcoplasmic reticulum, globally increasing the calcium concentration and activating actomyosin and contraction (Bers 2002; Catterall 2011). In vascular smooth muscle, the intravascular pressure regulates the depolarization and the subsequent LTCC activation. In these cells, calcium fluxes through the channel are directly responsible for the cytosolic calcium increase that activates the contractile processes (Amberg & Navedo 2013).

1.9 The L-type calcium channel regulation by Wnt signalling

Change in $[Ca^{2+}]_i$ is a ubiquitous signal used by different pathways. Among these, the evolutionarily conserved Wnt signalling pathway has a crucial role in cell fate determination, migration, cell polarity and organogenesis during embryonic development (Croce & McClay 2008). Wnt proteins are secreted glycoproteins, which via paracrine or autocrine activation, bind to the extracellular N-terminal domain of the Frizzled (Fzd) receptor family (Hendrickx & Leyns 2008). Upon Wnt binding the signal is transduced by

the cytoplasmic phosphoprotein Dishevelled (Dvl); the pathway can then proceed via three major cascades, the canonical and two non-canonical pathways: the planar cell polarity (PCP) and the Wnt/Ca^{2+} pathways. The accumulation and subsequent translocation of β-catenin into the nucleus is the hallmark of the Wnt canonical pathway. In the absence of Wnt signal, β-catenin is associated with the glycogen synthase kinase-3β (Gsk3β) and casein kinase-1 (Ck-1), which in collaboration with a destruction complex containing the adenomatous polyposis coli (Apc) protein, the Wilms tumor suppressor protein (WTX) and Axin, constantly phosphorylates the cytosolic β-catenin at specific regulatory Ser/Thr residues. The modified β-catenin is then recognized by β-transducing repeat-containing protein (β-TrCP), a component of an E3 ubiquitin ligase complex, and targeted for ubiquitination and proteasomal degradation (Spiegelman et al. 2000; Kohn & Moon 2005; Stamos & Weis 2013). Wnt activation induces a series of events, which disrupt the degradation complex and consequently promote β-catenin accumulation and translocation to the nucleus where it interacts with transcription factors to stimulate the transcription of target genes.

Non-canonical Wnt signalling is also called β-catenin independent. Indeed, the signal transduction is not mediated by β-catenin and appears to function without the transcription of target genes. The PCP pathway is one of the two branches of Wnt non-canonical signalling participating in cytoskeletal reorganization via stimulation of the Dishevelled-associated activator of morphogenesis 1 (Daam1). Fzd activation by Wnt stimulates the formation of a Dvl/Daam1 complex, which activates small GTPase proteins such as RhoA, leading to the activation of the Rho-associated kinase (ROCK) (Marlow et al. 2002) and myosin (Weiser et al. 2007), thus promoting cytoskeletal rearrangement and cellular polarization (Komiya & Habas 2008). The second branch of Wnt non-canonical signalling is the Wnt/Ca^{2+} pathway: Fzd receptor stimulates intracellular Ca^{2+} release from the endoplasmic reticulum through trimeric G-proteins (Slusarski & Pelegri 2007). Ca^{2+} release and cytosolic accumulation activates several Ca^{2+}-sensitive proteins such as protein kinase C (PKC) and Ca^{2+}/calmodulin-dependent kinase II (CamKII) (Kühl et al. 2000; Sheldahl et al. 2003).

Studies of heart development have revealed the critical role of Wnt non-canonical signalling (Eisenberg & Eisenberg 1999; Pandur et al. 2002; Flaherty & Dawn 2008; Cohen et al. 2012). In particular, Wnt11 stimulation as a key modulator of myocardial electrical cell coupling (Panakova et al. 2010), and heart chamber remodelling (Merks et al. 2018). During cardiac morphogenesis, intercellular coupling and the formation of electrical gradients between cardiomyocytes are crucial for electrical stability, which coordinates the mechanical movement of the adult heart (Watanabe et al. 1981). As the

heart is forming, impulse propagation progresses from being homogeneous along the whole organ into the formation of differentiated zones with slow and fast conductance (Panakova et al. 2010). It was shown that loss of Wnt11 signalling prevents the formation of the electrical gradient and the specification of different zones, resulting in homogeneous conductance velocities across the entire ventricle (Panakova et al. 2010). Further investigation of the Wnt11/PCP pathway in forming the electrical gradient, revealed that neither the loss of Vangl2 nor Prickle1, the two fundamental components of the PCP pathway, affected the gradient, suggesting that PCP signalling is not responsible for the gradient formation (Panakova et al. 2010). It was shown that the loss of Wnt11 increases the amplitude and the heterogeneity of the $[Ca^{2+}]_i$ transients across the entire ventricle. A similar effect was obtained with the stimulation of LTCC conductance. Together this suggests that Wnt11 regulates the electrical gradient patterning by reducing the LTCC activity (Panakova et al. 2010). Indeed, in a *cacna1c* mutant context, the loss of Wnt11 had no effect on the gradient of electrical coupling. Likewise, the electrical gradient was preserved in the *wnt11* mutant context in association with LTCC inhibition. This shows that Wnt11 acts upstream of LTCC, guiding the electrical gradient formation, modulating Ca^{2+} homeostasis by attenuating Ca^{2+} influx through the LTCC (Panakova et al. 2010).

1.10 Similarities between vascular and neuronal systems: the importance of the L-type calcium channel

Since the discovery of sprouting blood vessels, it was evident that the leading cell, the “tip cell”, resembles in cellular appearance and function the already well known specialized cellular structure at the tip of growing axons, the “axon growth cone”. Both are characterized by the presence of lamellipodia and long finger-like filopodia to sense the local environment and guide development (Gerhardt et al. 2003; Carmeliet & Tessier-Lavigne 2005; Carmeliet & Jain 2011).

Both vascular and neuronal systems form complex pattern networks to exchange information over long distances connecting and coordinating different organs in the body. The nervous system manipulates electrical signals to transport information, while the vascular system carries messenger molecules in the blood to connect and regulate far located organs. Because of these important functions, both systems require precise regulation of patterning and guidance of cellular and subcellular components (Wälchli et al. 2015).

The similarities between the nervous and vascular systems are not only limited to the morphologic structure, but they are also evident at the molecular level: both the endothelial tip cell and the axonal growth cone share common molecular pathways and respond to the same molecular cues (Melani & Weinstein 2010; Adams & Eichmann 2010). In the past years it has been shown that the main neuronal guidance molecule families, Netrins, Semaphorins, Ephrins, and Slits, in coordination with their receptors, guide not only neuronal development, but also vascular patterning (Carmeliet & Tessier-Lavigne 2005; Carmeliet & Jain 2011). Moreover, guidance molecules such as the morphogens: wingless-type proteins (Wnts), Bone Morphogenetic Proteins (BMPs) and Sonic Hedgehog (Shh) were revealed to participate in the process of attractive and repulsive signalling during axon pathfinding (Charron & Tessier-Lavigne 2007) as well as in vascular growth (Zacchigna et al. 2007; Wälchli et al. 2015).

In addition to the guidance molecules, one of the most crucial components controlling axonal turning and growth is calcium (Sutherland et al. 2014). Cytosolic calcium fluctuations have been reported as signals for both attractive and repulsive responses. As for other cell types the spatial distribution and the amplitude of $[Ca^{2+}]_i$ are crucial for accurate axon guidance. It has been shown that not only the amplitude of Ca^{2+} signals are important, but also the sources of Ca^{2+} entry and the environmental Ca^{2+} concentration (Sutherland et al. 2014; Gasperini et al. 2017). Asymmetric Ca^{2+} concentrations within the axonal growth cone were sufficient to generate the turning response (Zheng 2000); however the steepness of the Ca^{2+} gradient and the extracellular Ca^{2+} concentration are also important to determine the growth direction. A large Ca^{2+} increase in the condition of normal extracellular Ca^{2+} concentration evokes an attraction (Zheng 2000). On the contrary, small Ca^{2+} increases or large Ca^{2+} increases in the absence of extracellular Ca^{2+} result in repulsion (Wen et al. 2004).
Only the fine control of entry mechanisms can precisely regulate the calcium amplitude and distribution, and thus the axonal response. The most important way to increase $[Ca^{2+}]_i$ to control axon turning is through the VGCCs, which can activate the release of Ca^{2+} stores and therefore the store operated calcium entry (SOCE) from the extracellular space. Among the VGCCs the LTCC is the most important player in growth cone turning. It was shown that inhibition or activation of VGCC channels can switch the attractive response to netrin-1, an attractive chemotropic factor, into a repulsion reaction (Hong et al. 2000; Wang & Poo 2005; Gasperini et al. 2017). LTCC activity during axonal pathfinding is finely modulated by the balance of cGMP (promoting LTCC activation) and cAMP (promoting LTCC inactivation): high levels of cGMP result in axonal repulsion in response to a netrin-1 gradient, while high levels of cAMP result in axonal attraction

(Nishiyama et al. 2003). All together this data illustrate the importance of calcium fluxes through the plasma membrane and the critical role of the LTCC, together with its regulation, in controlling axon guidance and growth.

Given the commonalities between the nervous and vascular systems, it is plausible to speculate a physiological role of calcium signalling during the vascular formation as well. However, so far only few intensive studies have been done in this direction. Calcium signalling in developing vessels has been investigated mainly in relation to the VEGF response. It has been shown that different VEGF concentrations can evoke distinct calcium responses and oscillations, thus controlling diverse endothelial cell behaviour (Noren et al. 2016). Calcium oscillations have been detected also during the tip/stalk specification at the very early stage of the vessels sprouting in response to VEGF stimulation (Yokota et al. 2015). Moreover, hemodynamic forces due to blood flow, can trigger a calcium signalling response mediated by cilium bending in EC (Ando & Yamamoto 2013; Goetz et al. 2014). However the molecular mechanisms governing calcium signalling and its function during the different phases of sprouting angiogenesis and vascular formation remain elusive.

2 Aims

The formation of a functional vascular system is a critical step during embryonic development. Moreover, dysregulation of the vascular patterning is associated with several diseases. In the past years, studies on EC and angiogenesis *in vitro* and *in vivo*, have revealed the importance of VEGF signalling together with the Dll4/Notch pathway in regulating EC migration and proliferation during angiogenesis. Furthermore, it is well established that the endothelial tip cell and the axonal growth cone share not only similar morphology, but also common molecular pathways and respond to the same molecular cues. One of the most important players during axonal growth is calcium. Changes in the cytosolic Ca^{2+} concentration are ubiquitous intracellular signals activated by several different pathways and implicated in many biological processes thanks to their high versatility in amplitude, frequency, and distribution (Berridge et al. 2000). During axonal pathfinding, Ca^{2+} fluxes through the plasma membrane, in particular through the L-type Ca^{2+} channel, are essential to determine the axon turning and to guide the growth.

While in mature ECs changes in $[Ca^{2+}]_i$ are key regulators of many biological aspects (Tran et al. 2000; Munaron 2006), little is known about their role during angiogenic sprouting, a process akin to axonal pathfinding. Changes in $[Ca^{2+}]_i$ have been already associated with VEGF signalling cascade, however, its precise function and modulation of $[Ca^{2+}]_i$ in EC during angiogenesis are still debated. Moreover, the molecular mechanisms regulating the Ca^{2+} signalling at the level of the plasma membrane, the identity of the different channels involved, and their hierarchy are still not fully explored.

In summary, despite the large effort in understanding the Ca^{2+} regulation in non-excitable cells such as the ECs, there are still numerous aspects to be elucidated. Moreover, most of the information on the physiological role of Ca^{2+} in ECs were obtained through *in vitro* studies and little is known about the *in vivo* role of Ca^{2+} during vascular development. The central idea of my dissertation aims at understanding the role of calcium signalling during angiogenesis and focuses on elucidating the implication of calcium fluxes through the EC plasma membrane, in particular through the LTCC, on the angiogenic process utilizing the well-established zebrafish model.

3 Results

3.1 Intracellular calcium oscillation during the ISV outgrowth

Changes in cytosolic calcium concentration are key signals in the regulation of several biological processes, such as migration, vesicles segregation, contraction, adhesion, and gene expression (Munaron 2006; Moccia & Guerra 2016). Despite extensive efforts, *in vivo* approaches to accurately measure cytosolic calcium fluctuations in ECs are still limited. Here, I used a double transgenic zebrafish line *Tg(kdrl:Gal4; UAS:GCaMP5)*, expressing the Ca^{2+} indicator GCaMP5 (Akerboom et al. 2012) specifically in ECs, to evaluate changes in intracellular Ca^{2+} concentrations in ECs during angiogenic sprouting *in vivo*. Time-lapse imaging of growing ISVs uncovered Ca^{2+} oscillations in the tip cell at the forefront of the sprouting vessel, as well as in the stalk cells localized at the base of the vessel (Fig. 9 A, B). Moreover, analysis of the calcium fluctuations over time revealed a two-component nature of Ca^{2+} oscillations during angiogenic sprouting. The two components included slow Ca^{2+} transients with low amplitude and long duration and fast Ca^{2+} sparks with high amplitude and short duration (Fig. 9 B).
Furthermore, kymograph representations of a sprouting vessel showed simultaneous Ca^{2+} activity in the tip and stalk cell (Fig. 9 C, D), indicating a possible electrical coupling through the vessel. This data reveals dynamic cytosolic Ca^{2+} fluctuations during migration of ECs *in vivo*.

3.2 LTCC is expressed in endothelial cells

Increases in cytosolic calcium concentration are regulated by different pathways, by Ca^{2+} release from intracellular stores or by Ca^{2+} influx from the extracellular space through the plasma membrane. This last mechanism can be mediated by the VGCC such as the LTCC. The expression of VGCC, particularly the LTCC, in ECs is still disputed. Indeed, while LTCC is activated at depolarizing voltages, the depolarization of EC membrane abrogates the Ca^{2+} influx into the cells (Dora & Garland 2013). Moreover, it has been difficult to discriminate the contributions of different intracellular compartments to the increase of cytosolic calcium concentration, and obtain accurate measurements of

membrane Ca^{2+} influx upon EC membrane depolarisation (Dora & Garland 2013) such as the LTCC.

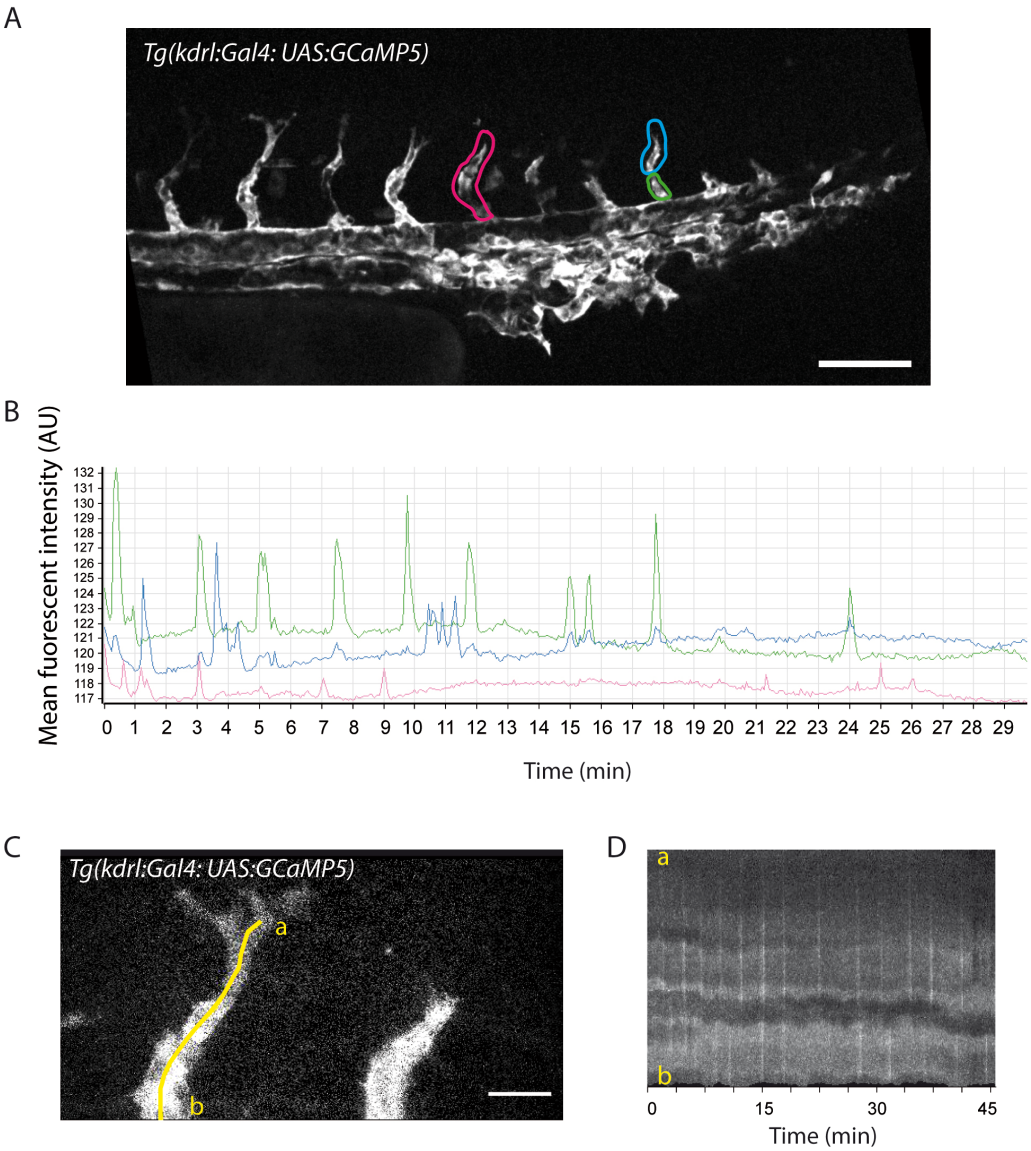

Figure 9: Ca^{2+}oscillations have a two-component nature during angiogenic sprouting. (A) Maximum intensity projection from time-lapse *in vivo* imaging of a *Tg(kdrl:Gal4; UAS:GCaMP5)* embryo from 30 hpf acquired by spinning disk confocal microscopy, images acquired using an interval of 4 seconds. Scale bar 100μm. **(B)** Average of Ca^{2+} signals over time (30min) in three different regions of interest (magenta, blue and green), in A, mean fluorescent intensity in arbitrary units (AU). **(C)** Maximum intensity projection from time-lapse *in vivo* imaging of a *Tg(kdrl:Gal4; UAS:GCaMP5)* embryo at 30 hpf acquired by confocal microscopy. Scale bar 20 μm. **(D)** Representative kymograph of a growing ISV in C (green line a, b) over time (45 min), images acquired using an interval of 8 seconds.

The expression of VGCC, particularly the LTCC, in ECs is still disputed. Indeed, while LTCC is activated at depolarizing voltages, the depolarization of EC membrane abrogates the Ca^{2+} influx into the cells (Dora & Garland 2013). Moreover, it has been difficult to discriminate the contributions of different intracellular compartments to the increase of cytosolic calcium concentration, and obtain accurate measurements of membrane Ca^{2+} influx upon EC membrane depolarisation (Dora & Garland 2013). Nonetheless, recent studies have shown the expression of the LTCC in human umbilical vascular endothelial cells (HUVEC) (Kim et al. 2016).

To address LTCC expression in zebrafish ECs during development, I performed RT qPCR analysis of the *cacna1c* gene, encoding the LTCC main pore forming subunit, in wildtype and in two *cacna1c*-mutant zebrafish lines as negative control. The first *cacna1c*-mutant line carries a non-sense mutation in exon 6/7 and the second affects an essential splice site in exon 35/36/37: *cacna1c*^{sa10930} and *cacna1c*^{sa15296}, respectively. The *cacna1c*^{sa10930} mutation may result in a complete loss of function of LTCC, while the *cacna1c*^{sa15296} mutation may create a truncated version of the main pore forming subunit missing the C-terminal tail, compromising the channel conductance (Hulme et al. 2006) and transcriptional activity (Gomez-Ospina et al. 2006; Schroder et al. 2009).

Taking into consideration that the *cacna1c* gene is characterized by the presence of different transcription start sites in its sequence (Gomez-Ospina et al. 2006; Schroder et al. 2009) and a cryptic promoter in exon 46 in the murine gene (Gomez-Ospina et al. 2013), I analysed the relative mRNA *cacna1c* expression with three different TaqMan probes, to cover the different isoform expression, targeting the 2-3 loop (N-terminal; exon 18), the proximal (pCt; exon 40) and the distal (dCt; exon 45) C-terminal region, (Fig. 10 A, B).

First, I verified the downregulation of the LTCC in the aforementioned mutant lines, analysing the relative mRNA *cacna1c* expression in whole embryo extracts. Compared to wildtype, both mutants showed between 30 and 40 percent decrease in *cacna1c* relative mRNA expression using the three different probes (Fig. 10 B). While the complete loss of protein in the aforementioned mutants could not be tested due to lack of working antibodies, the result confirms the downregulation of *cacna1c* expression in the mutant lines.

To determine whether LTCC is expressed in ECs, the *cacna1c* relative mRNA expression was measured in FACS-sorted ECs from the reporter line *Tg(kdrl:EGFP)*, which expresses EGFP specifically in ECs. The relative *cacna1c* expression detected in ECs from the *cacna1c*^{sa10930} mutant line was decreased compared to control ECs, confirming the presence of the LTCC in ECs (Fig. 10 C).

As predicted, the FACS-sorted non-ECs isolated from control embryos have higher expression of *cacna1c* compared to control ECs, due to the presence of cardiomyocytes and neuronal cells expressing high levels of LTCC. As a positive control, I measured 10-fold higher relative *cacna1c* expression level in FACS-sorted cardiomyocytes compared to control EC, as expected (Fig. 10 C).

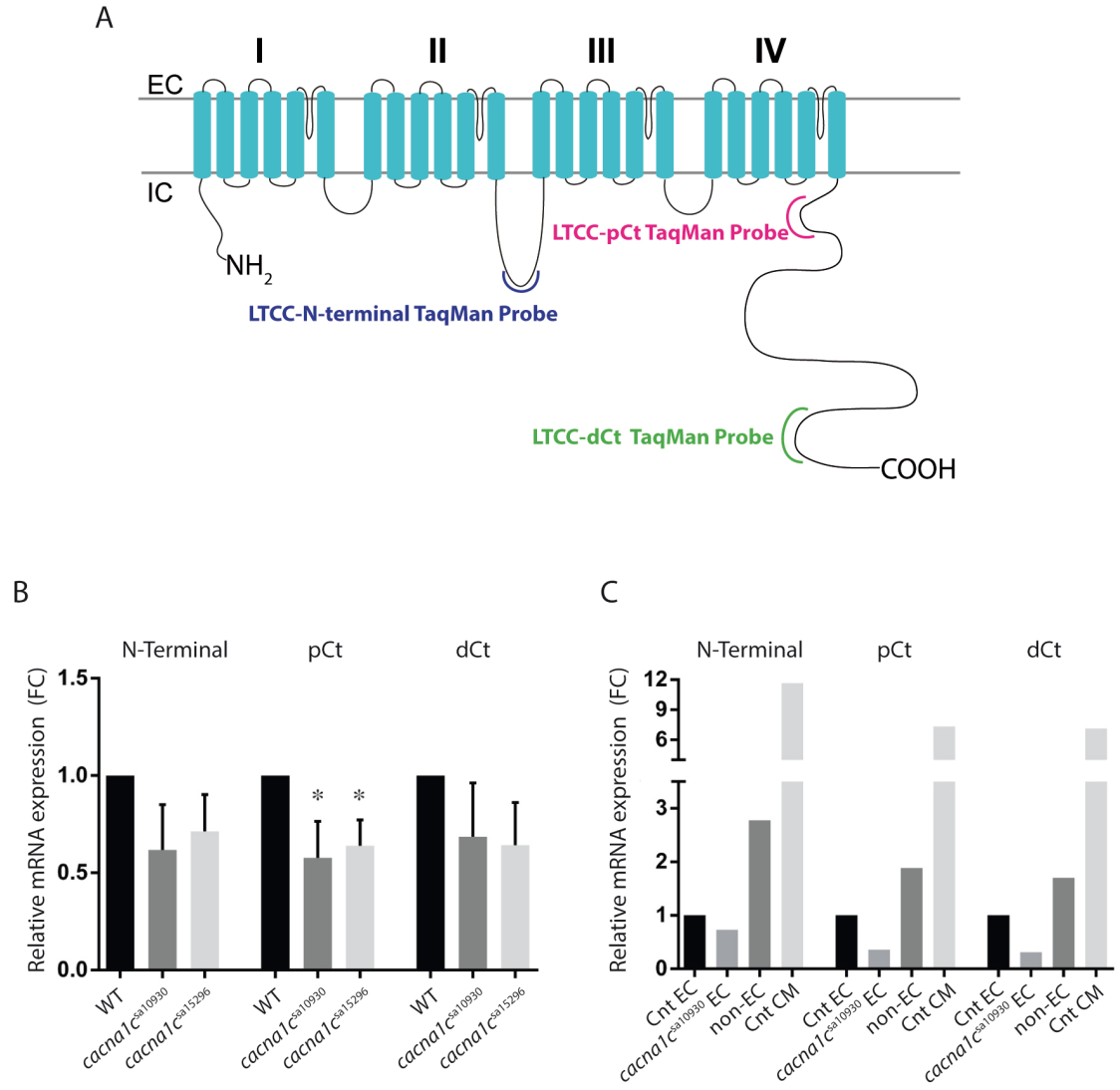

Figure 10: ECs express the LTCC. (A) Scheme of LTCCα1c main pore-forming subunit, different TaqMan probes targeting the 2-3 loop (N-terminal; exon 18), the proximal (pCt; exon 40) and the distal (dCt; exon 45) C-terminal region are represented. **(B)** RT qPCR analysis of *cacna1c* relative mRNA expression levels from two different *cacna1c* mutant lines (*cacna1c*^{sa10930} and *cacna1c*^{sa15296}) compared to wildtype control (WT, set to 1) in whole zebrafish embryos at 48 hpf, using three different TaqMan probes. **(C)** Relative mRNA expression levels of *cacna1c* in FACS-sorted ECs from control (Cnt EC, set to 1) and *cacna1c* mutant (*cacna1c*^{sa10930} EC), control non-endothelial cells (Cnt non-EC) and control cardiomyocytes (Cnt CM) using three different probes. Data were normalized to the reference gene *eef1α1* and represented as fold changes (FC). Mean ± SD. One-way ANOVA with Bonferroni Multiple Comparison correction. $n_{(WT)}$=3; $n_{(cacna1csa10930)}$=3, **P*=0.0160 with pCt probe; $n_{(cacna1csa15296)}$=3, **P*=0.0318 with pCt probe.

3.3 Alteration of Ca^{2+} fluxes through the LTCC results in morphological defects of ISVs

The formation of a functional vascular network is ensured by fine regulation of EC migration and proliferation to build the specific blood vessels' structure. By 30 hpf the vascular morphogenesis of the primary ISVs localized more rostrally in zebrafish embryos is complete. The sprouting vessel has reached the dorsolateral roof of the neural tube, divided into two branches, and formed the DLAV (Fig. 2 B, 11 A).
To determine the possible function of the LTCC during ISV outgrowth, a pharmaceutical and a genetic approach were used to inhibit or stimulate the channel conductance, and the ISV formation was analysed at 30 hpf.

3.3.1 Perturbation of Ca^{2+} fluxes through LTCC: a pharmaceutical approach

The main pore-forming subunit of the LTCC is sensitive to dihydropyridine (DHP) (Satin et al. 2011; Striessnig et al. 2006). For this reason the dihydropyridines Nifedipine and Bay K8644 (Bay K), the antagonist and agonist of the channel, respectively, were used to block and activate LTCC conductance. Transgenic *Tg(kdrl:EGFP)* embryos, expressing the EGFP marker only in ECs, were treated with Nifedipine or Bay K at 10 hpf, at the bud stage; the effect on ISV morphology was examined at 30 hpf and compared with untreated and DMSO-treated controls. At 30 hpf, Nifedipine-treated embryos were severely delayed in their development with profound morphological defects, whereas the development of Bay K-treated embryos was only slightly delayed. Both treatments resulted in heart function deficiency as expected. The decrease in Ca^{2+} fluxes through the LTCC due to the Nifedipine treatment resulted in morphological defects of ISVs during early embryonic development. The ISVs did not reach the dorsolateral roof of the neuronal tube and appeared shorter than in the controls (Fig. 11 A-C). Conversely, the stimulation of Ca^{2+} fluxes through the LTCC by Bay K treatment showed a completely opposite effect on the ISVs growth. The embryos showed enhanced angiogenic behaviour and an overbranching structure of the ISVs (Fig. 11 D). This phenotype partially phenocopied the one observed in the VEGF receptor-1 (*flt1*) mutant; the downregulation of *flt1* showed an overbranching ISV structure and an increase in the number of tip cells (Krueger et al. 2011). Increased of tip cell behaviour

together with higher number of cells forming the ISV was previously reported also in absence of Notch signalling in *dll4* MO-injected embryos (Siekmann & Lawson 2007).

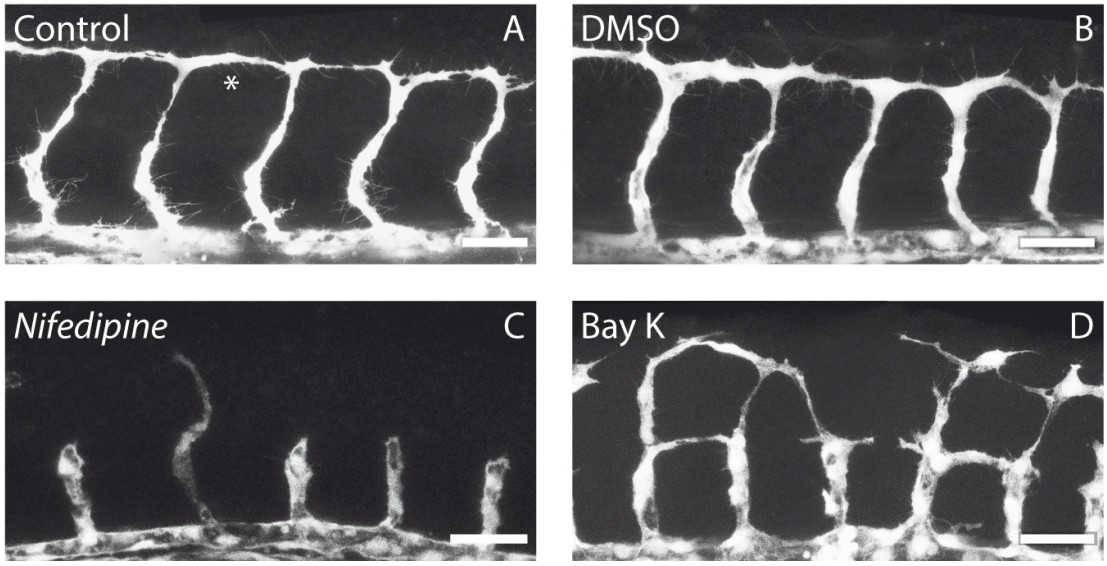

Figure 11: Alteration of calcium fluxes through the LTCC results in morphological defects of ISVs. **(A, B)** Maximum intensity projection of ISVs from the rostral area in *Tg(kdrl:EGFP)* zebrafish embryos at 30 hpf in control (A) and DMSO-treated embryos (B). **(C)** Inhibition of calcium fluxes through LTCC with 70µM Nifedipine results in ISV morphological defects. **(D)** On the contrary, stimulation of LTCC with 125µM Bay K induces an overbranching phenotype. Scale bar = 40µm.

3.3.2 Perturbation of Ca^{2+} fluxes through LTCC: genetic approach

In parallel to the pharmaceutical approach, I used genetic techniques to perturb the channel conductance to further investigate the role of Ca^{2+} fluxes through the LTCC during angiogenic sprouting. In addition to the aforementioned mutants, morpholino (MO) knockdown technology, targeting the spice-site acceptor of exon 4 in the *cacna1c* gene, was used to reduce LTCC levels. Decreased levels of LTCC, both in *cacna1c*^{ex4sa} MO-injected fish, as well as in the two *cacna1c*-mutants, led to a general developmental delay and profound heart defects characterised by a non-contractile myocardium and small unlooped hearts. The MO-injected embryos showed a strong effect on angiogenic sprouting, where the ISVs appeared strongly delayed in development or were completely missing (Fig. 12 B). Similarly, the LTCC loss of function in the *cacna1c*^{sa10930} mutants resulted in delayed ISV development: they were shorter

and sometimes completely missing (Fig. 12 C). Of note, the formation of the dorsal aorta and the cardinal vein were unaffected as they are formed by the process of vasculogenesis. The effect obtained with the morpholino approach was much stronger compared to the genetic mutant. This could be due to several reasons, with one possible explanation being the activation of an alternative transcription start site (as was identified in murine transcripts (Gomez-Ospina et al. 2013)) located downstream of the non-sense point mutation in the *cacna1c*^{sa10930} mutant.

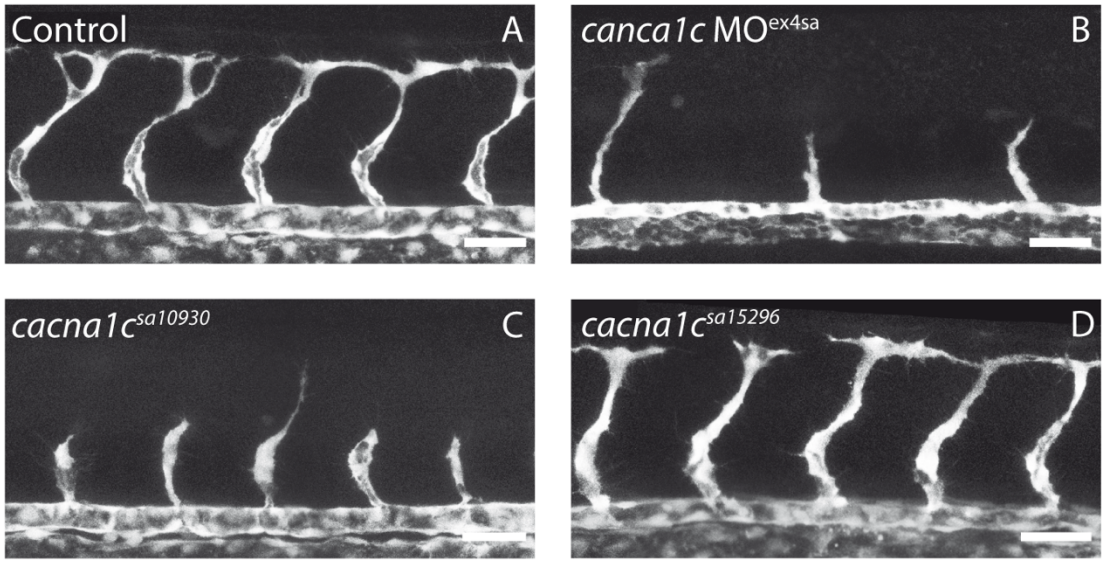

Figure 12: Alteration of calcium fluxes through the LTCC using genetic approaches results in morphological defects of ISVs. (A) ISVs morphological structure at 30 hpf in control *Tg(kdrl:EGFP)* zebrafish embryos. **(B, C)** The effect of LTCC downregulation on the ISVs morphology in *cacna1c*^{ex4sa} MO-injected embryos (B) is much stronger than the one observed in *cacna1c*^{sa10930} mutant line (C). **(D)** The *cacna1c*^{sa15296} mutant line does not show any visible defects in the ISV's structure. Scale bar = 40µm.

Although both mutant lines presented a general developmental delay and severe heart deficiency, the *cacna1c*^{sa15296} mutant did not present any morphological irregularity of ISV formation, suggesting that the main pore-forming subunit of the LTCC might be still present and also functional in this mutant. (Fig. 12 D). Furthermore, the RT qPCR analysis of the *cacna1c* expression showed only partial loss of *cacna1c* transcripts in both mutants (Fig.10), indicating potentially some residual activity of the LTCC.

3.4 Alteration of Ca^{2+} fluxes through the LTCC affects the number of cells in the ISVs

To better characterize the observed morphological phenotype after perturbing Ca^{2+} fluxes through the LTCC, the transgenic line *Tg(fli1a:nlsEGFP)* expressing the nuclear marker only in ECs was used to count the ISV cell number. I observed that the ISVs in the caudal region of the control embryos were shorter and had fewer ECs compared to the ISVs in the rostral region (Fig.13). To precisely analyse the cell number of ISVs across the whole length of the trunk, the image of each embryo was divided into two regions: i) the rostral region, extending from the first rostral ISV to the ISV at the end of the yolk extension (Fig. 13, blue ROI), and ii) the caudal region, extending from the adjacent ISV at the end of the yolk extension to the end of the tail (Fig. 13, green ROI). To investigate the effects of LTCC stimulation on the ISVs, the rostral and caudal regions were analysed separately and the cell number of each vessel was counted and compared within these two regions.

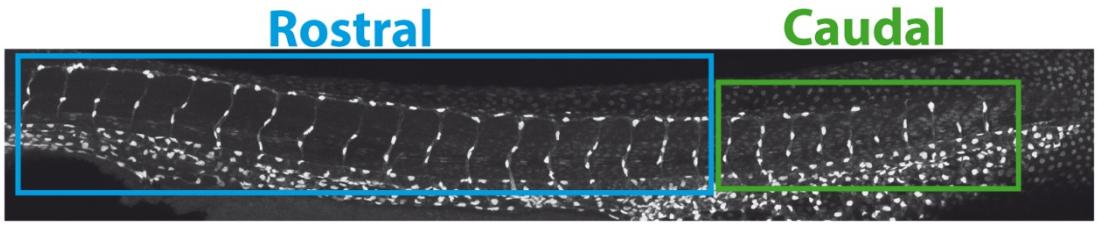

Figure 13: Arbitrary separation of ISVs into caudal and rostral regions. The rostral (blue box) and caudal (green box) regions of ISVs in a *Tg(fli1a:nlsEGFP)* zebrafish embryo at 30 hpf are indicated. The cell number in ISVs was compared separately in all experiments.

3.4.1 Stimulation of LTCC conductance increases the number of cells in the ISVs

In control embryos, untreated (Fig. 14 A) and DMSO-treated (Fig. 14 B), the quantification of cell number showed the differences between rostral and caudal regions as expected; on average, each rostral ISV has four cells, while each caudal ISV is made of only two cells (Fig. 14 D). The stimulation of Ca^{2+} fluxes through the LTCC upon Bay K treatment increased angiogenic cell behaviour at 30 hpf leading to an overbranching phenotype and a significant increase in cell number in both caudal and rostral regions (Fig. 14 C, D). The number of cells in the ISVs is increased up to six and four cells in

rostral and caudal regions, respectively (Fig. 14 D). This phenotype partially phenocopied the loss of VEGF receptor-1 (*flt1*) or *dll4*, which was previously reported to increase the tip cell behaviour (Siekmann & Lawson 2007).

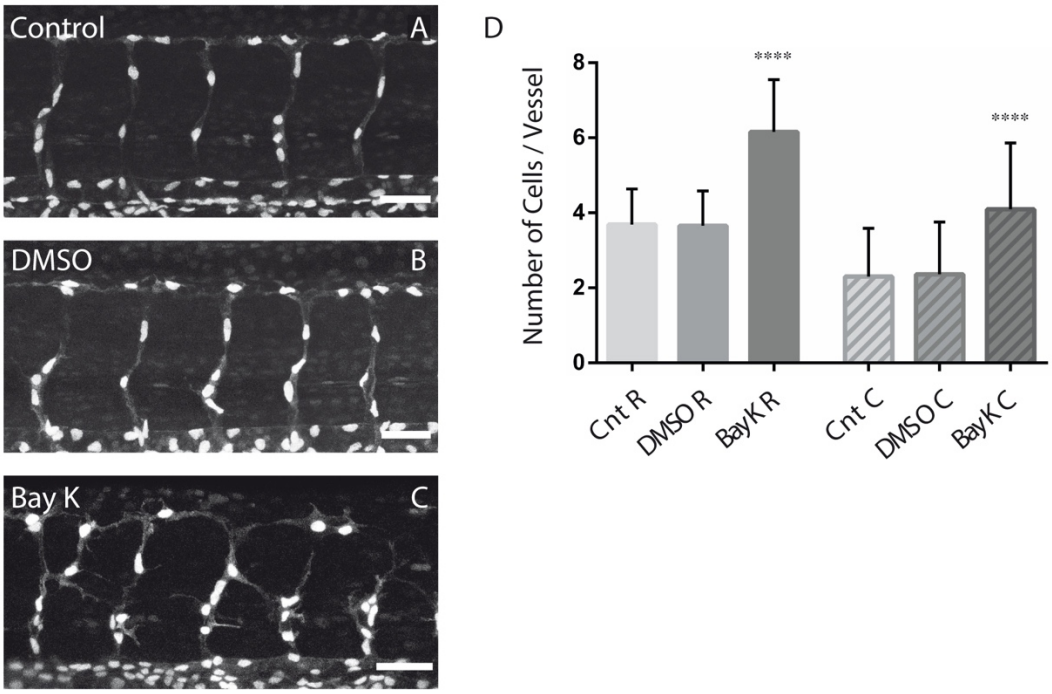

Figure 14: Stimulation of Ca^{2+} fluxes through the LTCC increases the number of cells in the ISVs. **(A-C)** Maximum intensity projection of ISVs from the rostral area in *Tg(fli1a:nlsEGFP)* at 30 hpf in control (A), DMSO (B), and 125µM Bay K-treated (C) zebrafish embryos. **(D)** Quantification of the number of cells per ISV in the rostral and caudal regions at 30 hpf. Mean ± SD. Rostral region: $n_{(cnt)}$=152; $n_{(DMSO)}$=87 $n_{(Bay\ K)}$=95; ****P <0.0001. Caudal region: $n_{(cnt)}$=120; $n_{(DMSO)}$=70; $n_{(Bay\ K)}$=80; ****P <0.0001. One-way ANOVA with Bonferroni Multiple Comparison correction. Scale bar = 40µm.

3.4.2 Loss of the LTCC reduces the number of cells in the ISVs

Inhibition of LTCC Ca^{2+} fluxes using either a pharmaceutical or genetic approach, compromised angiogenic sprouting, leading to morphological defects of the ISVs. To further characterize the consequences of LTCC inhibition on angiogenic development, I analysed the number of cells per vessel as described previously.

The *cacna1c*^{ex4sa} morphants and the previously described *cacna1c*^{sa10930} mutant line were used to study the effects of reduced LTCC levels on angiogenesis. I confirmed that at 30 hpf, the vessels were often missing or were very short, and composed by fewer cells in *Tg(fli1a:nlsEGFP)*, with a much stronger phenotype in the morphant than in the

genetic mutant, when compared to control embryos (Fig. 15 A-C). The quantification of cell number per vessel reflected the observed morphology. While in control embryos the average number of cells per ISV in the rostral region was four, in the *cacna1c*^{sa10930} mutant this was reduced to three, and in *cacna1c*^{ex4sa} MO-injected

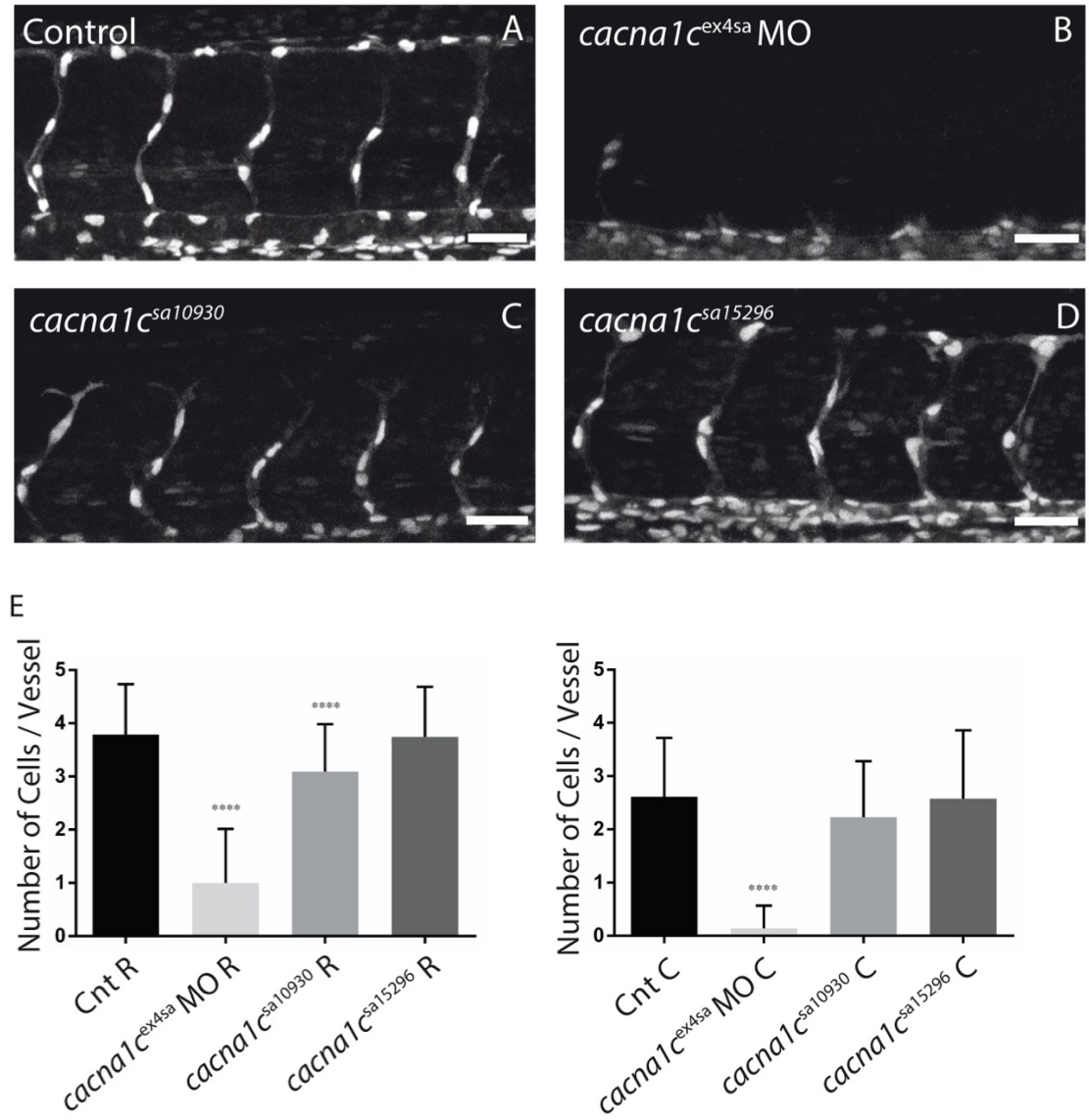

Figure 15: Loss of the LTCC affects the number of ECs in ISVs at 30 hpf. Maximum intensity projection of ISVs from the rostral area in *Tg(fli1a:nlsEGFP)* at 30 hpf. **(A)** ISVs in control embryos with an average of four cells per vessel. **(B)** Missing or severely delayed ISVs in *cacna1c*^{ex4sa}MO-injected embryos. **(C)** ISVs with fewer ECs in the *cacna1c*^{sa10930} mutant line **(D)** Normal looking ISVs with regular number of cells in the *cacna1c*^{sa15296} mutant embryo. **(E)** Quantification of the number of cells per ISV in the rostral (left panel) and caudal (right panel) regions at 30 hpf. Mean ± SD. Rostral region: $n_{(cnt)}$=152; $n_{(cacna1cMO)}$=32; $n_{(canca1csa10930)}$=75; $n_{(canca1csa15296)}$=70; ****P <0.0001. Caudal region: $n_{(cnt)}$=120; $n_{(cacna1cMO)}$=40; $n_{(canca1csa10930)}$=70; $n_{(canca1csa15296)}$=50 ****P <0.0001. One-way ANOVA with Bonferroni Multiple Comparison correction. Scale bar =40µm.

embryos the effect was even more profound with only one cell per ISV (Fig. 15 E, left panel). Similarly to what was observed in the rostral ISVs, analysis in the caudal region revealed a mild reduction in the *cacna1c*^{sa10930} mutant and a strong effect in the morphants, where the sprouting of ISVs was severely abolished (Fig. 15 E, right panel). To further study the role of the LTCC during angiogenic sprouting, the second mutant line *cacna1c*^{sa15296}, missing the C-terminal region of the LTCC, was investigated. I confirmed the previously observed morphology in the *cacna1c*^{sa15296}

EC quantification was repeated at 48 hpf to investigate whether the observed differences in the number of cells forming the ISV, in *cacna1c*-mutant and *cacna1c*^{ex4sa} MO-injected embryos were due to a delay in development.

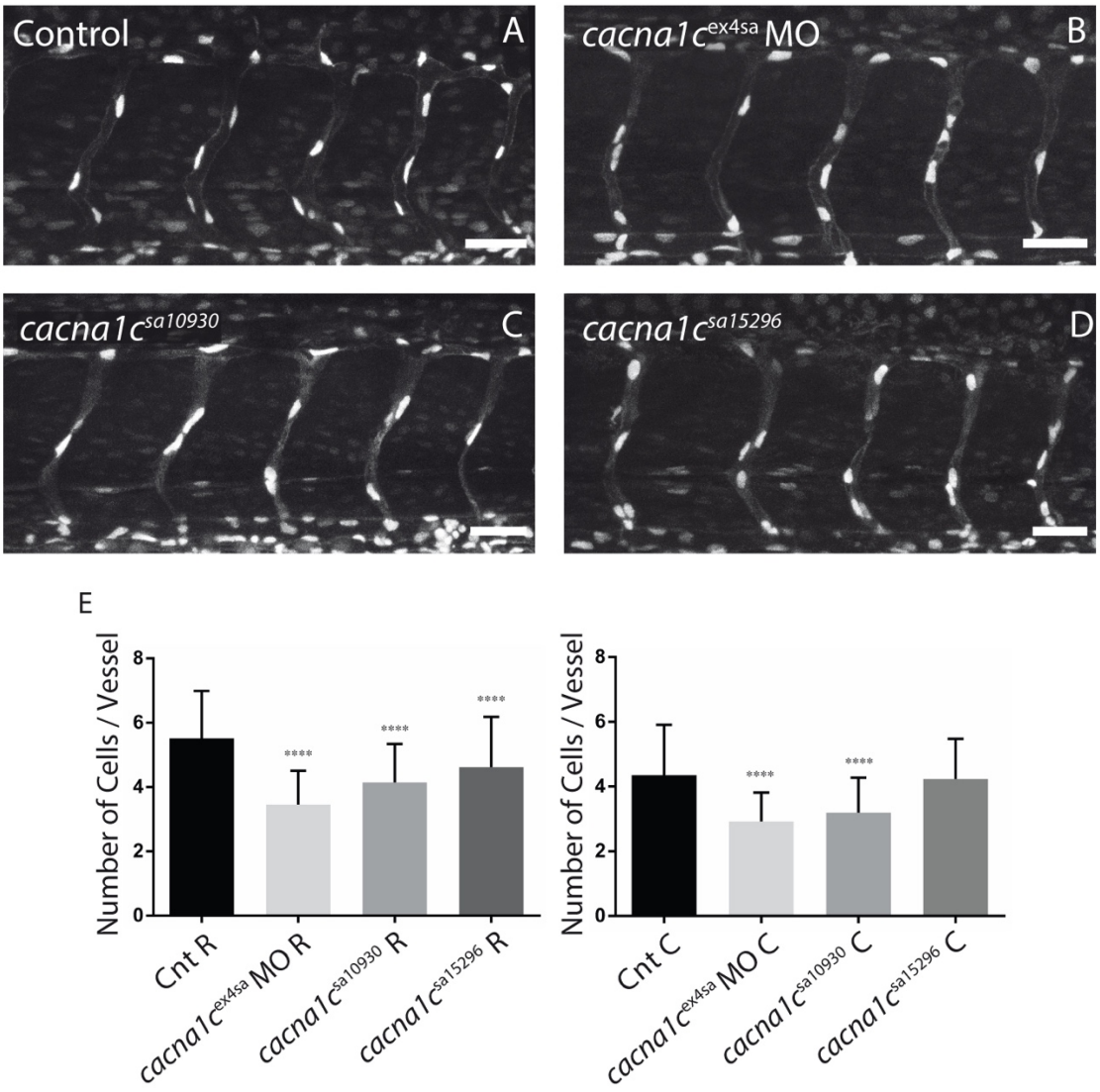

Figure 16: Perturbation of Ca^{2+} fluxes affects the number of ECs in the ISVs at 48 hpf. Maximum intensity projection of ISVs from the rostral area in *Tg(fli1a:nlsEGFP)* at 48 hpf. **(A)** ISVs in control embryos with an average of five cells per vessel. **(B-D)** Fewer cells compose the ISV in *cacna1c*^{ex4sa} MO-injected (B),

cacna1c^{sa10930} (C), and *cacna1c*^{sa15296} mutant lines (D), despite the structure of the ISVs being comparable to control embryos. **(E)** Quantification of the number of cells per ISV in the rostral (left panel) and caudal (right panel) regions at 48 hpf. Mean ± SD. Rostral region: $n_{(cnt)}$=342; $n_{(cacna1cMO)}$=92; $n_{(canca1csa10930)}$=112; $n_{(canca1csa15296)}$=92; ****P <0.0001. Caudal region: $n_{(cnt}$ =180; $n_{(cacna1cMO)}$=50; $n_{(canca1csa10930)}$=80; $n_{(canca1csa15296)}$=50 ****P <0.0001. One-way ANOVA with Bonferroni Multiple Comparison correction. Scale bar = 40µm.

Although the structure of the ISVs was comparable to the control embryos (Fig. 16 A-D), the decrease of Ca^{2+} fluxes through the LTCC in either *cacna1c*-mutants or morphants, led to an effect on the number of cells composing the vessels (Fig. 16 E). While in control embryos the average number of cells per ISV is five, in *cacna1c* morphants and mutants I observed a significant reduction of one or two cells per vessel, in both rostral and caudal regions (Fig. 16 E).

3.5 Alteration of LTCC conductance perturbs endothelial cell migration

Stimulation of Ca^{2+} fluxes though the LTCC via Bay K treatment, increased angiogenic cell behaviour, leading to an over-branching phenotype and an increase in the number of ECs forming the ISV. On the contrary, inhibition of LTCC conductance by MO treatment or in *cacna1c* mutant lines, results in a delayed phenotype with morphological vascular impairment and fewer ECs forming the vessels.

To elucidate whether the differences in the number of ECs per vessel were due to changes in ECs proliferation or migration, I performed long-term time-lapse imaging of the growing ISVs for 18 hours, from 28 hpf covering the angiogenic events in more caudal region of the embryo. Using this data, I defined the proliferative events: proliferation of tip or stalk EC, and migratory events: migration of cells from the DA to form the sprouting ISV (Fig. 17 A), and quantified the number of events per vessel (Fig. 17 B).

Interestingly, the stimulation of the LTCC Ca^{2+} fluxes by Bay K treatment strongly increased EC migration from the DA, without affecting tip or stalk cell proliferation (Fig. 17 B). Conversely, downregulation of the LTCC via *cacna1c*^{ex4sa} MO injection reduced the proliferation of tip and stalk cells, whereas EC migration was unchanged compared to control embryos. On the other hand, LTCC loss of function in the *cacna1c*^{sa10930}

A

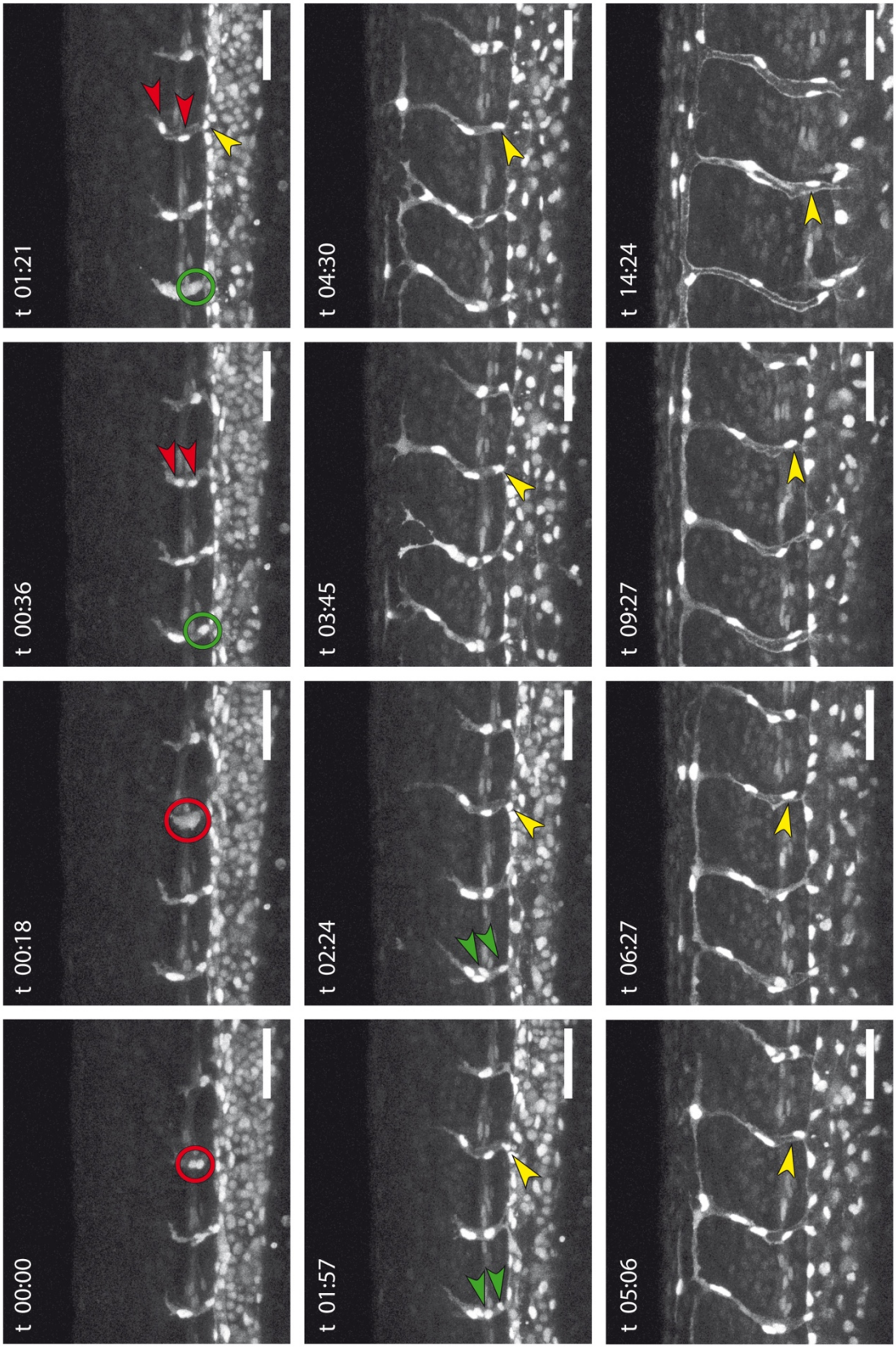
t 00:00
t 00:18
t 00:36
t 01:21
t 01:57
t 02:24
t 03:45
t 04:30
t 05:06
t 06:27
t 09:27
t 14:24

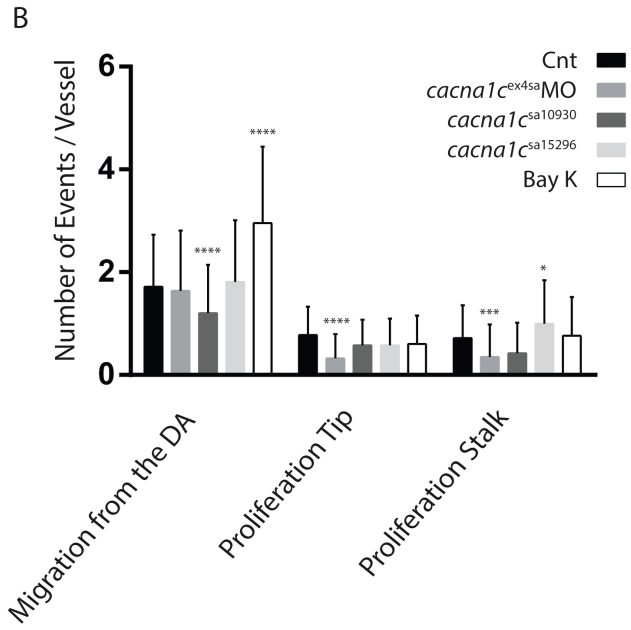

Figure 17: Increase of Ca^{2+} fluxes through the LTCC results in a higher rate of cell migration from the DA. (A) Long-term time-lapse *in vivo* imaging in a *Tg(fli1a:nlsEGFP)* control embryo acquired from 28 hpf onwards. A migratory event from the DA is highlighted (yellow arrow heads), tip and stalk cells (red and green circle, respectively) and their proliferation events (red and green arrow heads) are indicated. t = time in hours. **(B)** Quantification of migratory and proliferative (tip or stalk) events per vessel observed during 18 hours of development in long-term time-lapse imaging, in control, *cacna1c*^{ex4sa} MO-injected, *cacna1c*^{sa10930}, *cacna1c*^{sa15296} mutant lines, and Bay K-treated embryos. Mean ± SD. $n_{(cnt)}$=168; $n_{(cacna1cMO)}$=129; $n_{(canca1csa10930)}$=59, proliferation stalk ***P =0,0003; $n_{(canca1csa15296)}$=88, proliferation stalk *P =0.0293; $n_{(Bay\ K)}$=94; ****P <0.0001. Two-way ANOVA with Bonferroni Multiple Comparison correction. Scale bar =50µm.

mutants only mildly affected EC proliferation, while significantly decreased the migratory events (Fig. 17 B). In accordance with the previous morphological analysis, the perturbation of LTCC conductance in the cacna1c^{sa15296} mutant line did not alter EC migration, but mildly increased cell proliferation as stalk but not tip cells proliferated more (Fig. 17 B), suggesting a possible compensatory mechanism.

3.6 Directionality of cell migration in the absence of the LTCC

During angiogenic ISV formation, upon VEGF stimulation, ECs from the DA actively migrate out to start the sprout of the new vessel (Isogai et al. 2003; Gerhardt et al. 2003; Siekmann & Lawson 2007). Analysis of our time-lapse imaging data revealed that some ECs forming the ISV, regress and migrate back, leave the ISV and instead

A

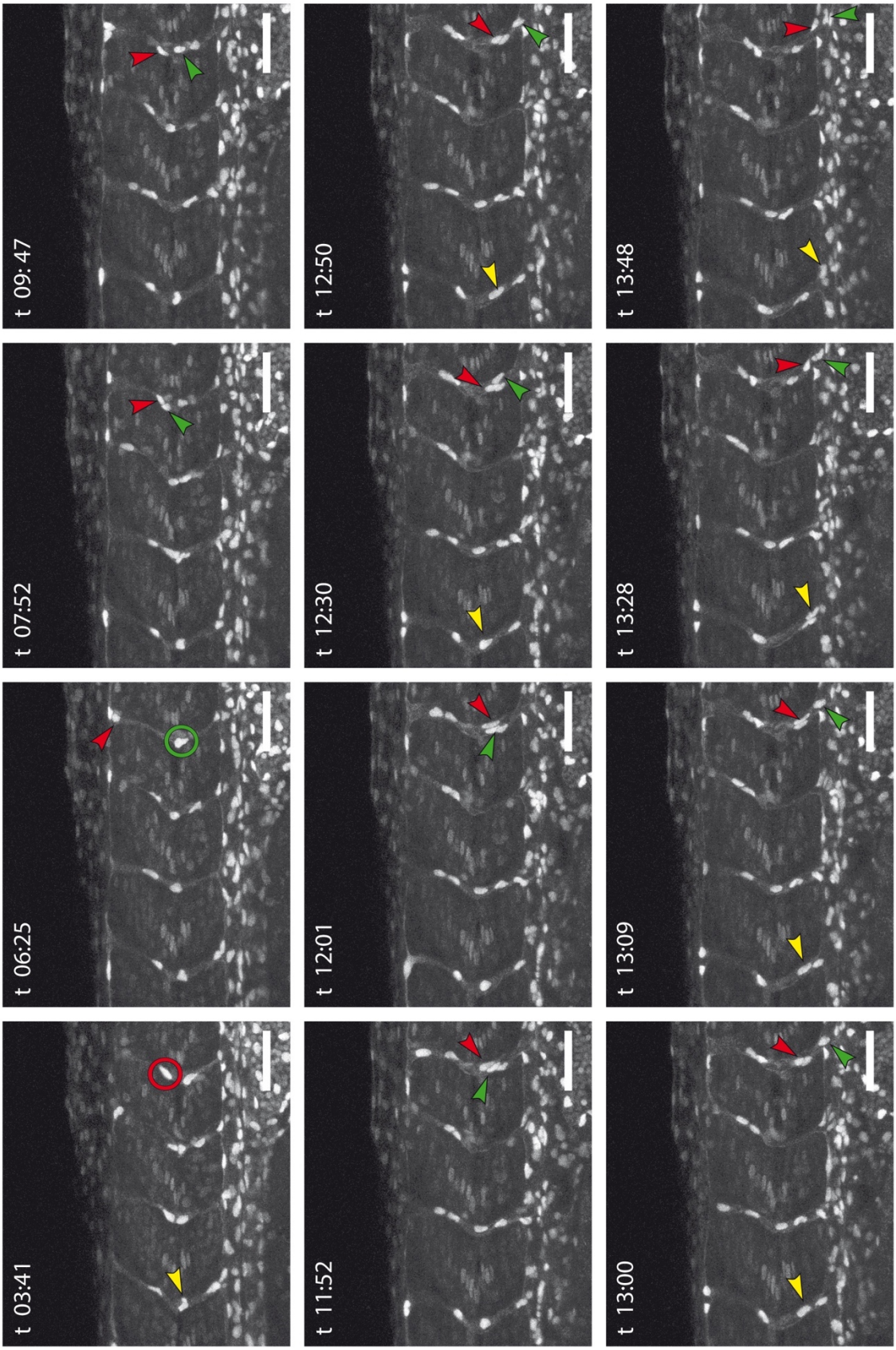
t 09: 47
t 12:50
t 13:48
t 07:52
t 12:30
t 13:28
t 06:25
t 12:01
t 13:09
t 03:41
t 11:52
t 13:00

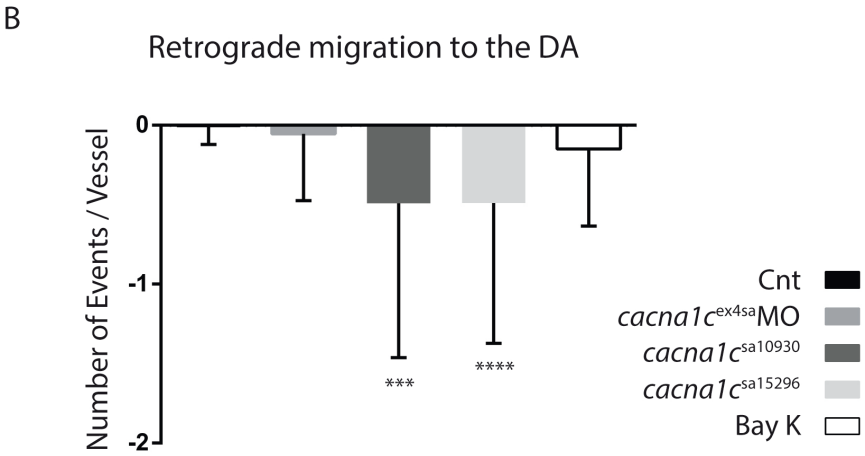

Figure 18: Loss of the LTCC induces retrograde migration from the ISV to the DA. (A) Long-term time-lapse *in vivo* imaging in a *Tg(fli1a:nlsEGFP) cacna1c*^{sa10930} mutant embryo acquired from 28 hpf onwards. The retrograde migration of cells that originated from a tip proliferation (red circle and arrows), a stalk proliferation (green circle and arrows) and a migratory event (yellow arrow) are highlighted. **(B)** Quantification of the retrograde migration events per vessel observed during 18 hours of development in long-term time-lapse imaging, in control, *cacna1c*^{ex4sa} MO-injected, *cacna1c*^{sa10930}, *cacna1c*^{sa15296} mutant lines and Bay K-treated embryos. Mean ± SD. $n_{(cnt)}$=168; $n_{(cacna1cMO)}$=129; $n_{(canca1csa10930)}$=59, ***P =0,0002; $n_{(canca1csa15296)}$=88, ****P <0.0001; $n_{(Bay\ K)}$=94. Two-way ANOVA with Bonferroni Multiple Comparison correction. Scale bar = 50µm.

contribute to the DA structure (Fig. 18 A), a process characteristic during pruning of the vessels (Chen et al. 2012; Franco et al. 2015). To better investigate the effects of the perturbation of LTCC conductance, the number of regressing cells was compared between different conditions. Markedly, upon LTCC downregulation, in both *cacna1c* mutant lines but not in the *cacna1c*^{ex4sa} MO-injected embryos, I observed enhanced retrograde cell migration from the ISVs back to the DA (Fig. 18 B). This observation can explain the fewer number of ECs in the ISVs of the *cacna1c*^{sa15296} mutant line observed at 48 hpf; a phenotype which was otherwise in disagreement with the migratory and proliferative events in the ISVs (Fig. 17 B). Interestingly, stimulation of the LTCC by Bay K treatment did not affect the retrograde migration**,** it was a rare event, but happened to the same extent as in untreated embryos (Fig. 18 B).

3.7 The effects of blood circulation on the development of ISVs

Numerous *in vitro* studies have demonstrated that vascular ECs are capable of sensing biomechanical stimuli, such as the shear stress due to blood flow (Hierck et al. 2008; Nauli et al. 2008). Between 22 and 24 hpf the zebrafish heart starts to pump and blood

circulation is observed in the dorsal artery and the posterior cardinal vein, resulting in production of haemodynamic forces that can influence the development of the ISVs. However, zebrafish embryos are able to survive for about seven days in the absence of blood circulation (Betz et al. 2016), providing the possibility to study the effects of haemodynamic forces and blood pressure on angiogenic development.
The stimulation as well as the inhibition of LTCC conductance using both pharmacological and genetic approaches, resulted in compromised heart function due to the disruption of the excitation-contraction coupling in cardiomyocytes, leading to the absence of blood flow during the development of ISVs. This prompted us to assess the role of haemodynamic forces on EC migration.

3.7.1 The blood flow is important for angiogenic sprouting

To understand the contribution of haemodynamic forces, ISV development was studied in the absence of blood flow. This was achieved by injection of a morpholino against the cardiac troponin T2 (*tnnt2* ^{ATG} MO) (Sehnert et al. 2002). The *tnnt2* ^{ATG} MO injection prevents cardiac contraction, and hence the formation of blood circulation. To analyse the ISVs, the previously described reporter lines *Tg(kdrl:EGFP)* and *Tg(fli1a:nlsEGFP)* were used. At 30 hpf, the morphological structure of the ISVs in *tnnt2* ^{ATG} MO-injected embryos was comparable to control (Fig. 19 A, B). As previously reported, (Schuermann et al. 2014) the first ISV sprout was independent of blood flow. However, the quantification of the number of cells per vessel revealed that fewer cells formed the vessel in *tnnt2* ^{ATG} morphants embryos compared to uninjected control (Fig. 19 C, D). This observed decrease was slight, yet significant (Fig. 19 E).
To better understand whether in the absence of blood circulation the mild alteration of ECs composing the ISVs, was due to a slight delay in development, EC quantification was repeated at 48 hpf. The analysis revealed that, although the ISVs' structure was not affected (Fig. 20 A, B), the number of ECs per vessel was still perturbed in the absence of blood flow (Fig. 20 C).

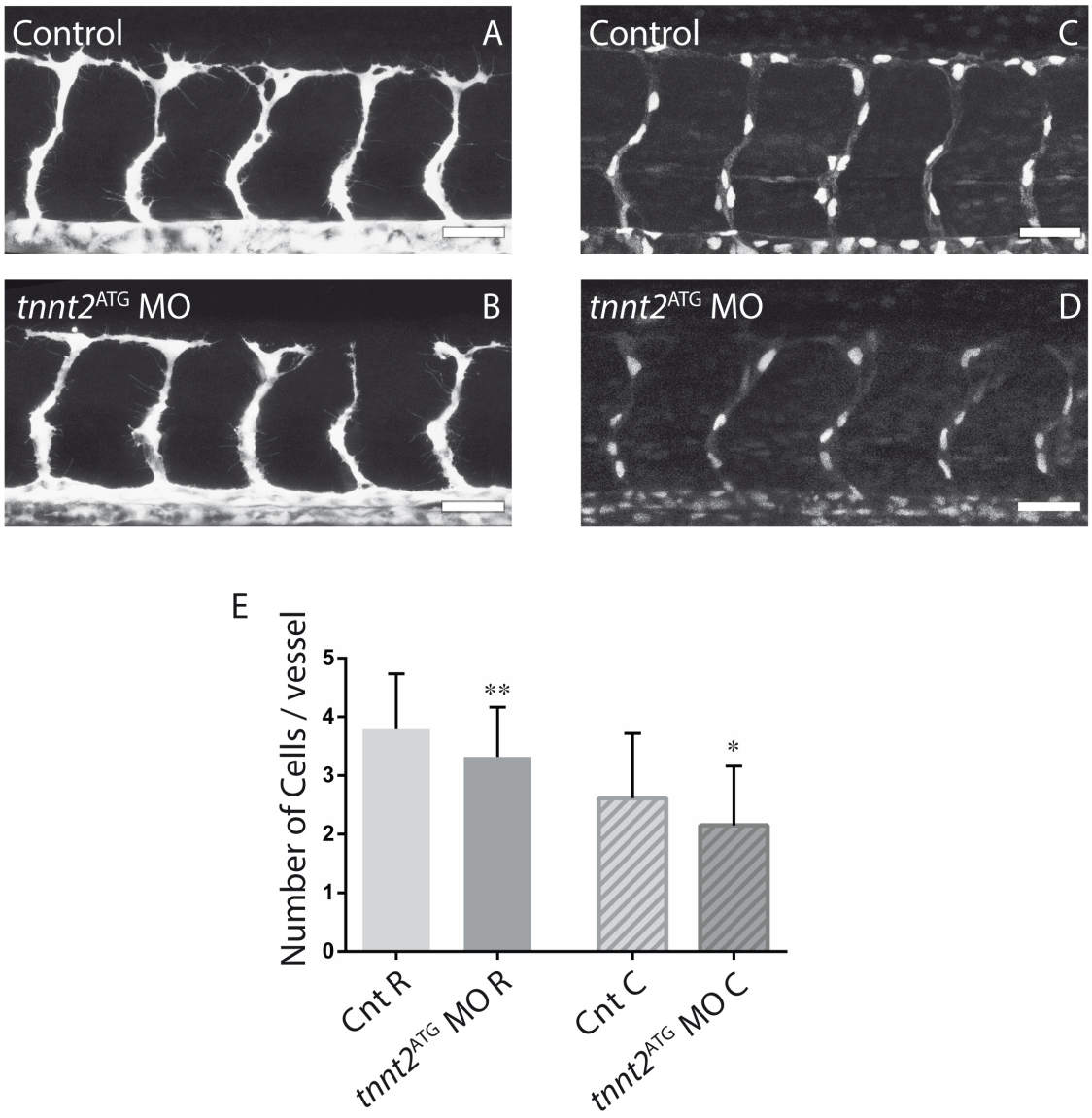

Figure 19: Lack of blood flow interferes with the number of cells in ISVs at 30 hpf. (A, B) ISVs from the rostral region, maximum intensity projections, in *Tg(kdrl:EGFP)* at 30 hpf in uninjected control (A) and *tnnt2*^{ATG} MO-injected embryos (B). **(C, D)** Maximum intensity projections of ISVs from the rostral region in *Tg(fli1a:nlsEGFP)* at 30 hpf in uninjected control (C), and *tnnt2*^{ATG} MO-injected embryos (D). **(E)** Quantification of the decreased number of cells per ISV in the rostral and caudal regions at 30 hpf. Mean ± SD. Rostral region: $n_{(cnt)}$=152; $n_{(tnnt2MO)}$=110, ***P* =0,0011. Caudal region $n_{(cnt)}$=120; $n_{(tnnt2MO)}$=100, ***P* =0,0383. One-way ANOVA with Bonferroni Multiple Comparison correction. Scale bar = 40µm.

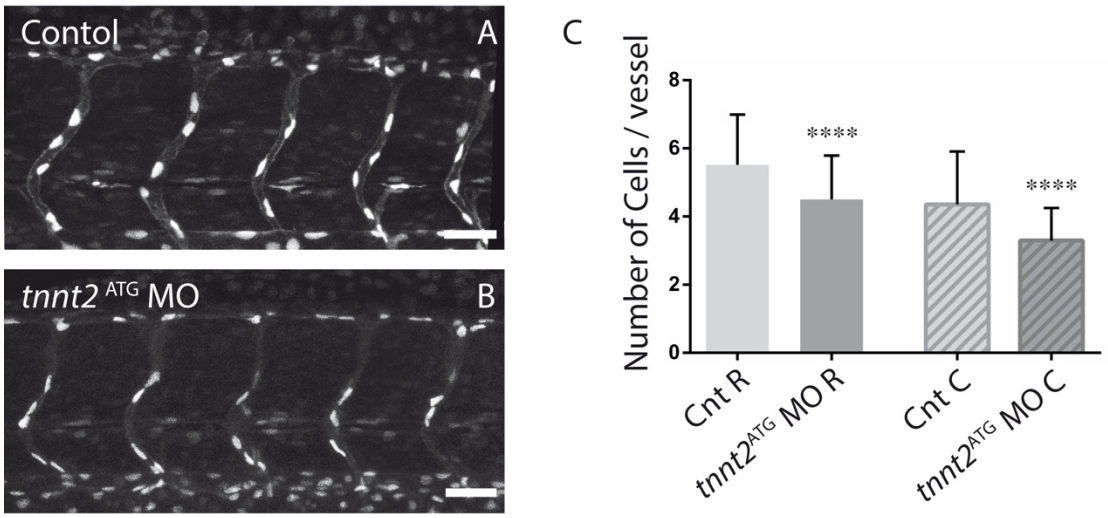

Figure 20: Lack of blood circulation interferes with the number of cells in ISVs at 48 hpf. (A, B) ISVs from the rostral region in *Tg(kdrl:EGFP)* at 48 hpf in uninjected control (A) and *tnnt2*^{ATG} MO-injected embryos (B). **(C)** Quantification of the decreased number of cells per vessel in *tnnt2*^{ATG} MO-injected embryos compared to uninjected control (Cnt) in both rostral and caudal regions. Mean ± SD. Rostral region: $n_{(cnt)}$=342; $n_{(tnnt2MO)}$=90. Caudal region: $n_{(cnt)}$ =180; $n_{(tnnt2MO)}$=50. ****P <0.0001. One-way ANOVA with Bonferroni Multiple Comparison correction. Scale bar = 40µm.

3.7.2 Absence of flow increases the retrograde endothelial cell migration

As previously reported, I confirmed that the first angiogenic process is not dependent on the presence of haemodynamic forces (Schuermann et al. 2014). Although, in absence of blood flow, the ISV structure was regularly formed, detailed observation revealed a mild decrease in the number of endothelial cells composing the ISVs at 30 and 48 hpf.
To assess the effects of lack of blood flow and clarify whether the differences in the number of cells per vessel is due to changes in EC proliferation or migration, long-term time-lapse imaging was performed on the growing vessels, as previously described (see chapter 3.5; Fig. 21 A). The number of migratory and proliferative events per vessel was quantified (Fig. 21 B). The absence of blood flow significantly increased retrograde migration from the ISV and slightly reduced the migration of ECs from the DA as well as the endothelial tip cell proliferation. This indicates that the reduction of ECs per vessel, in the absence of blood flow observed at 30 hpf, is mainly due to the strong increase of retrograde migration events.

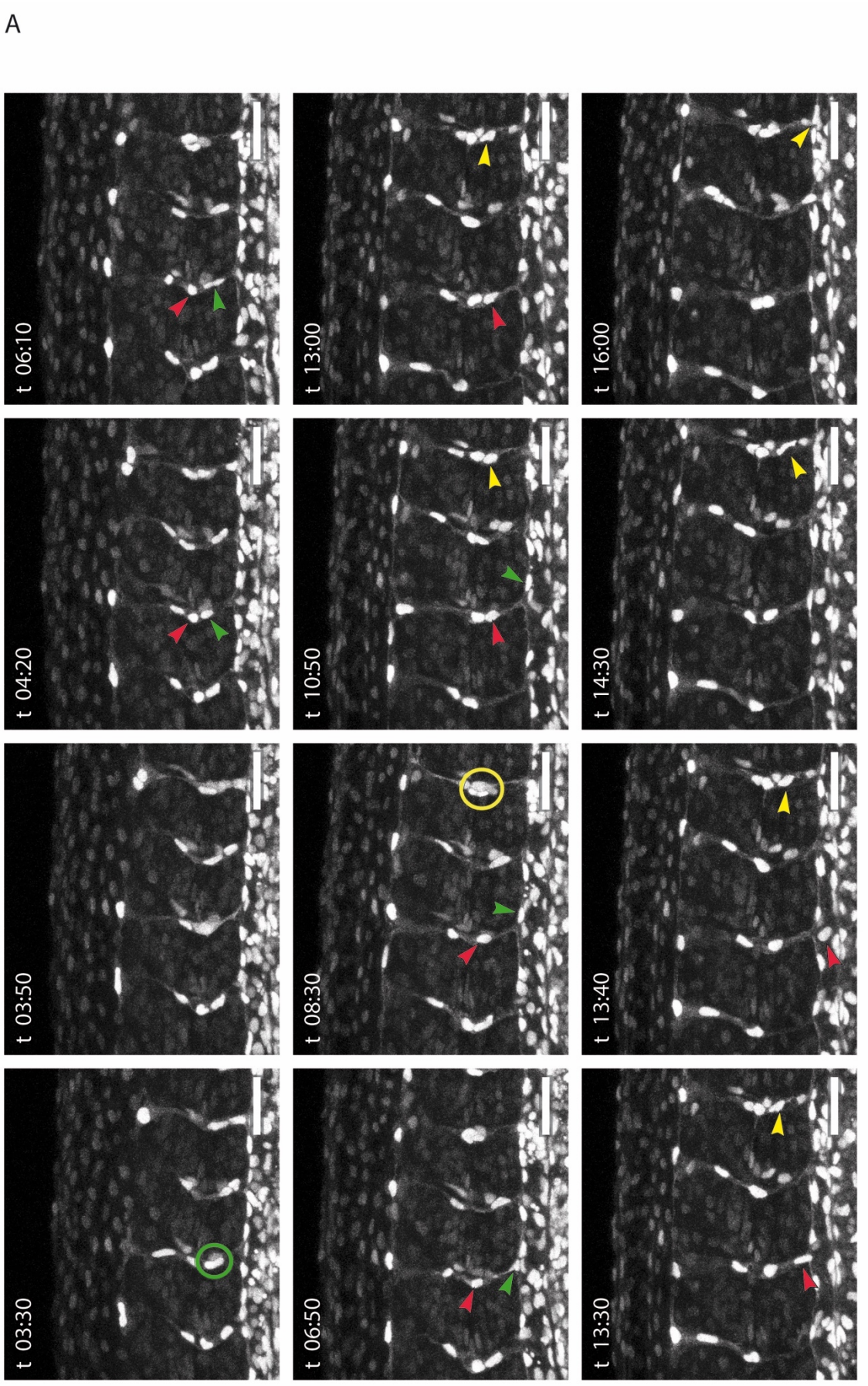
A
t 06:10
t 13:00
t 16:00
t 04:20
t 10:50
t 14:30
t 03:50
t 08:30
t 13:40
t 03:30
t 06:50
t 13:30

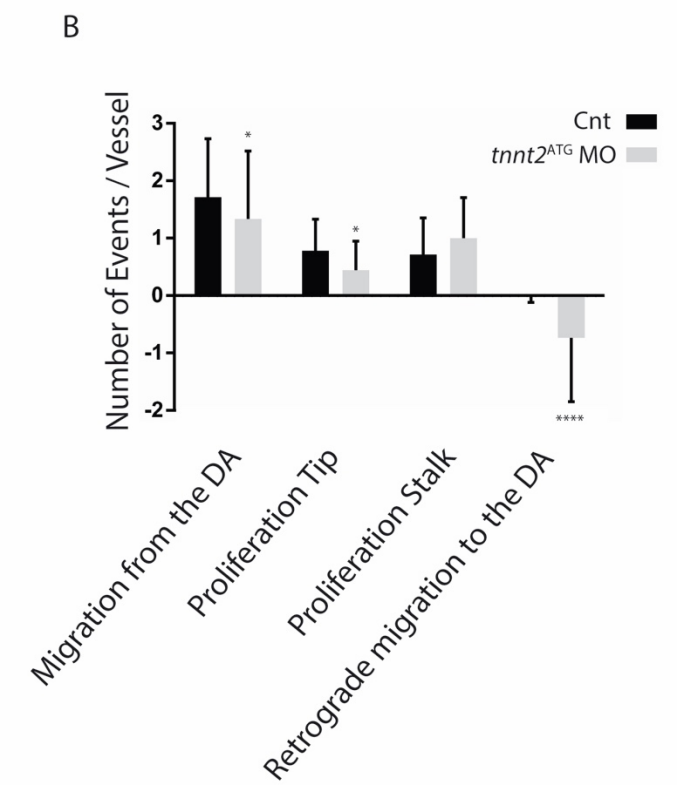

Figure 21: The absence of blood flow interferes with EC migration. **(A)** Long-term time-lapse *in vivo* imaging in a *Tg(fli1a:nlsEGFP), tnnt2*^{ATG} MO- injected embryo acquired from 28 hpf onwards. The retrograde migration of three different cells (green, yellow, and red arrows), originated from a stalk proliferation (red and yellow circle), are highlighted. Scale bar 40 µm. **(B)** Quantification of migratory, proliferative (tip or stalk), and retrograde migratory events per vessel observed during 18 hours of development in long-term time-lapse images from 28 hpf, in uninjected control and *tnnt2*^{ATG} MO-injected embryos. Mean ± SD. $n_{(cnt)}$=168; $n_{(tnnt2MO)}$=45, migration from the DA *P =0.0170, proliferation tip *P =0.0470. Two-way ANOVA with Bonferroni Multiple Comparison correction.

3.8 Loss of *wnt11*: an indirect way to stimulate the L-Type Ca^{2+} channel

Panáková et al., showed that the Wnt11 pathway reduces transmembrane Ca^{2+} influx attenuating the LTCC conductance in cardiomyocytes (Panakova et al. 2010).
Considering this data, downregulation of *wnt11* was used to indirectly stimulate LTCC conductance to assess whether the effect of Wnt11 signalling on the LTCC, previously shown in cardiomyocytes, occurs in ECs as well.

3.8.1 Loss of Wnt11 signalling affects ISV morphogenesis

Knowing that the Wnt11 pathway reduces the transmembrane Ca^{2+} influx, and thus attenuates LTCC conductance in cardiomyocytes (Panakova et al. 2010), the previously validated morpholino (Matsui et al. 2005; Merks et al. 2018) was used to reduce the Wnt11 levels and indirectly stimulate LTCC conductance in the described reporter line *Tg(kdrl:EGFP)*. As expected, downregulation of Wnt11 resulted in whole body morphological defects. In *wnt11*^{ATG} MO-injected embryos, the embryonic extension length was decreased, the brain was smaller and the embryos presented a cyclopia phenotype (data not shown), typical of Wnt signalling downregulation (Waxman et al. 2004; Yao et al. 2008). Moreover, I observed that loss of *wnt11* resulted in strong morphological vascular defects in comparison to uninjected control embryos at 48 hpf.

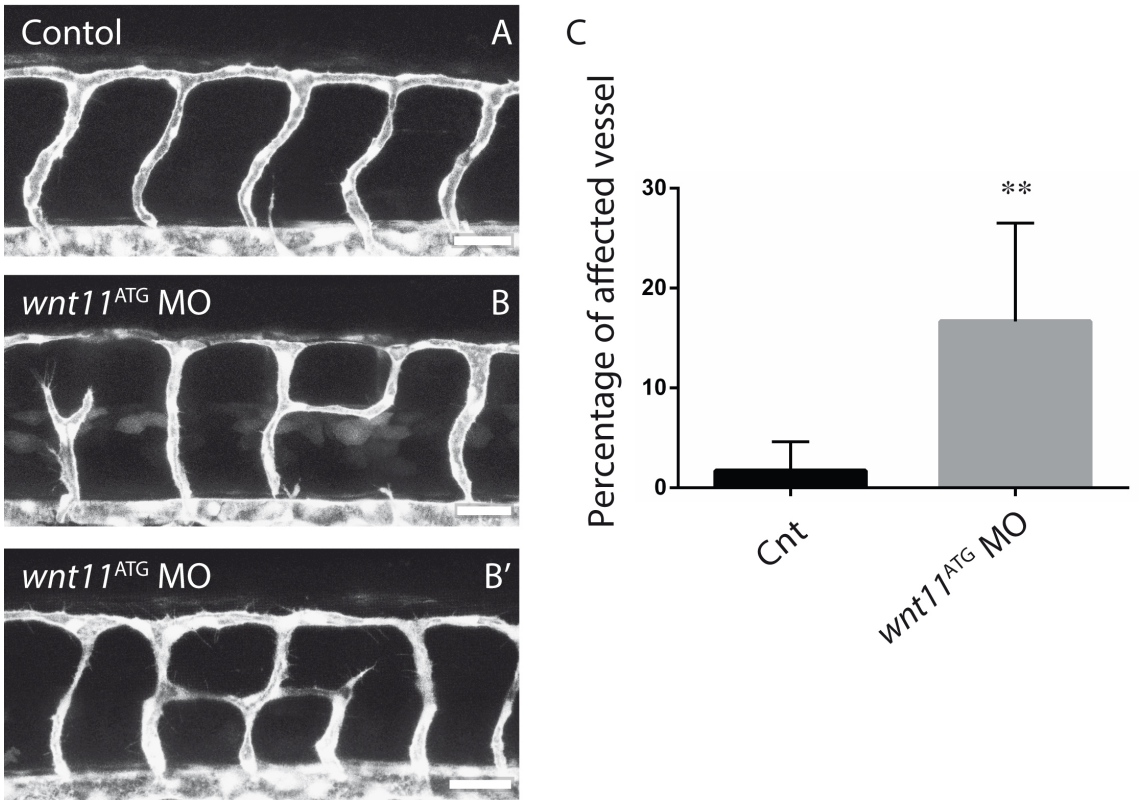

Figure 22: Loss of *wnt11* results in morphological ISV defects. **(A)** ISV morphological structure at 48 hpf in control *Tg(kdrl:EGFP)* zebrafish embryos. **(B-B')** ISVs morphological defects with disconnections to the DLAV, ectopic branches and loop connections in *wnt11*^{ATG} MO-injected embryos at 48 hpf. **(C)** Quantification in percentage of the affected ISV per embryo in uninjected control (cnt) and *wnt11*^{ATG}-MO injected embryos (C). Mean ± SD. n =6 for both groups ***P* =0.0051. Unpaired t-test. Scale bar = 40µm.

The ISVs presented ectopic branches and loop connections, as well as disconnections to the DA or to the DLAV (Fig. 22 A, B'). Quantification of ISV morphological defects showed a 15% increase of affected vessels per embryo in the *wnt11*^{ATG} MO-injected embryos compared to uninjected control (Fig. 22 C).

To better characterize the *wnt11*^{ATG} MO phenotype, the number of ECs composing the ISV structure at 48 hpf was quantified. I confirmed the morphological defects in the structure of the ISVs upon downregulating Wnt signalling at 48 hpf (Fig. 23 A, B), and observed a reduction of ECs per vessel localized in the rostral region (Fig. 23 C). Although the loss of *wnt11* clearly impacted the ISV formation, the result was dissimilar to what was predicted from the observed effects in the cardiomyocytes, and thus using such indirect way to stimulate the LTCC is rather inconclusive.

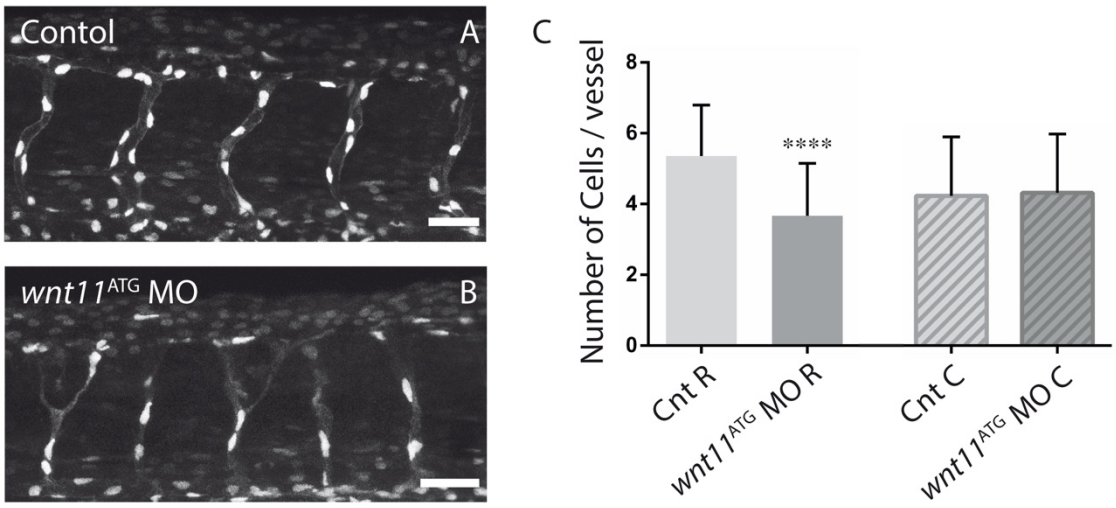

Figure 23: *wnt11* downregulation partially affects the number of cells in ISVs. **(A, B)** ISVs from the rostral region in *Tg(fli1a:nlsEGFP)* at 48 hpf in uninjected control (A) and *wnt11*^{ATG} MO-injected embryos (B). **(C)** Quantification of the number of cells per vessel in *wnt11*^{ATG} MO-injected embryos compared to uninjected control (Cnt) in both rostral and caudal regions. Mean ± SD. $n_{(cnt)}$=60; $n_{(wnt11ATG\ MO)}$=104 ****P <0.0001. Unpaired t-test. Scale bar = 40µm.

3.9 Interactions between the LTCC and TRPC1 during ISV development

Recent studies have shown that ECs express a large variety of membrane ion channels, in order to accomplish different functional roles, not only in the ECs themselves, but also

in the adjacent smooth muscle cells. An important contribution to Ca^{2+} regulation in ECs is given by the transient receptor potential (TRP) superfamily channels (Dietrich et al. 2014). All of the channels from the TRPC (for classical or canonical) subfamily, are non-selective cation channels and act as cellular mechanosensors and effectors (Nilius & Droogmans 2001). Moreover, all members have been reported to be expressed in ECs and smooth muscle cells. The TRPC1 was the first channel to be identified in mammalians and is the founding member of the subfamily, however, despite extensive research, its function as a cation channel in a physiological setting is still obscure (Beech 2013).

3.9.1 Loss of TRPC affects the number of cells in the ISV

Yu and collaborators studied the effects of *trpc1* downregulation on angiogenesis and ISV sprouting (Yu et al. 2010). Based on their observations, in the absence of TRPC1, the vessels are shorter and angiogenesis is compromised at 30 hpf, a phenotype similar to the one observed by me in the *cacna1c* mutants and *cacna1c*^{ex4sa} MO-injected embryos. This consideration prompted me to better investigate the TRPC1 during angiogenesis and the potential genetic interaction between *trpc1* and *cacna1c*.

To explore the effect of TRPC downregulation on angiogenesis during ISV development, the morpholino against *trpc1* was injected *in Tg(fli1a:nlsEGFP)* zebrafish embryos and the number of cells was counted at 30 hpf as described before (see chapter 3.4).

The inhibition of Ca^{2+} fluxes though the TRPC1 via *trpc1*^{ATG} MO injection perturbed the angiogenic sprouting, the resulting ISVs were shorter with fewer ECs compared to uninjected control embryos (Fig. 24 A, B). While in control embryos the average number of cells per vessel was four, the *trpc1* morphants revealed a significant reduction to one or two cells per vessel, in both rostral and caudal regions (Fig. 24 B, C). Beyond the defects observed in ISV outgrowth, the embryos developed normally, with a regular heart beat and blood circulation (data not shown).

To better characterize the phenotype and to understand if the differences observed in the number of cells per vessel, after inhibiting the Ca^{2+} fluxes through TRPC1, was the consequence of a developmental delay in ISV formation, EC quantification was repeated at 48 hpf. Upon loss of TRPC1, the structure of the ISVs was maintained (Fig. 25 A, B), however, fewer ECs were assembling the vessel even at 48 hpf (Fig. 25 C).

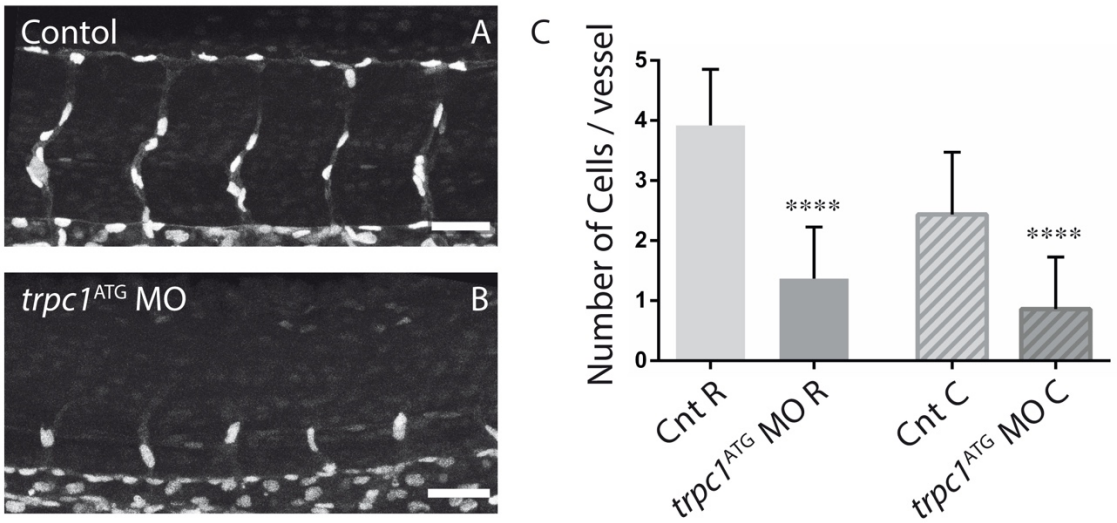

Figure 24: Loss of *trpc1* affects the number of cells per vessel at 30 hpf. (A, B) Maximum intensity projection of ISVs from the rostral region in *Tg(fli1a:nlsEGFP)* at 30 hpf in uninjected control (A) and *trpc1*^{ATG} MO-injected embryos (B). **(C)** Quantification of the number of cells per vessel in *trpc1*^{ATG} MO-injected embryos compared to uninjected control (Cnt) in both rostral and caudal regions. Mean ± SD. Rostral region $n_{(cnt)}$=152; $n_{(trpc1ATG\ MO)}$=45. Caudal region $n_{(cnt)}$=120; $n_{(trpc1ATG\ MO)}$=40; ****P <0.0001. One-way ANOVA with Bonferroni Multiple Comparison correction. Scale bar = 40µm.

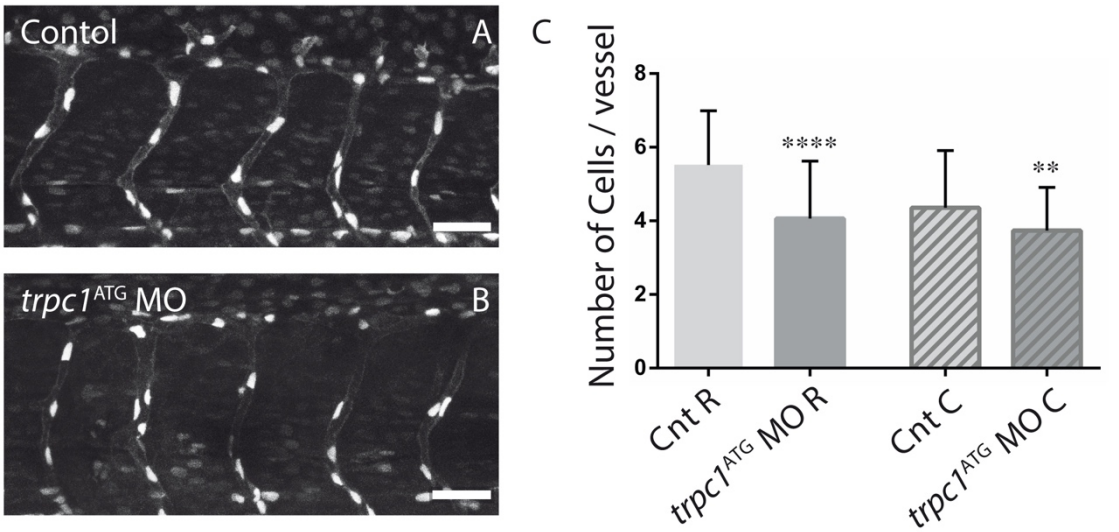

Figure 25: Downregulation of *trpc1* affects the number of ECs per vessel at 48 hpf. (A, B) Maximum intensity projections of ISVs from the rostral region in *Tg(fli1a:nlsEGFP)* at 48 hpf in uninjected control (A) and regularly formed ISVs in *trpc1*^{ATG} MO-injected embryos (B). **(C)** Quantification of the decreased number of cells per vessels in *trpc1*^{ATG} MO-injected embryos compared to uninjected control (Cnt) in both rostral and caudal regions. Mean ± SD. Rostral region $n_{(cnt)}$ =342; $n_{(trpc1ATG\ MO)}$ =97; ****P <0.0001. Caudal region $n_{(cnt)}$ =180; $n_{(trpc1ATG\ MO)}$ =60; **P =0.0062. One-way ANOVA with Bonferroni Multiple Comparison correction. Scale bar = 40µm.

3.9.2 Loss of TRPC1 affects endothelial cell migration and proliferation in ISVs

The inhibition of ion fluxes through the TRPC1 channel compromised the development of ISVs during angiogenesis. The vessels appear shorter and formed by fewer ECs compared to uninjected control embryos. To understand whether the differences in the number of ECs is due to changes in proliferation or migration, I performed long term time-lapse imaging to observe ISV outgrowth and measure the number of proliferative and migratory events per vessel as described before (see chapter 3.5). The reduction of TRPC1 activity in *trpc1*^{ATG} MO-injected embryos strongly decreased the number of migration events from the DA as well as EC proliferation of both tip and stalk cells (Fig. 26). The loss of *trpc1* did not affect heart function and the circulation was still present. In agreement with my previous observations, retrograde migration from the ISVs to the DA was not affected in *trpc1* morphants (Fig. 26).

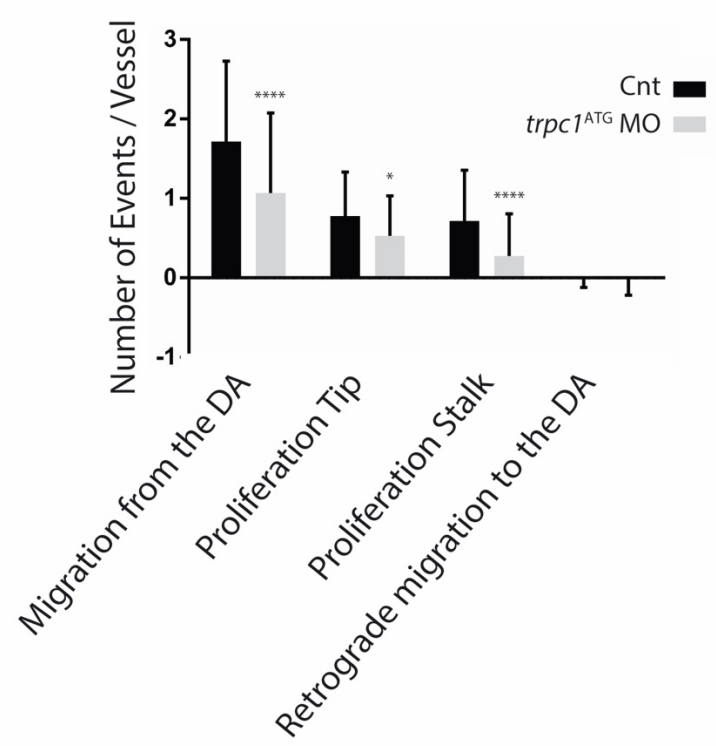

Figure 26: The loss of *trpc1* affects EC migration and proliferation. Quantification of migratory, proliferative (tip or stalk), and retrograde migratory events per vessel observed during 18 hours of development in long-term time-lapse imaging, in uninjected control (Cnt) and *trpc1*^{ATG} MO-injected embryos. Mean ± SD. $n_{(cnt)}$=168; $n_{(trpc1ATG\text{-}MO)}$=102, proliferation tip *P =0.0475; ****P <0.0001. Two-way ANOVA with Bonferroni Multiple Comparison correction.

3.9.3 The LTCC and TRPC1 interact during angiogenic sprouting

The loss of Ca^{2+} fluxes through the LTCC as well as TRPC1 channels affected the migratory and proliferative behaviour of ECs during angiogenesis, decreasing the number of cells forming the ISVs at 30 and 48 hpf.

To investigate to what extent LTCC and TRPC1 might interact to modulate the angiogenic behaviour of ECs, subthreshold levels of *trpc1*^{ATG} and *cacna1c*^{ex4sa} MOs were co-injected in *Tg(fli1a:nlsEGFP)* embryos, in order to question an epistatic relation by reducing to a lesser extent both channels. The single injection at a subthreshold concentration for each of the two MOs, had a mild or no effect on the architecture and number of cells composing the ISVs (Fig 27 A-C). However, the concomitant loss of both channels by co-injection of both MOs at subthreshold concentrations, had a significantly stronger effect on the development of the ISVs and the number of their cells (Fig. 27 D), indicating a genetic interaction and synergy between these two channels.

On average ISVs in the rostral region of uninjected embryos are formed by four cells. Single injection at subthreshold concentration mildly reduced the average number of cells per vessel to three, however co-injection at subthreshold concentration of both *trpc1*^{ATG} and *cacna1c*^{ex4sa} MOs, strongly decreased the ECs to one or none per vessel (Fig. 27 E). These data also suggest that Ca^{2+} fluxes across the plasma membrane might, in general, modulate the angiogenic behaviour of the ECs, which might be in part regulated by haemodynamic forces.

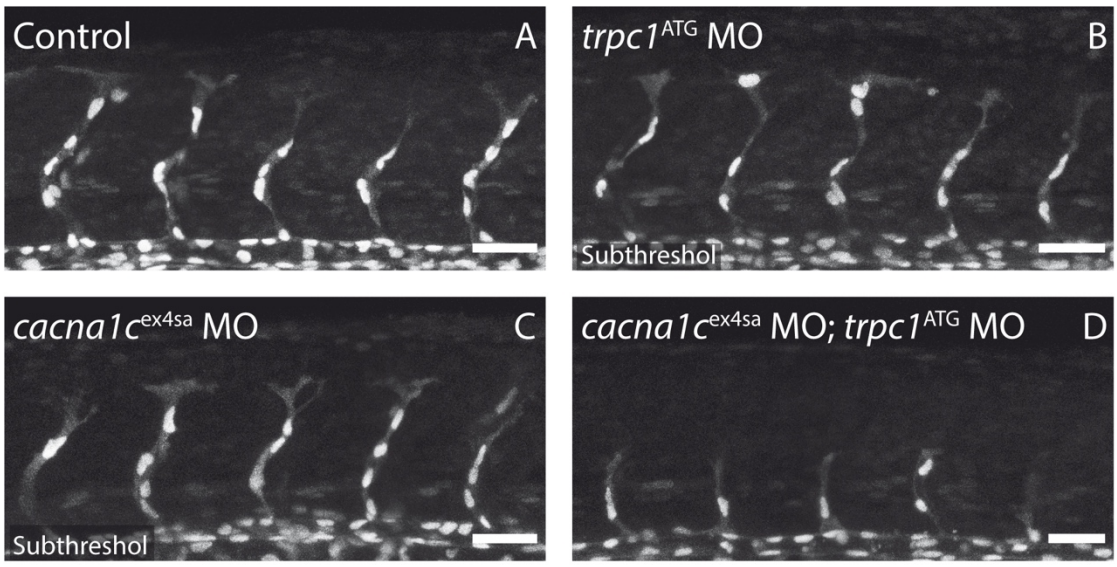

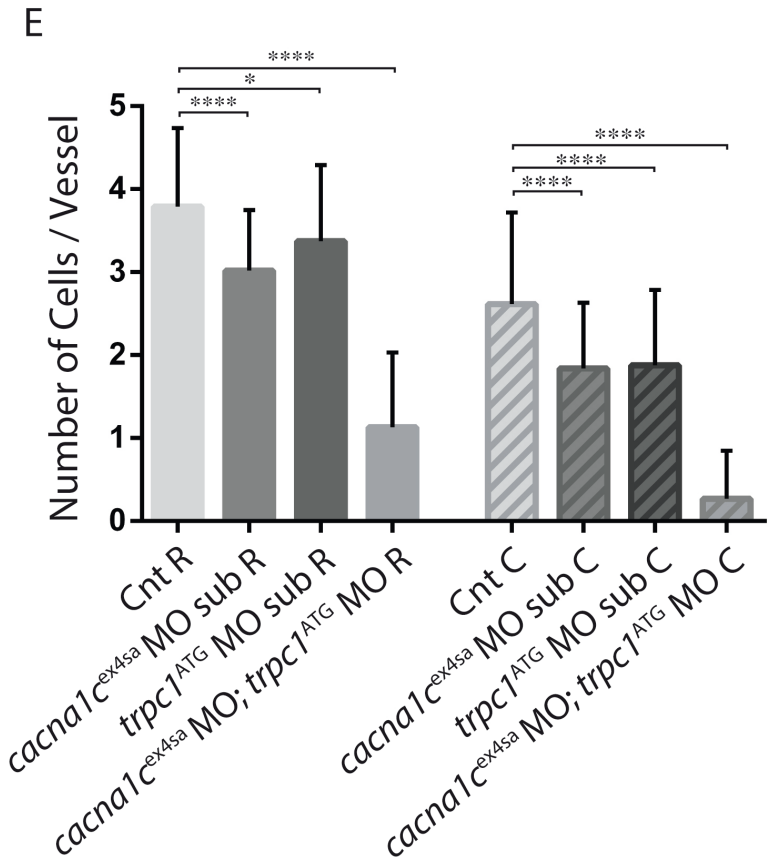

Figure 27: Synergistic effect of TRPC1 and LTCC. (A-D) Maximum intensity projections of ISVs from the rostral region in *Tg(fli1a:nlsEGFP)* at 30 hpf in uninjected control (A), *trpc1*^{ATG} MO-injected at subthreshold concentration (1,6 ng) (B) or *cacna1c*^{ex4sa} MO-injected at subthreshold concentration (1,68 ng) (C), and of both MOs co-injected at subthreshold concentrations (D). **(E)** Quantification of the number of cells in the ISVs at 30 hpf in embryos injected with subthreshold concentrations of *cacna1c*^{ex4sa} MO or *trpc1*^{ATG} MO, and co-injected with both MOs, revealing the synergistic effect between the two genes. Mean ± SD. Rostral region $n_{(cnt)}$=152; $n_{(cacna1c\text{-}MO\ sub)}$=52; $n_{(trpc1c\text{-}MO\ sub)}$=51, **P* =0.0136; $n_{(cacna1c\text{-}MO;trpc1\text{-}MO)}$=30; *****P* <0.0001. Caudal region $n_{(cnt)}$=120; $n_{(cacna1c\text{-}MO\ sub)}$=50; $n_{(trpc1c\text{-}MO\ sub)}$=40; $n_{(cacna1c\text{-}MO;trpc1\text{-}MO)}$=30; *****P* <0.0001. One-way ANOVA with Bonferroni Multiple Comparison correction. Scale bar = 40µm.

3.10 The LTCC affects VEGF-Dll4-Notch signalling

The development of a functional vascular network is achieved by the precise coordination of different signalling pathways to regulate EC angiogenic behaviour.

It has been shown that pharmacological or genetic disruption of Dll4/Notch signalling leads to an overbranching phenotype, increasing tip cell formation, and EC migration and proliferation (Leslie et al. 2007; Siekmann & Lawson 2007). Conversely, stimulation of Notch signalling decreases EC migration and proliferation (Liu et al. 2006; Leslie et al.

2007; Siekmann & Lawson 2007; Harrington et al. 2008). Moreover, perturbation on the VEGF pathway can alter the angiogenic EC behaviour, directly or indirectly modulating the Dll4/Notch cascade. In particular it has been shown that loss of *flt1* enhanced the tip cell formation leading to an overbranching phenotype (Krueger et al. 2011; Chappell et al. 2013). Overall, these studies have highlighted the crucial role of VEGF-Dll4-Notch interplay in the regulation of sprouting angiogenesis and in particular endothelial tip/stalk cell differentiation, migration, and proliferation.

3.10.1 Dynamics of the Notch pathway activity during ISV outgrowth

As shown in section 3.9., perturbation of the Ca^{2+} fluxes through the LTCC interfered with cell migration during the development of the ISVs. Furthermore, it is known that the Notch pathway is involved in angiogenic sprouting and tip/stalk cell specification. Considering this, it is plausible to hypothesize that the observed changes in the number of cells per ISVs after modulation of LTCC conductance, were the result of impaired Notch signalling.

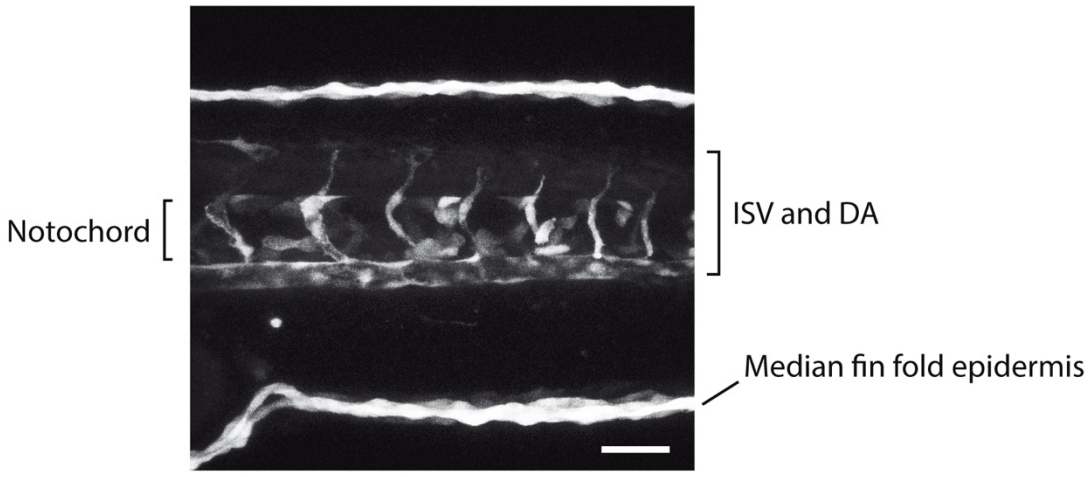

Figure 28: Notch signalling pathway is active in different cells. Maximum intensity projection of ISVs from the rostral region in *Tg(TP1:VenusPEST)* at 30 hpf indicating the Notch activity in different tissue such as the median fin fold epidermis and the notochord. Scale bar = 50μm.

To test this hypothesis the Notch reporter line *Tg(Tp1:VenusPEST)* (Ninov et al. 2012), was used to visualize all the cells where the Notch pathway was active.

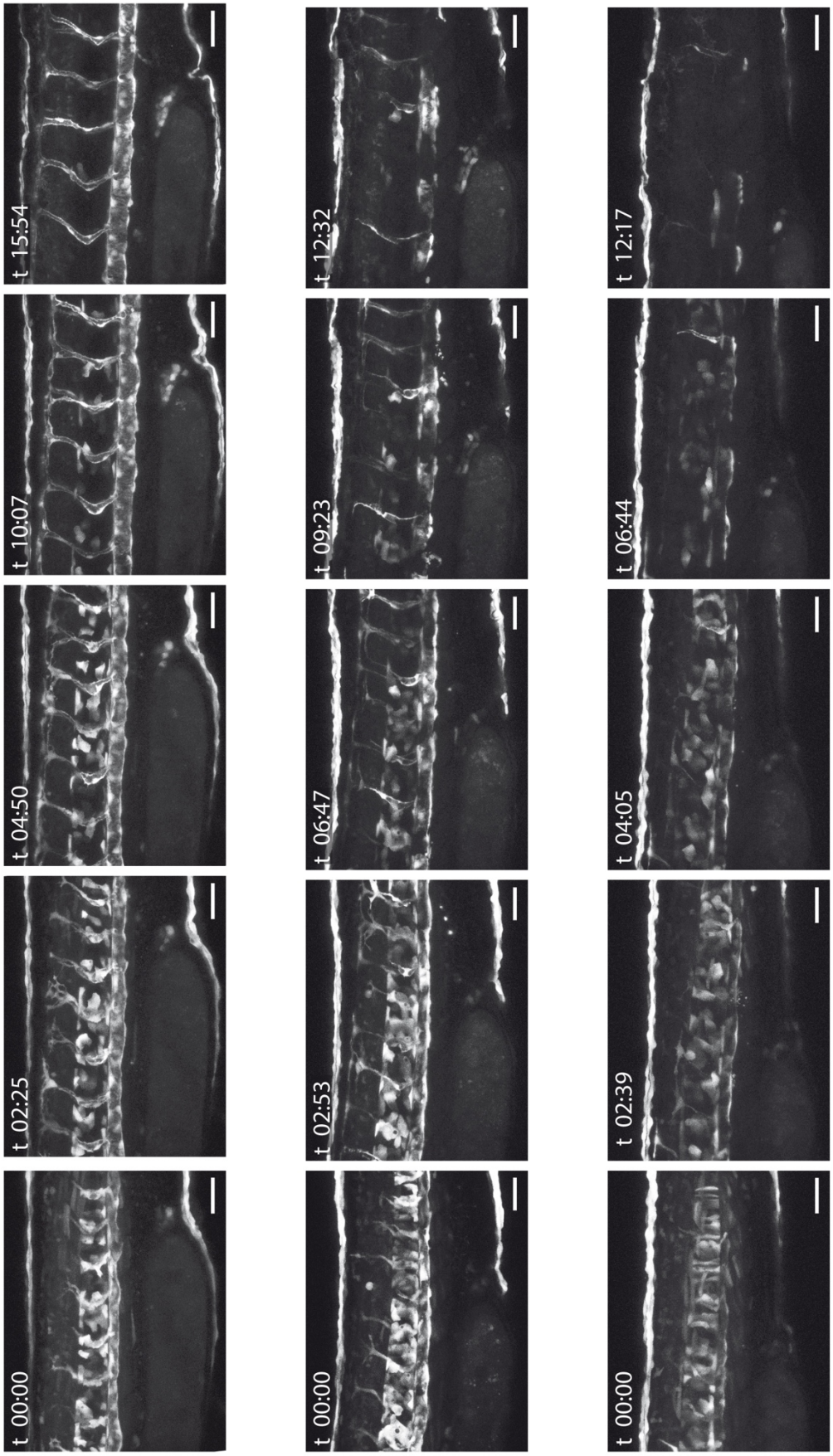
t 15:54
t 10:07
t 04:50
t 02:25
t 00:00
t 12:32
t 09:23
t 06:47
t 02:53
t 00:00
t 12:17
t 06:44
t 04:05
t 02:39
t 00:00
Control I
Control II
Control III

Figure 29: Notch signalling is dynamically active during ISV outgrowth. Maximum intensity projection from long-term time-lapse *in vivo* imaging of three different *Tg(TP1:VenusPEST)* control embryos (I-III), at the same developmental stage acquired from 28 hpf onwards. The embryos show different Notch activation patterns. t = time in hours. Scale bar = 50μm.

In this particular reporter line, the fluorescent marker VenusPEST was expressed under the control of a synthetic promoter composed of a repetition of Notch target sequences (Ninov et al. 2012). Thanks to the PEST sequence (Li et al. 1998) the fluorescent marker is rapidly degraded allowing a dynamic visualization of the signal only in those cells which have an active Notch pathway. The strength of the fluorescence reflects the Notch signalling activity

To better characterize the transgenic line, long-term time-lapse movies were acquired. To avoid multiple expression of the VenusPEST protein, the *Tg(Tp1:VenusPEST)* line was outcrossed with the control WT line and only the offspring were treated and analysed. As expected, along the zebrafish trunk, I observed the fluorescent signal not only in ECs, but also in other tissues such as the median fin fold epidermis and the notochord (Fig. 28), indicating that the Notch pathway is active in different cells at 30 hpf. As development proceeds, the fluorescent signal from the Notch activation decreases in the notochord and increases in ECs, allowing the visualization of ISV structures (Fig. 29). However, the acquired long-term time-lapse images revealed that the signal was highly dynamic and very heterogeneous among different control fish even within the same clutch and at the same time frame (Fig. 29). This made the comparison between control and treated embryos rather challenging.

3.10.2 The perturbation of LTCC conductance affects the Notch pathway

To assess the physiological functions of calcium fluxes at the plasma membrane on the Notch signalling during angiogenesis, I analysed the *Tg(Tp1:VenusPEST)* reporter line in perturbed Ca^{2+} flux conditions during ISVs development.

Loss of the LTCC, in the *cacna1c*^{sa10930} mutant or in *cacna1c*^{ex4sa} MO-injected embryos, as well as the stimulation of LTCC by Bay K treatment, decreased Notch signalling at 30 hpf, compared to uninjected control embryos (Fig. 30). In contrast, downregulation of TRPC1 in *trpc1*^{ATG}MO-injected embryos and the absence of blood flow in *tnnt2*^{ATG} MO-injected embryos did not affect Notch signalling (Fig. 30). The γ-secretase inhibitor DBZ, which suppresses Notch receptor cleavage, was used as a positive control of Notch

pathway downregulation. This data suggested that the perturbation of Ca^{2+} fluxes specifically through the LTCC, but not through TRPC1, affects the Notch signalling pathway.

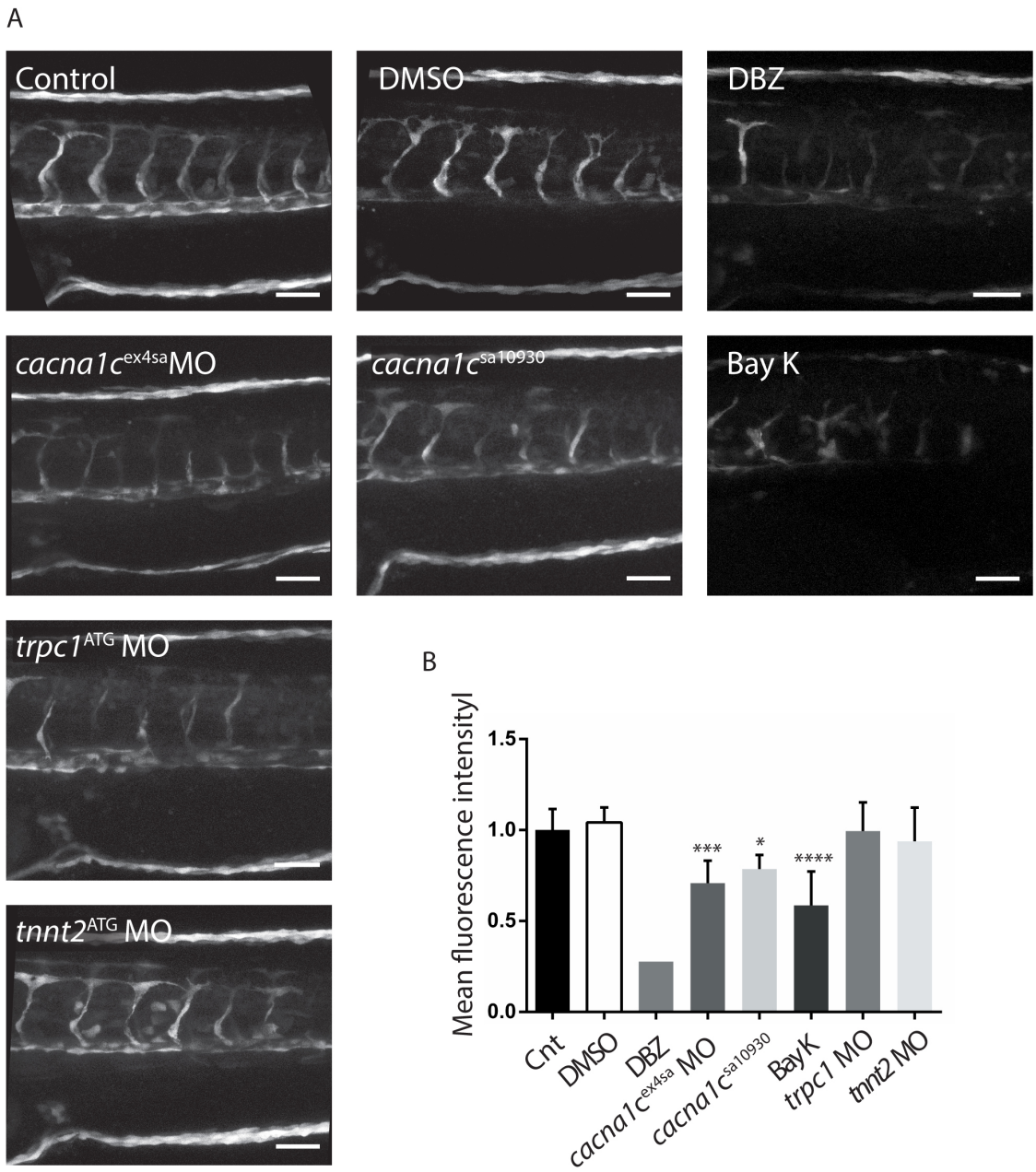

Figure 30: Perturbation of LTCC conductance downregulates Notch signalling. (A) Maximum intensity projections of ISVs from the rostral region in *Tg(TP1:VenusPEST)* at 30 hpf in different conditions. **(B)** Quantification of the mean fluorescence intensity signal in different conditions, data were normalized to the control values, set to 1. DBZ, a γ-secretase inhibitor, was used as a positive control of Notch pathway inhibition. Mean ± SD. $n_{(cnt)}$=8; $n_{(DMSO)}$=5; $n_{(cacna1cMO)}$=10, ***P =0.0004; $n_{(cacna1csa10930)}$=7, *P =0.0304; $n_{(Bay\ K)}$ =4, ****P <0.0001; $n_{(trpc1MO)}$=11; $n_{(tnnt2MO)}$=10. One-way ANOVA with Bonferroni Multiple Comparison correction. Scale bar = 50μm.

To better investigate the effect of LTCC conductance on the VEGF and Notch pathways specifically in ECs, RT qPCR experiments were performed at 30 hpf on FACS sorted ECs. Inhibition or stimulation of LTCC conductance was achieved by *cacna1c*^{ex4sa} MO injection or by Bay K treatment respectively; while the *trpc1*^{ATG} MO injection was used to affect the contribution of the TRPC1 current. Moreover, I examine the contribution of blood flow on the VEGF and Notch pathway components expression by *tnnt2* ^{ATG} MO injection.

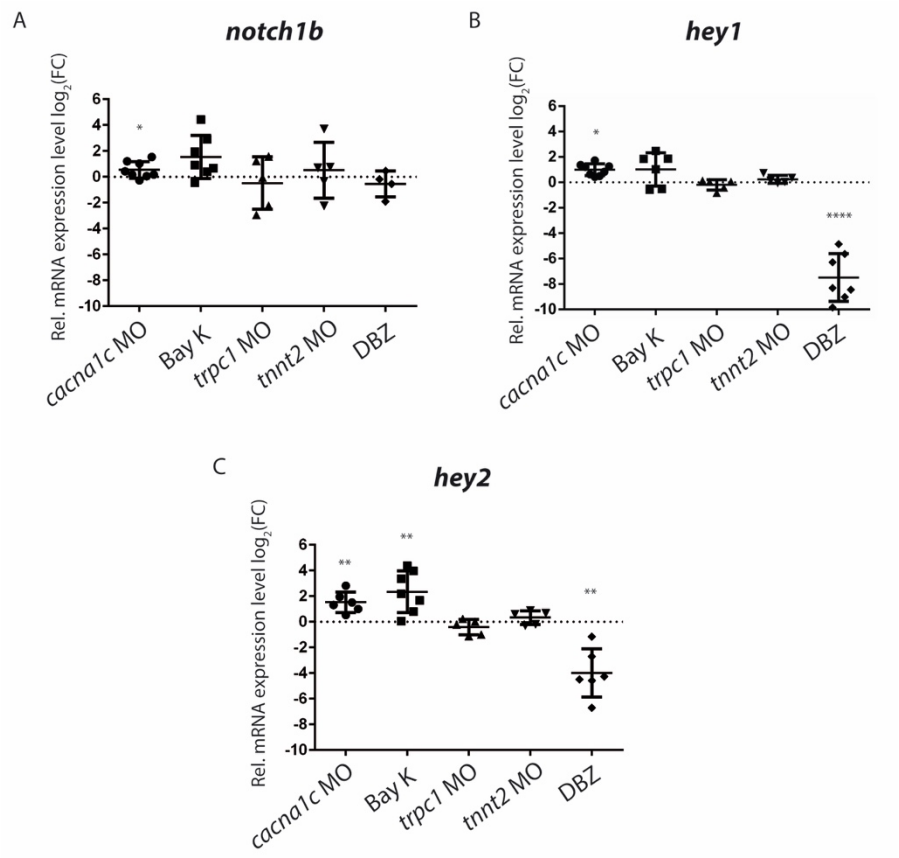

Figure 31: Perturbation of calcium fluxes via LTCC increases Notch target genes expression. (A-C) RT qPCR analysis of *notch1b* (A) and its target genes *hey1* (B) and *hey2* (C) in FACS-sorted ECs from zebrafish embryos at 30 hpf in different conditions, compared to FACS-sorted ECs from uninjected control embryos (set to 0). The perturbation of the LTCC conductance (via *cacna1c*^{ex4sa} MO injection (n =8)) mildly increased *notch1b* relative expression level. On the other hand LTCC stimulation by Bay K treatment (n =7) or TRPC1 downregulation (via *trpc1*-MO injection (n =5)), did not result in any effect on *notch1b* expression, neither did the loss of haemodynamic forces (via *tnnt2*-MO injection (n=5)) (A). Downregulation of the LTCC increased *hey1* (**P* =0,0242) and *hey2* (n=6; ***P* =0,0054) expression, while its stimulation upregulated only *hey2* (***P* =0,0089) (B, C). The γ-secretase inhibitor DBZ, used as a positive control for the Notch downregulation, decreased the expression levels of the *hey1* (n=7; *****P* <0,0001) and *hey2* (n =7; ***P* =0,0035) genes without affecting *notch1b* (n=4) expression. Data were normalized to the reference gene *eef1a1l1* and represented as $\log_2$ of the fold change (FC) ($\log_2$(FC)). Mean ± SD. Paired t-test.

Based on this results, downregulation of the LTCC mildly increases the expression level of the Notch receptor encoded by the *notch1b* gene (Geudens et al. 2010) (Fig. 31 A). However, neither LTCC stimulation nor loss of *trpc1* affected the *notch1b* expression level. The expression of the receptor was not altered even in the absence of haemodynamic forces due to the absence of blood flow via *tnnt2*-MO injection (Fig. 31 A). This demonstrates that the regulation of the Notch receptor expression, in this context, is independent of these pathways (Fig. 31 A).

Interestingly, the specific perturbation of LTCC conductance but not TRPC1, nor the absence of blood flow, increased the expression of the Notch target gene *hey1* and *hey2* (Fig. 31 B, C). In particular, the inhibition of LTCC conductance increased *hey1* and *hey2* expression levels, likewise, the stimulation of the channel increased *hey2* but not the *hey1* expression level (Fig. 31 B, C). As expected, the inhibition of the Notch pathway by the γ-secretase inhibitor DBZ, used as an internal control, decreased the expression level of the *hey1* and *hey2* genes without affecting *notch1b* expression (Fig. 31 A-C). Overall these data suggest that perturbing calcium fluxes through haemodynamic forces does not affect the expression of Notch signalling components. However, the specific inhibition or stimulation of LTCC activity induces the expression of the Notch target genes *hey1* and *hey2* (Fig. 31 B, C).

3.10.3 Perturbation of LTCC conductance affects VEGF signalling pathway

During angiogenesis and tip/stalk EC differentiation, Notch signalling is activated by its transmembrane ligand Dll4, expressed in neighbour cells and upregulated by the VEGFR-2 signalling cascade (Jakobsson et al. 2010). To better understand the implication of calcium fluctuation at the level of the plasma membrane on angiogenic signals, I investigated the expression level of the VEGF cascade components, upstream of the Notch pathway.

Interestingly, the specific perturbation of LTCC conductance but not TRPC1, nor the absence of flow, increased the expression level of VEGF receptors: *kdrl* (*vegfr-2*) and *flt1* (*vegfr-1*), which were shown to be a target genes of the Notch cascade (Jakobsson et al. 2010) (Fig. 32 A, B). In accordance with these results, I also observed an increase of *dll4* expression (Fig. 32 C), which is regulated by the VEGFR-2 cascade (Liu et al. 2003; Lobov et al. 2007; Suchting et al. 2007). Moreover, the increase of *dll4* is in

agreement with the observed increase in expression of the Notch target genes *hey1* and *hey2* (Fig. 31 B, C).

Importantly, neither the perturbation of TRPC1 nor the absence of haemodynamic forces affected any components of the VEGF or Dll4/Notch cascades. Furthermore, the inhibition of Notch signalling by DBZ treatment, used as a positive control, decreased *dll4* expression (Fig. 32 A) as previously reported (Leslie et al. 2007).

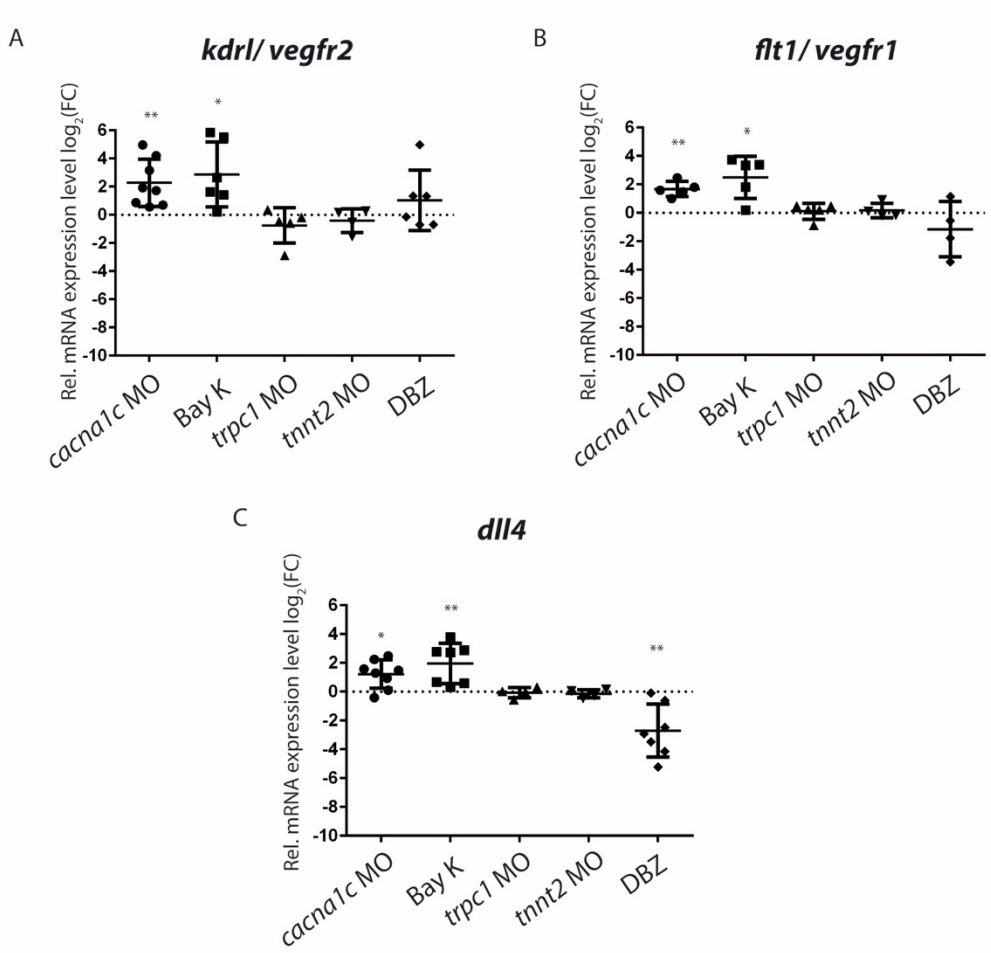

Figure 32: Perturbation of LTCC conductance affects the VEGF signal. (A-C) RT qPCR analysis of *kdrl* (*vegfr-2*) (A), *flt1* (*vegfr-1*) (B) and *dll4* (C) in FACS sorted ECs from zebrafish embryos at 30 hpf in different conditions, compared to FACS sorted ECs from uninjected control embryos (set to 0). Inhibition of LTCC conductance, via *canca1c*-MO injection, increased the expression levels of *kdrl* (*vegfr-2*) (n=8; ***P*=0,0064) (A) and *flt1* (*vegfr-1*) (n=6; ***P*=0,0022) (B), as well as the Notch ligand *dll4* (n=8; **P*=0,0101) (C). Stimulation of LTCC conductance by Bay K treatment also increased the expression level of *kdrl* (n=6; **P*=0,0283) (A) and *flt1* (n=5; **P*=0,0200) (B), as well as the Notch ligand *dll4* (n=7; ***P*=0,0098) (C). Loss of *trpc1* or the absence of flow via injection of *tnnt2*-MO, did not affect the expression of *vegfr-2* ($n_{(trpc1\text{-MO})}$=4; $n_{(tnnt2\text{-MO})}$=4) (A), *vegfr-1* ($n_{(trpc1\text{-MO})}$=5; $n_{(tnnt2\text{-MO})}$=4) (B), or *dll4* ($n_{(trpc1\text{-MO})}$=4; $n_{(tnnt2\text{-MO})}$=4) (C). The γ-secretase inhibitor (DBZ), decreased *dll4* (n=7; ***P*=0,0082) expression levels, as expected (positive control for Notch pathway downregulation). DBZ treatment barely affects the expression level of *kdrl* (n=6) (A) or *flt1* (n=4) (B). Data were normalized to the reference gene *eef1a1l1* and represented as $\log_2$ of the fold changes (FC) ($\log_2$(FC)). Mean ± SD. Paired t-test.

4 Discussion

Oscillations in cytosolic calcium concentrations ($[Ca^{2+}]_i$) are ubiquitous intracellular signals participating in different pathways and are fundamental to regulation of several biological processes. Because of its high versatility in amplitude, speed, frequency and spatiotemporal organization, this unique signal is adopted by different pathways in controlling cell behaviour. Due of this central role, Ca^{2+} signalling has been largely studied particularly in excitable cells such as neuron and muscle cells. However, the information on Ca^{2+} fluxes in non-excitable cells such as the endothelial cells are limited. During the neuronal development, Ca^{2+} signalling is one of the most important signals controlling the axonal turning: source and amplitude of Ca^{2+} fluctuations are crucial in order to promote attraction or repulsion in response to a molecular cue. Especially the Ca^{2+} fluxes through the LTCC were shown to be essential for the neuronal turning (Hong et al. 2000; Wang & Poo 2005; Gasperini et al. 2017). Given the similarities between the neuronal and vascular systems, it is reasonable to hypothesize that Ca^{2+} signalling may play a critical role in ECs during vascular development. The main goal of this dissertation was to explore the contribution of Ca^{2+} oscillations and with that associated signalling during angiogenic sprouting *in vivo*.

Ca^{2+} signalling in EC was mainly investigated in relation to the regulation of vascular tone by vascular smooth muscle cells (vSMCs) and the excitation-contraction coupling. Increase in $[Ca^{2+}]_i$ in the EC was associated with the production of soluble vasoconstrictor (or vasodilator), as well as with the initiation of the SMC hyperpolarization thus stimulating the vasodilation (Emerson et al. 2001; Taylor et al. 2012). Recently it has been shown that Ca^{2+} transients in vSMC can also propagate to the endothelium through the gap junctions located on the EC protrusion where the two cells make contact (Garland et al. 2017). This Ca^{2+} signal is sufficient to be amplified and stimulate the Ca^{2+} signalling response in the EC to promote vasodilation (Garland et al. 2017). Localised increase in $[Ca^{2+}]_i$ have been reported to be essential for the EC migration (Tsai et al. 2015; Yokota et al. 2015). Moreover, different Ca^{2+} distribution along the migrating cells was observed to polarize the EC and to promote their cytoskeletal reorganization (Tsai et al. 2014). Nevertheless, most of these studies have been accomplished in cultured ECs and are studied in the context of mature vessels. *In vivo* approaches to resolve the EC Ca^{2+} dynamics at molecular level and the role of Ca^{2+} signalling during angiogenesis is still poorly understood (Yokota et al. 2015; Noren et al. 2016). In addition, how Ca^{2+} is regulated during angiogenesis, which channels are

responsible for the increase of $[Ca^{2+}]_i$, and how the different signals modulate their activation remain to be elucidated. The data presented here have revealed the importance of Ca^{2+} fluxes through the plasma membrane, and specifically through the LTCC, in the regulation of EC migration during angiogenesis. Stimulation of the LTCC strongly induced the EC migration from the DA and resulted in an overbranching phenotype. On the other hand, the inhibition of the LTCC, as well as downregulation of the TRPC1, reduced the EC migration and proliferation. Furthermore, my results point to the high level of synergy between different Ca^{2+} channels regulating Ca^{2+} influx into the EC. Although on some level these channels act synergistically, the data reveal that LTCC play a distinct role in VEGF-Dll4-Notch signalling circuit.

4.1 Calcium oscillations: in vivo approach

The change in $[Ca^{2+}]_i$ is the result of integrated outcome of multiple Ca^{2+} release and influx pathways, occurring in a range of millisecond from the Ca^{2+} channel opening. The possibility to capture this very dynamic signal relies on the development of new sensitive Ca^{2+} sensors and fast microscopy technologies. Moreover, the lack of different molecular compounds to specifically inhibit or stimulate distinct Ca^{2+} channels, make their identification difficult. Furthermore, tailored algorithms and customised image processing analysis is necessary to parse out different Ca^{2+} pools; because of these obstacles the analysis of Ca^{2+} signals remains challenging.

Due to the tissue transparency and the relative easy establishment of reporter lines, the zebrafish embryo is a powerful model system for studying angiogenesis *in vivo*. For the purpose of this study, I have generated the zebrafish transgenic line *Tg(kdrl:Gal4; UAS:GCaMP5)* expressing the calcium indicator GCaMP5 specifically in the ECs. The rapid turnover of the GCaMP5 indicator (Akerboom et al. 2012) allowed for the visualization of calcium changes during the ISV outgrowth *in vivo*. In comparison to *ex vivo* studies, this approach guarantees a minimal interference with local Ca^{2+} pools and does not modify the extracellular environment of ECs. In particular, the extracellular Ca^{2+} concentrations, which have been shown to be a key regulator for the neuronal growth (Sutherland et al. 2014), are not interfered. Different calcium distributions in the filopodia extensions or into the main cell body can be appreciated and monitored during the angiogenic development. In this study, I present evidence of different components of calcium fluctuations during the angiogenesis in ECs. I observed slow Ca^{2+} transients with low amplitude and long durations, and fast Ca^{2+} sparks with high amplitude and short

duration (Fig. 9). The observed Ca^{2+} oscillation patterns are consistent with previous reports on ECs (Tsai et al. 2015). The Ca^{2+} response may be formed by an initial Ca^{2+} spike, due to the fast Ca^{2+} release from the intracellular stores, followed by an intermediate plateau level, resulted by the Ca^{2+} entry from the plasma membrane (Nilius & Droogmans 2001).

In addition to intracellular Ca^{2+} oscillations, at some instances Ca^{2+} waves appeared to propagate between sprouting ECs. This observation could provide evidence for the intercellular coupling between migrating ECs. More quantitative analysis of this potential coupling between neighbouring ECs has to be performed to provide conclusive evidence. Nevertheless, it is well documented that one of the gap junctional proteins, Connexin45 is highly expressed in DA (Desplantez et al. 2003; Christie et al. 2004), and thus my observation does not preclude the existence of tight intercellular communication between migrating ECs.

Taken together, zebrafish is an excellent model to study Ca^{2+} oscillations during angiogenesis *in vivo*. Growing number of genetically encoded indicators, fast *in vivo* imaging approaches such as light sheet microscopy, and improved image processing algorithms provide new exciting tools to explore physiological cues such as Ca^{2+} and their role in developmental processes in the very near future.

4.2 The role of LTCC in angiogenic sprouting

The expression of voltage gated Ca^{2+} channels in the endothelial cell has been long disputed over the last years. Recent data show the expression of the LTCC main pore forming subunit in human umbilical vascular endothelial cells (Kim et al. 2016). In this study I provide evidence that *cana1c* (a gene encoding LTCC) is expressed in zebrafish ECs during development. I used three different probes targeting different regions of the gene covering all predicted transcripts (Fig. 10). Moreover, the decrease in the relative mRNA expression level in ECs isolated from *cacna1c* mutant line compared to control demonstrated that the LTCC is indeed expressed in the endothelial cells. Imaging of Ca^{2+} oscillations in the presence of LTCC inhibitors and/or agonists is necessary to show the contribution of LTCC to Ca^{2+} transient amplitudes, duration and frequency.

To address the role of LTCC during angiogenesis different approaches were used: on one hand a pharmacological approach targeting the 1,4-dihydropyridine sensitive subunit of the LTCC, and on the other hand a genetic approach to test the loss-of-function with either MO oligonucleotide-mediated knock-down or available *cacna1c*

mutant lines. Unfortunately, to this day no gain-of-function mutations in *cacna1c* have been identified. The pharmacological approach to inhibit the LTCC conductance by Nifedipine treatment severely affected not only the ISVs formation, but also embryo development (Fig. 12). Due to this fact I adopted genetic approaches for the subsequent experiments.

In accordance with the Nifedipine treatment, the downregulation of calcium fluxes through the LTCC by MO injection or in the *cacna1c*^{sa10930} mutant compromised the ISV primary angiogenic sprout. The vessels were shorter and formed by less ECs at 30 hpf (Fig. 15) as well as at 48 hpf (Fig. 16). As expected, both approaches affected the cardiac function leading to the loss of heartbeat, and thus blood circulation.

MO approach represents an acute loss-of-function phenotype, and thus differs from genetic mutant. As previously reported for other genes (Kok et al. 2015), I noticed that the MO knock-down had a stronger phenotype compared to the one observed in the mutants. Nevertheless, the MO used in this work has been previously well established (Ramachandran et al. 2013), and the phenotypes observed were comparable and differ only in strength. This discrepancy could be explained by the genetic compensation mechanisms present in mutant lines (Rossi et al. 2015).

Notably, the perturbation of calcium influx through LTCC affected the EC behaviour during angiogenesis, decreasing the migration as well as the proliferation of ECs during primary angiogenic sprouting (Fig. 17). Curiously, LTCC downregulation in *cacna1c* morphants affected specifically EC proliferation but not migration, while the *cacna1c*^{sa10930} mutants revealed a decrease in EC migration but not proliferation (Fig. 17). This could be explained by the differences in timing and site of action between the MO and the mutant line. MO blocks translation by binding to the RNA of the target gene and causes a transient and concentration-dependent knockdown. The genetic mutation causes the permanent change in the DNA sequence; it has been recently demonstrated that some mutations are subjected to compensatory mechanisms leading to increased expression of other genes (Rossi et al. 2015). This possibility needs to be further tested by injecting the *cacna1c*^{ex4sa} MO into the *cacna1c*^{sa10930} mutants as indicated by recurrent guidelines (Stainier et al. 2017). If the MO does not cause additional defects, it confirms its specificity. Other possible explanation for this discrepancy in EC behaviour could be that the genetic mutant *cacna1c*^{sa10930} is not a complete null but a hypomorph; if the *cacna1c*^{ex4sa} MO caused enhanced phenotype upon injection into *cacna1c*^{sa10930}, it might indicate that this mutation is indeed a hypomorph. Further work is required to fully understand these differences. It also indicates that even though both strategies cause overall the same phenotype, the lower endothelial cell number per ISV, the mechanisms leading to this phenotype vary, and the result interpretation warrants caution.

Interestingly, the stimulation of the LTCC achieved via Bay K treatment resulted in an opposite effect on the ISV outgrowth: the ECs enhanced their angiogenic behaviour leading to an aberrant overbranching structure of the ISV (Fig. 11 D) formed by numerous ECs (Fig. 14). The increase of calcium influx through the LTCC by Bay K stimulation, positively impacted the EC migration from the DA, without affecting their proliferation. This phenotype partially phenocopied the one observed upon loss of *dll4* as well as in the VEGFR-1 (*flt1*) mutants. The inhibition of Notch signalling, via *dll4*-MO as well as *Rbpsuh*-MO, strongly increase the number of EC within the ISVs (Siekmann & Lawson 2007). Conversely, stimulation of Notch signalling decreases the ECs migration and proliferation (Liu et al. 2006; Leslie et al. 2007; Siekmann & Lawson 2007; Harrington et al. 2008). Furthermore, loss of *flt1* causes overbranching ISVs and increases the number of tip cells (Krueger et al. 2011). Indeed, the overbranching phenotype could result from the failure in the balance between tip and stalk cells differentiation, which is determined by the VEGF pathway and the Dll4/Notch cascade suggesting a possible regulatory role of LTCC in the VEGF-Dll4-Notch signalling circuit. The C-terminal tail of the LTCC is responsible for the channel regulation, harbouring binding sites for a number of proteins (Takahashi et al. 1987; Christel & Lee 2012; Weiss et al. 2013). To address the role of this key region during angiogenesis we adopted the *cacna1c*^{sa15296} mutant line with the mutation in the splicing site that should yield a truncated version of the main pore forming subunit missing the C-terminal tail, compromising the channel conductance (Hulme et al. 2006) and C-terminal transcriptional activity (Gomez-Ospina et al. 2006; Schroder et al. 2009). However, the analysis of the ISV structure (Fig. 11) and the EC number (Fig. 15) in the *cacna1c*^{sa15296} mutant line were comparable to the control zebrafish embryos, indicating that the main pore forming subunit may be still present and functional. Curiously, the investigation of migratory and proliferative events revealed a slight increase of the stalk cell proliferation (Fig. 17). The conductance of this mutant has to be yet determined. Moreover, the lack of working antibodies precluded me to test the mobility of the LTCC on the SDS-PAGE, and to accurately determine what is the nature of sa15296 allele at the protein level. Further analysis are required to address the specific issue of whether the observed effects in *cacna1c*^{sa15296} mutant are solely due to the increased Ca^{2+} conductance through the LTCC or they are result of the absence of the C-terminal function. Altogether, my data indicate that the fine regulation of Ca^{2+} influx through the LTCC is required for controlling the angiogenic behaviour in EC and modulates the angiogenic sprouting of ISVs in zebrafish.

4.3 Calcium oscillations: contribution of different channels

Oscillations in $[Ca^{2+}]_i$ result from the joined activity of different channels. The VEGF mediated increase of $[Ca^{2+}]_i$ in EC *in vitro* was associated with the PLCγ-IP_3-IP_3R cascade (Brock et al. 1991; Koch & Claesson-Welsh 2012; Moccia & Guerra 2016), and with the SOCE involving the ER low Ca^{2+} sensor STIM1, the pore forming subunit Orai1 (Li et al. 2011), and TRPC1 (Jho et al. 2005; Shi et al. 2017). Furthermore, an *in vivo* study revealed VEGF-mediated Ca^{2+} oscillation in EC sprouting from the DA (Yokota et al. 2015). However, *in vivo* studies are still limited: since the Ca^{2+} oscillations are generally mediated by different channels and transporters, further studies are required to fully understand the molecular mechanisms and to identify all the participating members.

Among the calcium channels, the TRPC family provides an important contribution to the calcium signalling in EC. Studies on ECs highlighted the role of TRPC1 in VEGF-induced $[Ca^{2+}]_i$ increase (Jho et al. 2005), and its positive contribution to angiogenesis (Yu et al. 2010) and to vascular tone permeability (Ahmmed et al. 2004; Jho et al. 2005). However, the physiological role of TRPC1 during vessel formation *in vivo*, and the interactions with the VEGF signalling components or with other ion channels are still poorly understood. My results, in accordance with previously published data (Yu et al. 2010), confirmed the requirement of TRPC1 in regulating the EC angiogenic behaviour during the primary ISV sprouting; TRPC1 downregulation decreased the migratory and proliferative events during ISVs angiogenesis (Fig. 26).

Increasing evidence from studies of vascular SMC suggests that TRPC1 and Orai1 cooperate in the SOCE and functionally interact with the LTCC (Bolotina 2012; Ávila-medina et al. 2016). SOCE could serve not only as a Ca^{2+} entry to restore the ER supply, but also as a depolarizing tool to trigger a secondary activation of the voltage gated LTCC (Bolotina 2012; Ávila-medina et al. 2016). Further studies are needed to delineate whether a similar process is present in non-excitable endothelial cells as well, and to establish its implication during the angiogenesis. However, I observed that TRPC1 interact synergistically with the LTCC promoting the ISV development (Fig. 27). This suggests the general requirement of Ca^{2+} fluxes at the plasma membrane for the regulation of the angiogenic process, rather than Ca^{2+} influx through a specific channel. Moreover, study on cell migration in diverse cell types have revealed the importance of calcium oscillations located at the front end of the migrating cell, and the increasing front-to-rear Ca^{2+} gradient to maintain the cell polarity (Tsai et al. 2014; Tsai et al. 2015). Furthermore, *in vitro* studies highlighted the role of LTCC to establish a front-to-rear

increasing Ca^{2+} gradients during EC migration (Kim et al. 2016). My data indicate the importance of the concerted action between the TRPC1 and the LTCC to promote the accurate ISV angiogenic development. Moreover, given the detailed analysis of the EC behaviour, it is evident that such synergies need to exist not only in polarized cell migration, but also in regulating cell proliferation.

It has to be noted that other channels can contribute to generating Ca^{2+} oscillations and to maintain the cell polarity, indeed TRPC3 and TRPC6 may mediate the DAG-dependent Ca^{2+} entry in several types of ECs (Antigny et al. 2011; Weissmann et al. 2012). Finally, it has to be taken into consideration that mechanical stimuli as laminar shear stress due to the hemodynamic forces can elicit Ca^{2+} influx, stimulating several mechanosensitive channels like the TRP polycystin 2 (TRPP2) the TRP vanilloid 4 (TRPV4), the heteromeric complex TRPC1-TRPP2-TRPCV4 and Piezo1 (Dietrich et al. 2007; Filosa et al. 2013; Du et al. 2014; Moccia 2018). However, these studies were mainly accomplished *in vitro* or in mature vessels, and integrative in vivo approaches are required to further understand the role of ionic cues during the vessels formation.

4.4 The angiogenic signalling

The VEGF-Dll4-Notch cascade is responsible for the maturation and maintenance of the EC angiogenic behaviour during the vessel formation. Given the morphological defects in the ISVs and the changes in the EC migration upon perturbing the LTCC conductance during angiogenesis, prompted me to better investigate the VEGF-Dll4-Notch signalling circuit. Using the Notch reporter line *Tg(Tp1:VenusPEST)* (Ninov et al. 2012) to visualise all the cells in which the Notch pathway was active, I observed downregulation of the Notch signalling upon LTCC perturbations, However, this result was in contrast with the subsequent RT qPCR analysis of the Notch-target genes in FACS-sorted ECs that show a significant increase in expression (Fig. 31, 32). This discrepancy could be explained by the high heterogeneity observed in the *Tg(Tp1:VenusPEST)* zebrafish line. Although, only the offspring from the outcross between the reporter and a wildtype control line were treated and analysed in order to avoid the heterogeneous effect of possible multiple insertion of VenusPEST transgene. The decrease of signal over time could be also due to the photobleaching and instability of the VenusPEST signal under the specific microscopy conditions applied.

The analysis of the expression level of Notch cascade components in FACS-sorted ECs gave more consistent results. My analysis revealed that downregulation of LTCC conductance during angiogenesis mildly increased the *notch1b* expression and stimulated the Notch target gene *hey1* and *hey2* as well as the VEGF receptor 1 (*flt1*), which was shown to also be a Notch target gene (Jakobsson et al. 2010). Moreover, we observed an increase of the VEGF receptor 2 (*kdrl*) expression level, which is in agreement with the observed upregulation of the Notch ligand *dll4* expression as the VEGFR-2 activation stimulate the *dll4* expression (Blanco & Gerhardt 2013; Simons et al. 2016). Bay K treatment resulted in a similar effect on the expression levels of different VEGF and Notch signalling components (Fig. 31 and 32). This indicates that the maintenance of the correct Ca^{2+} homeostasis via LTCC is required for the regulation of the gene expression; any changes in LTCC conductance in either direction can evoke the observed alterations. Notably, only the perturbation of the LTCC but not the TRPC1 affected the angiogenic pathways. The downregulation of the TRPC1 did not affect any components of the VEGF signalling nor the Notch-Dll4 cascade, suggesting an exclusive role for the LTCC in the regulation of the angiogenic signalling represented by VEGF-Dll4-Notch circuit (Fig. 31 and 32).

Previous *in vitro* studies have investigated the interplay between VEGF signalling and TRPC1, revealing how the VEGF-mediated increase of $[Ca^{2+}]_i$ is associated with the TRPC1 activity, which is stimulated by Ca^{2+} store depletion through the SOCE mechanisms (Jho et al. 2005; Moccia & Poletto 2015; Shi et al. 2017). However, the possible interplay between the VEGF signalling and the LTCC is still unexplored. The C-terminal region of the LTCC main pore forming subunit harbours the binding sites for several proteins that regulate the channel gating, offering the possibility that other pathways may modulate the channel activity. VEGFR activation leads to the recruitment of the phosphoinositide 3-kinase (Simons et al. 2016), which was also shown to ensure the stability of the $\alpha 1$ LTCC subunit via the Akt- (protein kinase B) mediated phosphorylation of the β subunit (Ghigo et al. 2017). Moreover, the VEGF cascade can stimulate the protein kinase C activity. It has been shown that the phosphorylation of the LTCC by PKC can either decrease the channel conductance or elicits a transient increase followed by a decrease (Lacerda et al. 1988; Tseng & Boyden 1991). Furthermore, evidences in vascular SMC suggest that the SOCE mechanism, which is also activated by the VEGF signalling, would work not only as a Ca^{2+} entry system to restore the ER supply, but also as a depolarizing tool to stimulate the LTCC activation (Bolotina 2012; Ávila-medina et al. 2016). However, further studies are required to

understand whether this mechanism is present in ECs as well, and to establish the crosstalk between the VEGF signalling and the LTCC regulation.
Study in developing cardiomyocytes has shown that the LTCC conductance is attenuated by the Wnt11 signalling (Panakova et al. 2010). For this reason, the MO-mediated loss of *wnt11* was used to indirectly stimulate the LTCC conductance. At 48 hpf, the loss of *wnt11* resulted in morphological vascular defects. In comparison to uninjected control embryos, the ISVs presented ectopic branches and loop connections, as well as disconnections to the DA or to the DLAV (Fig. 22). This was in line with previous results showing that the balance between the Notch and the Wnt signalling is required to stabilise or break new vessel connection (Phng et al. 2009). However, Phng and colleagues addressed the specific contribution of the Wnt3a to the vascular formation, further research would be required to understand the implication of Wnt11 on the angiogenic process, which remains poorly explored.

4.5 The contribution of the hemodynamic forces

The alteration of the LTCC conductance compromised the cardiac function, resulting in loss of heartbeat and thus blood flow. It has been shown that blood flow itself is required for the remodelling of vascular network (Chen et al. 2012; Kochhan et al. 2013; Franco et al. 2015) as well as for the lumen formation during sprouting angiogenesis (Gebala et al. 2016). Moreover, EC are able to sense and transduce the biomechanical stimuli, as the hemodynamic shear stress, in biological responses by the activation of multiple intracellular signalling pathways mediated by a variety of mechanosensors. The EC reaction to shear stress is mediated by an increase of $[Ca^{2+}]_i$, which can be modulated through primary cilia (Hierck et al. 2008; Nauli et al. 2008; Ando & Yamamoto 2013; Goetz et al. 2014).
We observed the contribution of the hemodynamic forces in our model by blocking the cardiac function, and thus the blood flow via *tnnt2*^{ATG}-MO injection. As previously reported, the primary angiogenic sprout of the ISVs is independent of the blood circulation (Schuermann et al. 2014) and the ISVs morphology at 30 hpf was comparable to the uninjected control. However, accurate observations uncovered that the structure of the ISVs was formed by slightly less ECs compared to the control (Fig. 19). Furthermore, I determined that loss of blood flow mildly affected the EC migration and proliferation, and strongly increased the rate of retrograde migration events (Fig. 21), thus explaining the decrease of ECs forming the vessels.

This retrograde migration was defined as an event when the ECs located in the ISV and forming the prospective vessel, migrated back to the DA. This event of cell regression only rarely appears in the wildtype ISVs at this stage, however, is typical for the vessel pruning during the vessel maturation (Chen et al. 2012). The regression is strongly associated with the blood flow directionality and from that implied hemodynamic forces (Chen et al. 2012; Franco et al. 2015).
Overall these data confirmed the crucial role of hemodynamic forces in stabilising the formation of the newly formed vessels. I also noticed that downregulation of LTCC in the *cacna1c* mutant, but surprisingly not in morphant embryos, increased the amount of EC retrograde migrations (Fig. 17). However, these events were occurring in the late stage of the vessel development, indicating that the lack of stability in the vessels due to the absence of flow promoted the retrograde migration. Importantly, the lack of blood flow did not perturb the expression levels of any components of the VEGF-Dll4-Notch cascade, showing that the balance of these pathways is independent from hemodynamic forces at 30 hpf during primary angiogenic sprouting (Fig. 31, 32).

In conclusion, our data uncovered a new role of LTCC underlying the endothelial cell behaviour, to modulate the primary angiogenic sprout of ISV in zebrafish.
This present work provide evidence that different Ca^{2+} channels interact with a high level of synergy to promote the ISV development. However, only the specific modulation of the LTCC conductance pointed to a new possible regulatory role of the LTCC on the VEGF-Dll4-Notch signalling circuit. Understanding the endothelial calcium responses and its molecular mechanisms in physiological condition during angiogenesis, have the potential to provide deeper insight into the regulation of vasculature formation and contribute to the generation of new targets for therapeutic applications.

5 Materials and Methods

5.1 Materials

5.1.1 Critical commercial assays

Table 1: List of critical commercial assays.

Kit	Manufacturer	Cat#
First Stand cDNA Synthesis Kit	ThermoFisher ScientificTM	K1612
GeneJET Gel Extraction Kit	ThermoFisher ScientificTM	K0691
mMESSAGE MMACHINE T7 Kit	Ambion	AM1344
Phusion High-Fidelity PCR Kit	ThermoFisher ScientificTM	F553
RNaesy Mini Kit	Qiagen	74104

5.1.2 Zebrafish line

Transgenic zebrafish lines were used to visualize the vascular development during time.

Table 2: List of zebrafish lines

Zebrafish line	Source	ZFIN-ID
Wild Type Lines		
AB	ZIRC	ZDB-GENO-960809-7
TL (Tupfel long fin)	ZIRC	ZDB-GENO-990623-2
WIK	ZIRC	ZDB-GENO-010531-2
Transgenic Lines		
***Tg(fli1a:nlsEGFP)*^{y7}**	ZIRC	(Roman et al. 2002)
***Tg(kdrl:EGFP)*^{s843}**	ZIRC	ZDB-ALT-050916-14
***Tg(kdrl:Gal4-VP16)*^{sd14}**		(A. D. Kim et al. 2014)
***Tg(Tp1bglob:H2BmCherry)*^{S939}**	EZRC	ZDB-ALT-110503-3
***Tg(Tp1bglob:venusPEST)*^{S940}**	EZRC	ZDB-ALT-120419-6
Tg(UAS:GCaMP5)		(Akerboom et al. 2012)
Mutant Lines		
Tg(cacna1c*^{sa10930}*)	EZRC	Item # 11056
Tg(cacna1c*^{sa15296}*)	EZRC	Item # 14832

5.1.3 Morpholino oligonucleotides

Table 3: Morpholino antisense oligonucleotides from GeneTools

Morpholino	[c]E	Target	Sequence 5'-3'	ZDB-MRPHLNO
***cacna1c*-MO**	4,5 ng; 1,68 ng	SSA ex 4	CCCGTTCCTAGACAGACGAAACAGA	130802-1
***tnnt2*-MO**	1 ng	ATG	CATGTTTGCTCTGATCTGACACGCA	060317-4
***trpc1*-MO**	4 ng; 1,6 ng	ATG	CATCCCACTGAGCAGAGCCTTACAC	100621-1
***wnt11*- MO**	1,2ng	ATG	GTTCCTGTATTCTGTCATGTCGCTC	050318-3

5.1.4 Chemicals and Reagents

Table 4: List of essential chemicals and reagents

Chemical/Reagent	Source	Cat #
BayK-8644 (Bay K), 125μM	Calbiochem	196878
DBZ (LY-41157), 100μM	Sigma-Aldrich	SML0649
Dimethyl sulfoxide (DMSO)	Sigma-Aldrich	276855
Dream*Taq* DNA Polymerase (5 U μl^{-1})	ThermoFisher Scientific™	EP0701
GlycoBlue™ Coprecipitant (15 mg $^{ml-1}$)	Invitrogen™	AM9515
Nifedipine (Nif), 70μM	Sigma-Aldrich	N7634
NuSieve® GTG Agarose	Lonza	50084
Pronase	Sigma-Aldrich	10165921001
Proteinase K, recombinant, PCR Grade	Roche	3115879001
TaqMan™ Gene Expression Master Mix	Applied Biosystems™	10525395
Tricane	Sigma-Aldrich	E10521
TRIzol® Reagent	Invitrogen™	15596026
Trypsin-EDTA solution, 0.25%, sterile-filtered	Sigma-Aldrich	T4049

5.1.5 Genotyping

Table 5: List of oligonucleotides used for mutant genotyping

Gene	Oligo	Sequence 5'-3'	Size
***cacna1c*^{sa10930}**	fw	TTTGCAGATTTTTGCGAGTG	595 bp
	rv	GCCGATACTGGAGCAGACTC	
***cacna1c*^{sa15296}**	fw	TTCCTCAGGCTGTTCTGCTT	431 bp
	rv	TCACAAACCCCTGAATCACA	

5.1.6 TaqMan probes for qRT-PCR

All the TaqMan probes were designed to target the gene expression in *Danio rerio* (Dr). With the exception for the *eef1α1* probe tagged with the covalently bound fluorophore VIC™, the remaining probes were tagged with the reporter dye FAM(6-carboxyfluorescein). The reference gene *eef1α1* was used as internal control within the same well of the gene-of-interest.

Table 6: List of TaqMan Probes for qRT-PCR

Gene	Order No.	Exon Boundary	Fluorophore
cacna1c	Dr03093556_g1	44-45	FAM - MGB
cacna1c	Dr03093552_g1	40-41	FAM - MGB
cacna1c	Dr03093552_g1	18-19	FAM - MGB
dll4	Dr03428642_m1	4-5	FAM - MGB
eef1α1	Dr03432748_m1	1-2	VIC - MGB
flt1	Dr03109249_m1	11-12	FAM - MGB
hey1	Dr03438953_g1	1-2	FAM - MGB
hey2	1376891 A8	-	FAM - MGB
kdrl	Dr03432890_m1	18-19	FAM - MGB
notch1b	Dr03086770_m1	28-29	FAM - MGB

5.1.7 Equipment and software

Table 7: Overview of Equipment

Equipment	Manufacturer
BD FACSAriaTM I Flow Cytometer	BD Biosciences
Centrifuge 5427 R	Eppendorf
Centrifuge 5920 R	Eppendorf

FemtoJet 4i Microinjector	Eppendorf
Flaming/Brown Micropipette Puller, Model P-97	Sutter Instrument®
Leica TCS SP8 Confocal Microscopy	Leica
M-152 Three-Dimensional Manipulator	Narishige Group
M165	Leica
Mastercycler® pro vapo.protect	Eppendorf
NanoDrop ND-1000 Spectrophotometer	peqLAB
SZX7 Brightfield Microscopy	Olympus
ViiATM 7 Real-Time PCR System	Life Technologies
inverted 3i spinning-disc confocal microscope (VIVO-SDC—CSU W1)	(Coxam & Gerhardt 2018)

Table 8: Overview of Software

Software	Purpose	Vendor /URL
A Plasmid Editor (APE) by M. Wayne Davis	sequence alignment	http://biologylabs.utah.edu/jorgensen/wayned/ape/
Adobe Illustrator CS5.1	illustration of data	Adobe Systems, Inc. (San Jose, US)
Adobe Photoshop CS5.1	image processing	Adobe Systems, Inc. (San Jose, US)
GraphPad Prism 7 for Mac OS X, Version 7.0b	statistical analysis	GraphPad Software, Inc. (La Jolla, US)
ImageJ	image processing	http://imagej.nih.gov/ij/
Mendeley	reference manager	https://www.mendeley.com/
Microsoft® Excel for Mac	spreadsheet application	Microsoft
Microsoft® Word for Mac	text processing	Microsoft
SlideBooks	image processing	www.slidebooks.com
ViiA™ 7 RUO software	qPCR processing	ThermoFisher Scientific™

5.2 Methods

5.2.1 Zebrafish methods

5.2.1.1 Zebrafish husbandry

Zebrafish were maintained under standard laboratory condition in accordance with the guidelines of the Max-Delbrück Center for Molecular Medicine and the local authority for animal protection (Landesamt für Gesundheit und Soziales, Berlin, Germany) for the use of laboratory animals, and followed the 'Principles of Laboratory Animal Care' (NIH publication no. 86–23, revised 1985) as well as the current version of German Law on the Protection of Animals. Embryos were kept in E3 Medium (see below) for practical reasons at 31,5°C for the first 10 hours post fertilization (hpf) and then transferred at 28°C standard temperature. When pigmentation started beyond 30 hpf, PTU (1-phenyl-2-thiourea, Sigma-Aldrich) at the concentration of 0,003% was added to the E3 medium to prevent the melanogenesis (D. Burrill & S. Easter 1994). Staging was calculated as described before by hpf or by somites counting (Kimmes 2004). Zebrafish strains AB, TL and WIK (Table 2) were used for the analysis of wild type phenotype.

E3 Medium	**5mM NaCl; 0,17mM KCl; 0,33mM CaCl; 0,33mM $MgSO_4$; pH 7,4**

5.2.1.2 Microinjection and morpholino mediated gene knockdown

Genetic manipulations were performed by microinjection of *in vitro* transcribed mRNA, expression construct or antisense morpholinos oligonucleotides (GeneTools) into zebrafish fertilized eggs at one-cell stage. Morpholino antisense oligonucleotides are translational blockers, which bind to the complementary sequences of the mRNA. The injection was performed either in the yolk or into the zygote using a FemtoJet microinjector, all the desired concentrations were obtained in Danieau's buffer (see below). Different morpholinos and concentrations are described in Table 3.

Danieau's Buffer	**17,4mM NaCl; 0,21mM KCl; 0,12mM $MgSO_4$ 0,18mM $Ca(NO_3)$; 1,5 mM HEPES; pH 7,6**

5.2.1.3 *In vivo* imaging

To obtain *in vivo* imaging and time-lapse imaging, embryos were anaesthetized with 0,016% Tricaine in E3 medium and then embedded in 0,5% low melting point agarose (Lonza) for immobilization in a microwell glass bottom dishes (MatTek). The imaging was then performed using a Leica TCS SP8 Confocal Microscope with a 25X water immersion objective or a 20X glycerol immersion objective. During acquisition embedded embryos were kept in a chamber at 28°C and covered with E3 medium containing 0.016% Tricaine.

5.2.1.4 Nifedipine, BayK-8644, and γ-secretase inhibitor (DBZ) treatment

To pharmacologically interfere with the L-type calcium channel (LTCC) we used BayK-8644 (Bay K) and Nifedipene (Nif), the agonist and the antagonist of the channel, respectively. The indirect inhibition of Notch signalling was performed using the γ-secretase inhibitor (DBZ), which prevents the cleavage of Notch receptor stopping the signalling cascade. All the substances were dissolved in DMSO to reach the stock concentration of 50mM, Nifedipine and Bay K or 100mM DBZ. The compounds were dissolved in E3 medium to reach the desired concentration (Table 4), zebrafish embryos were treated from 10 hpf at the bud stage until the moment of the analysis. Embryos in E3 medium containing only DMSO were used as controls.

5.2.2 Molecular biology methods

5.2.2.1 Genomic DNA isolation from zebrafish fins for mutant identification

Genomic DNA was isolated from fins samples to identify the ones carrying the mutation in the *cacna1c* gene. Adult fish were anaesthetized in 0,016% of Tricaine in E3 medium before the fin dissection. The fin tissue was lysed in 50μl of 50mM NaOH solution at 95°C for 10min. The reaction was stopped by adding 5μl of 1M Tris buffer (pH 8.0). The primers used for PCR amplification to identify the *cacna1c* mutants are listed in Table 5.

5.2.2.2 Fluorescent activated cell sorting (FACS)

In order to analyze the gene expression levels specifically in the vasculature we isolated endothelial cells using the fluorescent activated cell sorting (FACS) of the transgenic line *Tg(kdrl:EGFP)*. Approximately 100 embryos were first dechorionated using 0,5 mg/ml of Pronase solution in E3 Medium, then dissociated to obtain a homogeneous single cells suspension via trypsinization in 10ml of 0.25% Trypsin-EDTA solution (Trypsin with 0,25% EDTA, Sigma Aldrich) for 2-3 hours at 28°C on rotation with a gentle resuspension every 30 min through a 1 ml filter tip. The following operations were then performed on ice. The cells suspension was put through a 70μm nylon cell strainer (Cat#734-0003, Neolab) then centrifuged at 200g for 20 min at 4°C. Supernatant was removed until 1ml and 100μl of FBS (Fetal Bovine Serum) was added to stop the trypsinization. The pellet was then resuspended and centrifuged at 200g for 10 min at 4°C; supernatant was removed, cells washed in 2% FBS/PBS and the centrifugation repeated. The cells were resuspended in 400μl of 100% PBS and strained through an ice-cold 5 ml polystyrene round-bottom tube, with 75μm cell-strainer cap (Cat#10585801, Corning™) to prevent clogging. Using the FACS Aria I Flow Cytometer, EGFP positive labeled cells were sorted and collected at 4°C in 500μl of TRIzol® Reagent, shock frozen in liquid nitrogen and stored at -80°C.

5.2.2.3 Total RNA Isolation from FACS sorted cells

Total RNA isolation from FACS sorted cells was achieved using Chloroform/ Isopropanol and GlycoBlue precipitation. Upon FACS sorting procedures the samples aliquots containing 500 µl of TRIzol® Reagent, were thawed on ice and shaken for 5 min at 25 °C before to be resuspended five times. 100 µl ice-cold chloroform were added to the tube, shaken vigorously for 20 s in between the fingertips and incubated for 5 min on ice. Full speed centrifugation was then performed for 15 min at 4°C to achieve phase separation into a lower red colored phenol-chloroform phase, an interphase, and a color-less upper aqueous phase containing the RNA. Approximately 200 µl of upper phase was transferred in a fresh 1.5 ml Eppendorf tube and diluted 1:2 in ice-cold Isopropanol, carfully mixed before 1 µl GlycoBlue™ Coprecipitant was added to the mixture to facilitate the RNA visualization. The reaction was gently mixed before to start the RNA precipitation at –20 °C over night. Upon 30 min full speed centrifugation at 4 °C, the supernatant was removed without disturbing the RNA pellet, which was then washed

with 500 µl 75% Ethanol/H_2O (RT, freshly prepared), followed by full speed centrifugation at 4 °C for 10 min. The obtained pellet was air-dried for 10 min at RT, resuspended in 10 µl H_2O. Quality and quantity of the purified RNA was measured photometrically using NanoDrop according to the manufacturer's instructions. The total isolated RNA was then stored at -80°C or directly used for TR qPCR analysis.

5.2.2.4 Total RNA Isolation from Zebrafish embryos

Total RNA isolation was performed from 15-100 zebrafish embryos by Chloroform/ Isopropanol and GlycoBlue precipitation as for FACS sorted cells. First the embryos were washed several time with sterile egg water, anesthetized and transferred into a 1.5 ml tube. After the water was removed, 500 µl TRIzol® Reagent were added and tissue homogenization was performed by sucking the lysate 20 times each through a 23 G (Ø 0.6 x 30 mm) and a 27 G (Ø 0.4 x 20 mm) needle (B. Braun Sterican). 500 µl of TRIzol® Reagent were then added to reach a total volume of 1 ml, and the lysate was mixed by pipetting up and down six times. To allow the complete dissociation of nucleoprotein complexes the homogenized samples were incubated at RT for 5 min. 200 µl of ice-cold chloroform were then added and the samples were vigorously rocked for 15 s, incubated at RT for 5 min and full speed centrifuged at 4 °C for 15 min. Upon the complete phase separation the RNA isolation was performed as described before (see chapter 5.2.2.3), the RNA pellet was resuspended in 87.5 µl nuclease-free H_2O by flicking the tube for 3 min to facilitate RNA rehydration. The total RNA was then stored at -80°C or directly used for TR qPCR analysis.

5.2.2.5 DNase I Treatment and cDNA Synthesis

On-column DNase I treatment (Appendix D: DNase Digestion of RNA before RNA Cleanup), clean-up and determination of RNA concentration were performed according to the RNeasy Mini Kit. Upon determination of RNA quantity and quality with the NanoDrop ND-1000 spectrophotometer (Table 8): complementary DNA (cDNA), required for quantitative RT-PCR, was obtained using First-Stand cDNA Synthesis Kit according to manufacturer's protocol. The reverse transcription was performed according to the manufacturer's instructions using a random hexamers primer, the reaction was incubated for 5 min at 25 °C followed by 60 min at 37 °C in the

Mastercycler® pro *vapo.protect*. cDNA samples were directly used for qRT-PCR analysis.

5.2.2.6 Quantitative RT-PCR

In order to analyze the expression levels of specific genes, quantitative RT-PCR using TaqMan® Gene Expression Assey (Applied Biosystems) was performed. The amplification was performed on 25-100 ng of cDNA using FAM or VIC dye-labeled TaqMan® MGB probes (Table 6) and TaqMan® Gene Expression Master Mix and carried out on a ViiA™ 7 Real-Time PCR System. The reaction was performed in technical triplicates, minus-reverse transcriptase (–RT) and no-template were used as negative control conditions. The following condition were applied:

PCR condition steps	Temperature	Time
1-UNG Incubation annealing	50°C	2 min
2-UNG inactivation **Taq activation**	95°C	10 min
3-Denaturation	95°C	15 sec
4-Elongation	60°C	1 min
Repeat steps 3-4: 40X		

UNG: uracil-N-glycosylase is a component of the TaqMan Master Mix that prevent the reaplification of carryover PCR poducts by removing any uracil incorporated into single- or double-stranded DNA.

Data were analyzed using ViiA^{TM}7 RUO software (Table). The software reported the threshold cycle (C_T) values and baseline. The C_T represents the number of cycle (C), during the early phase of the exponential growth, in which the detected fluorescence probe crossed a threshold (T). The Ct value is a relative measurement of the target gene concentration: low C_T value corresponds to high abundance of the target gene, on the other hand, high C_T represents poor amount of the initial target gene.
The data were normalized to the internal housekeeping gene *eef1α1*, labeled with VIC^{TM} dye (Table 6), the reaction was performed in the same well as the gene of interest. Fold induction (fold change, FC) was determined applying ΔΔCt calculation (Livak & Schmittgen 2001) and plotted as $\log_2$(FC) with the control set to 0; or as FC with the

control set to 1, using GraphPad Prism 7 (Table 8). Statistics analysis was performed with GraphPad Prism 7 on the ΔC_T values comparing the untreated control situation to the treated situation using paired t-test.

5.2.3 Confocal microscopy

To image *in vivo* growing ISVs of mounted zebrafish embryos, long time lapse confocal microscopy was performed using a Leica SP8 microscope either with a 25X water immersion objective, for live imaging or a 20X glycerol immersion objective for 18 hours from 28hpf. To acquire different confocal plane through the tissue each stack was formed by 40-70 single images separated by 1,04μm. For the long time lapse imaging every stack was acquired at 10-15 min interval. Live calcium imaging was performed either on Leica SP8 microscope with a 25X water immersion objective, acquiring each stack in 8 sec interval; or on an inverted 3i spinning-disc confocal microscope (VIVO-SDC—CSU W1), with a Zeiss W Plan-Apochromat 20X/1.0NA WD1.8 mm Water Dipping Objective for Vivo™, acquiring each stack in 4 sec interval. Images were then analyzed using either ImageJ or SlideBooks software (Table 8).

5.2.4 Statistics

Statistical analysis was performed using GraphPad Prism 7 (Table 8). Significant differences between 2 experimental groups were determined applying One-way ANOVA with Bonferroni Multiple Comparison correction, paired or unpaired t-test. Unless otherwise stated, significant differences are indicated as p values: *P*<0,05= *; *P*<0,01= **; *P*<0,001= *** ; *P*<0,0001 = ****. All data are plotted as mean ± standard deviation (SD).

6 References

AbouAlaiwi, W. A., Takahashi, M., Mell, B. R., Jones, T. J., Ratnam, S., Kolb, R. J., & Nauli, S. M. (2009). Ciliary Polycystin-2 Is a Mechanosensitive Calcium Channel Involved in Nitric Oxide Signaling Cascades. *Circulation Research*, *104*(7), 860–869. https://doi.org/10.1161/CIRCRESAHA.108.192765

Abramowitz, J., & Birnbaumer, L. (2009). Physiology and pathophysiology of canonical transient receptor potential channels. *The FASEB Journal*, *23*(2), 297–328. https://doi.org/10.1096/fj.08-119495

Abu-Ghazaleh, R., Kabir, J., Jia, H., Lobo, M., & Zachary, I. (2001). Src mediates stimulation by vascular endothelial growth factor of the phosphorylation of focal adhesion kinase at tyrosine 861, and migration and anti-apoptosis in endothelial cells. *Biochemical Journal*, *360*(Pt 1), 255–264. Retrieved from http://www.ncbi.nlm.nih.gov/pmc/articles/PMC1222225/

Adams, R. H., & Eichmann, A. (2010). Axon Guidance Molecules in Vascular Patterning. *Cold Spring Harbor Perspectives in Biology*, *2*(a001875), 1–28. https://doi.org/10.1101/cshperspect.a001875

Ahmmed, G. U., Mehta, D., Vogel, S., Holinstat, M., Paria, B. C., Tiruppathi, C., & Malik, A. B. (2004). Protein kinase Cα phosphorylates the TRPC1 channel and regulates store-operated Ca2+ entry in endothelial cells. *Journal of Biological Chemistry*, *279*(20), 20941–20949. https://doi.org/10.1074/jbc.M313975200

Akerboom, J., Chen, T. W., Wardill, T. J., Tian, L., Marvin, J. S., Mutlu, S., … Looger, L. L. (2012). Optimization of a GCaMP calcium indicator for neural activity imaging. *J Neurosci*, *32*(40), 13819–13840. https://doi.org/10.1523/JNEUROSCI.2601-12.2012

Albert, A. P. (2011). Gating Mechanisms of Canonical Transient Receptor Potential Channel Proteins: Role of Phosphoinositols and Diacylglycerol. In M. S. Islam (Ed.), *Transient Receptor Potential Channels* (pp. 391–411). Dordrecht: Springer Netherlands. https://doi.org/10.1007/978-94-007-0265-3_22

Alonso, D., & Radomski, M. W. (2003). The Nitric Oxide-Endothelin-1 Connection, 107–115.

Amali, A. A., Sie, L., Winkler, C., & Featherstone, M. (2013). Zebrafish hoxd4a Acts Upstream of meis1.1 to Direct Vasculogenesis, Angiogenesis and Hematopoiesis. *PLoS ONE*, *8*(3). https://doi.org/10.1371/journal.pone.0058857

Amberg, G. C., & Navedo, M. F. (2013). Calcium Dynamics in Vascular Smooth Muscle. *Microcirculation*, *20*(4), 281–289. https://doi.org/10.1111/micc.12046

Ando, J., & Yamamoto, K. (2013). Flow detection and calcium signalling in vascular endothelial cells. *Cardiovascular Research*, *99*, 260–268. https://doi.org/10.1093/cvr/cvt084

Antigny, F., Jousset, H., König, S., & Frieden, M. (2011). Thapsigargin activates Ca2+ entry both by store-dependent, STIM1/Orai1-mediated, and store-independent, TRPC3/PLC/PKC-mediated pathways in human endothelial cells. *Cell Calcium*, *49*(2), 115–127. https://doi.org/https://doi.org/10.1016/j.ceca.2010.12.001

Ávila-medina, J., Calderón-sánchez, E., González-rodríguez, P., Monje-quiroga, F., Antonio, J., Castellano, A., … Smani, T. (2016). Orai1 and TRPC1 Proteins Co-localize with Ca V 1 . 2 Channels to Form a Signal Complex in Vascular Smooth Muscle Cells *, *291*(40), 21148–21159.

https://doi.org/10.1074/jbc.M116.742171

Bacon, C. R., Cary, N. R., & Davenport, A. P. (1995). Distribution of endothelin receptors in atherosclerotic human coronary arteries. *Journal of Cardiovascular Pharmacology*, *26*, S439-41.

Beech, D. J. (2013). Characteristics of Transient Receptor Potential Canonical Calcium-Permeable Channels and Their Relevance to Vascular Physiology and Disease. *Circulation Journal*, *77*(3), 570–579. https://doi.org/10.1253/circj.CJ-13-0154

Berridge, M. J., Bootman, M. D., & Roderick, H. L. (2003). Calcium signalling: dynamics, homeostasis and remodelling. *Nat Rev Mol Cell Biol*, *4*(7), 517–529. https://doi.org/10.1038/nrm1155

Berridge, M. J., Lipp, P., & Bootman, M. D. (2000). The versatility and universality of calcium signalling. *Nature Reviews. Molecular Cell Biology*, *1*(1), 11–21. https://doi.org/10.1038/35036035

Bers, D. M. (2002). Cardiac excitation contraction coupling. *Nature*, *415*, 198–205. https://doi.org/10.1016/B978-0-12-378630-2.00221-8

Betz, C., Lenard, A., Belting, H., & Affolter, M. (2016). Cell behaviors and dynamics during angiogenesis, 2249–2260. https://doi.org/10.1242/dev.135616

Blanco, R., & Gerhardt, H. (2013). VEGF and Notch in tip and stalk cell selection. *Cold Spring Harbor Perspectives in Medicine*, *3*(1), 1–20. https://doi.org/10.1101/cshperspect.a006569

Blasi, F., & Carmeliet, P. (2002). uPAR: a versatile signalling orchestrator. *Nature Reviews Molecular Cell Biology*, *3*, 932. Retrieved from https://doi.org/10.1038/nrm977

Bodi, I., Mikala, G., Koch, S. E., Akhter, S. a, & Schwartz, A. (2005). The L-type calcium channel in the heart : the beat goes on, *115*(12). https://doi.org/10.1172/JCI27167.3306

Böhm, F., Ahlborg, G., Johansson, B. L., Hansson, L. O., & Pernow, J. (2002). Combined endothelin receptor blockade evokes enhanced vasodilatation in patients with atherosclerosis. *Arteriosclerosis, Thrombosis, and Vascular Biology*, *22*(4), 674–679. https://doi.org/10.1161/01.ATV.0000012804.63152.60

Bolotina, V. M. (2012). Orai1, STIM1, and iPLA2β Determine Arterial Vasoconstriction. *Arteriosclerosis, Thrombosis, and Vascular Biology*, *32*(5), 1066–1067.

Bossu, J. L., Elhamdani, A., & Feltz, A. (1992). Voltage-Dependent Calcium Entry in Confluent Bovine Capillary Endothelial Cells. *FEBS.Lett.*, *299*(3), 239–242.

Bournele, D., & Beis, D. (2016). Zebrafish models of cardiovascular disease. *Heart Failure Reviews*, *21*(6), 803–813. https://doi.org/10.1007/s10741-016-9579-y

Brailoiu, G. C., Gurzu, B., Gao, X., Parkesh, R., Aley, P. K., Trifa, D. I., … Brailoiu, E. (2010). Acidic NAADP-sensitive Calcium Stores in the Endothelium: AGONIST-SPECIFIC RECRUITMENT AND ROLE IN REGULATING BLOOD PRESSURE. *The Journal of Biological Chemistry*, *285*(48), 37133–37137. https://doi.org/10.1074/jbc.C110.169763

Brevetti, G., Giugliano, G., Brevetti, L., & Hiatt, W. R. (2010). Contemporary Reviews in Cardiovascular Medicine Inflammation in Peripheral Artery Disease, 1862–1875. https://doi.org/10.1161/CIRCULATIONAHA.109.918417

Brock, T. A., Dvorak, H. F., & Senger, D. R. (1991). Tumor-secreted vascular permeability factor increases cytosolic Ca2+ and von Willebrand factor release in human endothelial cells. *The American Journal of Pathology*, *138*(1), 213–221.

Retrieved from https://www.ncbi.nlm.nih.gov/pubmed/1987767

Brown, E. B., Campbell, R. B., Tsuzuki, Y., Xu, L., Carmeliet, P., Fukumura, D., & Jain, R. K. (2001). In vivo measurement of gene expression, angiogenesis and physiological function in tumors using multiphoton laser scanning microscopy. *Nature Medicine*, *7*, 864. Retrieved from https://doi.org/10.1038/89997

Burri, P. H., Hlushchuk, R., & Djonov, V. (2004). Intussusceptive angiogenesis: Its emergence, its characteristics, and its significance. *Developmental Dynamics*, *231*(3), 474–488. https://doi.org/10.1002/dvdy.20184

Burri, P. H., & Tarek, M. R. (1990). A novel mechanism of capillary growth in the rat pulmonary microcirculation. *The Anatomical Record*, *228*(1), 35–45. https://doi.org/10.1002/ar.1092280107

Busse, R., & Mülsch, A. (1990). Calcium-dependent nitric oxide synthesis in endothelial cytosol is mediated by calmodulin. *FEBS Letters*, *265*(1–2), 133–136. https://doi.org/10.1016/0014-5793(90)80902-U

Bussmann, J., Wolfe, S. A., & Siekmann, A. F. (2011). Arterial-venous network formation during brain vascularization involves hemodynamic regulation of chemokine signaling. *Development*, *138*(9), 1717–1726. https://doi.org/10.1242/dev.059881

Bychkov, R., Burnham, M. P., Richards, G. R., Edwards, G., Weston, A. H., Félétou, M., & Vanhoutte, P. M. (2002). Characterization of a charybdotoxin-sensitive intermediate conductance Ca(2+)-activated K(+) channel in porcine coronary endothelium: relevance to EDHF. *British Journal of Pharmacology*, *137*(8), 1346–1354. https://doi.org/10.1038/sj.bjp.0705057

Cahill, L. S., Rennie, M. Y., Hoggarth, J., Yu, L. X., Rahman, A., Kingdom, J. C., … Sled, J. G. (2018). Feto- and utero-placental vascular adaptations to chronic maternal hypoxia in the mouse. *The Journal of Physiology*, *596*(15), 3285–3297. https://doi.org/10.1113/JP274845

Carafoli, E., Santella, L., Branca, D., & Brini, M. (2001). Generation, Control, and Processing of Cellular Calcium Signals. *Critical Reviews in Biochemistry and Molecular Biology*, *36*(2), 107–260. https://doi.org/10.1080/20014091074183

Carmeliet, P. (2005). Angiogenesis in life, disease and medicine. *Nature*, *438*(7070), 932–936. https://doi.org/10.1038/nature04478

Carmeliet, P., De Smet, F., Loges, S., & Mazzone, M. (2009). Branching morphogenesis and antiangiogenesis candidates: tip cells lead the way. *Nat Rev Clin Oncol*, *6*(6), 315–326. Retrieved from http://dx.doi.org/10.1038/nrclinonc.2009.64

Carmeliet, P., Ferreira, V., Breier, G., Pollefeyt, S., Kieckens, L., Gertsenstein, M., … Nagy, A. (1996). Abnormal blood vessel development and lethality in embryos lacking a single VEGF allele. *Nature*, *380*(6573), 435–439. Retrieved from http://dx.doi.org/10.1038/380435a0

Carmeliet, P., & Jain, R. K. (2000). Angiogenesis in cancer and other diseases. *Nature*, *407*, 249. Retrieved from https://doi.org/10.1038/35025220

Carmeliet, P., & Jain, R. K. (2011). Molecular mechanisms and clinical applications of angiogenesis. *Nature*, *473*, 298. Retrieved from http://dx.doi.org/10.1038/nature10144

Carmeliet, P., & Tessier-Lavigne, M. (2005). Common mechanisms of nerve and blood vessel wiring. *Nature*, *436*, 193. Retrieved from http://dx.doi.org/10.1038/nature03875

Catterall, W. A. (2011). Voltage-gated calcium channels. *Cold Spring Harb Perspect*

Biol, *3*(8), a003947. https://doi.org/10.1101/cshperspect.a003947

Chakrabarti, S., Streisinger, G., Singer, F., & Walker, C. (1983). Frequency of γ-Ray Induced Specific Locus and Recessive Lethal Mutations in Mature Germ Cells of the Zebrafish, BRACHYDANIO RERIO . *Genetics*, *103*(1), 109–123. Retrieved from http://www.ncbi.nlm.nih.gov/pmc/articles/PMC1202016/

Chappell, J. C., Mouillesseaux, K. P., & Bautch, V. L. (2013). Flt-1 (vascular endothelial growth factor receptor-1) is essential for the vascular endothelial growth factor-Notch feedback loop during angiogenesis. *Arteriosclerosis, Thrombosis, and Vascular Biology*, *33*(8), 1952–1959. https://doi.org/10.1161/ATVBAHA.113.301805

Charron, F., & Tessier-Lavigne, M. (2007). The Hedgehog, TGF-β/BMP and Wnt Families of Morphogens in Axon Guidance BT - Axon Growth and Guidance. In D. Bagnard (Ed.) (pp. 116–133). New York, NY: Springer New York. https://doi.org/10.1007/978-0-387-76715-4_9

Chávez, M. N., Aedo, G., Fierro, F. A., Allende, M. L., & Egaña, J. T. (2016). Zebrafish as an Emerging Model Organism to Study Angiogenesis in Development and Regeneration. *Frontiers in Physiology*, *7*, 56. https://doi.org/10.3389/fphys.2016.00056

Chen, Q., Jiang, L., Li, C., Hu, D., Bu, J., Cai, D., & Du, J. (2012). Haemodynamics-Driven Developmental Pruning of Brain Vasculature in Zebrafish, *10*(8). https://doi.org/10.1371/journal.pbio.1001374

Cheng, H.-W., James, A. F., Foster, R. R., Hancox, J. C., & Bates, D. O. (2006). VEGF Activates Receptor-Operated Cation Channels in Human Microvascular Endothelial Cells. *Arteriosclerosis, Thrombosis, and Vascular Biology*, *26*(8), 1768 LP-1776. Retrieved from http://atvb.ahajournals.org/content/26/8/1768.abstract

Chevalier, M., Gilbert, G., Roux, E., Lory, P., Marthan, R., Savineau, J. P., & Quignard, J. F. (2014). T-type calcium channels are involved in hypoxic pulmonary hypertension. *Cardiovascular Research*, *103*(4), 597–606. https://doi.org/10.1093/cvr/cvu166

Christel, C., & Lee, A. (2012). Ca2 +-dependent modulation of voltage-gated Ca2 + channels. *Biochimica et Biophysica Acta - General Subjects*. Retrieved from http://ovidsp.ovid.com/ovidweb.cgi?T=JS&PAGE=reference&D=emed10&NEWS=N&AN=2012332506

Christie, T. L., Mui, R., White, T. W., & Valdimarsson, G. (2004). Molecular cloning, functional analysis, and RNA expression analysis of connexin45.6: a zebrafish cardiovascular connexin. *Am J Physiol Heart Circ Physiol*, *286*(5), H1623-32. https://doi.org/10.1152/ajpheart.00800.2003

Claxton, S., & Fruttiger, M. (2004). Periodic Delta-like 4 expression in developing retinal arteries. *Gene Expression Patterns*, *5*(1), 123–127. https://doi.org/10.1016/J.MODGEP.2004.05.004

Cohen, E. D., Miller, M. F., Wang, Z., Moon, R. T., & Morrisey, E. E. (2012). Wnt5a and Wnt11 are essential for second heart field progenitor development. *Development (Cambridge, England)*, *139*(11), 1931–1940. https://doi.org/10.1242/dev.069377

Coleman, H. A., Tare, M., & Parkington, H. C. (2001). EDHF is not K+ but may be due to spread of current from the endothelium in guinea pig arterioles. *American Journal of Physiology-Heart and Circulatory Physiology*, *280*(6), H2478–H2483. https://doi.org/10.1152/ajpheart.2001.280.6.H2478

Cooke, V. G., LeBleu, V. S., Keskin, D., Khan, Z., O'Connell, J. T., Teng, Y., … Pathway, S. (2012). Pericyte depletion results in hypoxia-associated epithelial-to-

mesenchymal transition and metastasis mediated by met signaling pathway. *Cancer Cell*, *21*(1), 66–81. https://doi.org/10.1016/j.ccr.2011.11.024.Pericyte

Coultas, L., Chawengsaksophak, K., & Rossant, J. (2005). Endothelial cells and VEGF in vascular development. *Nature*, *438*(7070), 937–945. https://doi.org/10.1038/nature04479

Coxam, B., & Gerhardt, H. (2018). Imaging of Endothelial Cell Dynamic Behavior in Zebrafish BT - Lymphangiogenesis: Methods and Protocols. In G. Oliver & M. L. Kahn (Eds.) (pp. 181–195). New York, NY: Springer New York. https://doi.org/10.1007/978-1-4939-8712-2_12

Crane, G. J., Gallagher, N., Dora, K. A., & Garland, C. J. (2003). Small- and intermediate-conductance calcium-activated K(+) channels provide different facets of endothelium-dependent hyperpolarization in rat mesenteric artery. *The Journal of Physiology*, *553*(Pt 1), 183–189. https://doi.org/10.1113/jphysiol.2003.051896

Croce, J. C., & McClay, D. R. (2008). Evolution of the Wnt pathways. *Methods in Molecular Biology*. https://doi.org/10.1007/978-1-60327-469-2_1

Cunningham, S. A., Arrate, M. P., Brock, T. A., & Waxham, M. N. (1997). Interactions of FLT-1 and KDR with Phospholipase C γ: Identification of the Phosphotyrosine Binding Sites. *Biochemical and Biophysical Research Communications*, *240*(3), 635–639. https://doi.org/10.1006/BBRC.1997.7719

D. Burrill, J., & S. Easter, S. (1994). *Development of the retinofugal projections in the embryonic and larval zebrafish (Brachydanio rerio)*. *The Journal of comparative neurology* (Vol. 346). https://doi.org/10.1002/cne.903460410

Dao Thi, M.-U., Trocmé, C., Montmasson, M.-P., Fanchon, E., Toussaint, B., & Tracqui, P. (2012). Investigating Metalloproteinases MMP-2 and MMP-9 Mechanosensitivity to Feedback Loops Involved in the Regulation of In Vitro Angiogenesis by Endogenous Mechanical Stresses. *Acta Biotheoretica*, *60*(1), 21–40. https://doi.org/10.1007/s10441-012-9147-3

Davenport, A. P., Kuc, R. E., Maguire, J. J., & Harland, S. P. (1995). ETA receptors predominate in the human vasculature and mediate constriction. *Journal of Cardiovascular Pharmacology*, *26*, S265-7.

Davis, G. E., Koh, W., & Stratman, A. N. (2007). Mechanisms controlling human endothelial lumen formation and tube assembly in three-dimensional extracellular matrices. *Birth Defects Research Part C: Embryo Today: Reviews*, *81*(4), 270–285. https://doi.org/10.1002/bdrc.20107

Dejana, E., Tournier-Lasserve, E., & Weinstein, B. M. (2009). The Control of Vascular Integrity by Endothelial Cell Junctions: Molecular Basis and Pathological Implications. *Developmental Cell*, *16*(2), 209–221. https://doi.org/10.1016/J.DEVCEL.2009.01.004

Desplantez, T., Marics, I., Jarry-Guichard, T., Veteikis, R., Briand, J.-P., Weingart, R., & Gros, D. (2003). *Characterization of Zebrafish Cx43.4 Connexin and its Channels*. *Experimental physiology* (Vol. 88). https://doi.org/10.1113/eph8802584

DeVries, M. E., Kelvin, A. A., Xu, L., Ran, L., Robinson, J., & Kelvin, D. J. (2005). Defining the Origins and Evolution of the Chemokine/Chemokine Receptor System. *The Journal of Immunology*, *176*(1), 401–415. https://doi.org/10.4049/jimmunol.176.1.401

Dietrich, A., Fahlbusch, M., & Gudermann, T. (2014). Classical Transient Receptor Potential 1 (TRPC1): Channel or Channel Regulator? *Cells*, *3*(4), 939–962. https://doi.org/10.3390/cells3040939

Dietrich, A., Kalwa, H., Storch, U., Mederos Y Schnitzler, M., Salanova, B.,

Pinkenburg, O., … Gudermann, T. (2007). Pressure-induced and store-operated cation influx in vascular smooth muscle cells is independent of TRPC1. *Pflugers Archiv European Journal of Physiology*, *455*(3), 465–477. https://doi.org/10.1007/s00424-007-0314-3

Djonov, V., Baum, O., & Burri, P. H. (2003). Vascular remodeling by intussusceptive angiogenesis. *Cell and Tissue Research*, *314*(1), 107–117. https://doi.org/10.1007/s00441-003-0784-3

Dolmetsch, R. E. (2001). Signaling to the Nucleus by an L-type Calcium Channel-Calmodulin Complex Through the MAP Kinase Pathway. *Science*, *294*(5541), 333–339. https://doi.org/10.1126/science.1063395

Dora, K. A., Gallagher, N. T., McNeish, A., & Garland, C. J. (2008). Modulation of endothelial cell K(Ca)3.1-channels during EDHF signaling in mesenteric resistance arteries. *Circulation Research*, *102*(10), 1247–1255. https://doi.org/10.1161/CIRCRESAHA.108.172379

Dora, K. A., & Garland, C. J. (2013). Linking hyperpolarization to endothelial cell calcium events in arterioles. *Microcirculation*, *20*(3), 248–256. https://doi.org/10.1111/micc.12041

Dorrell, M. I., Aguilar, E., & Friedlander, M. (2002). Retinal Vascular Development Is Mediated by Endothelial Filopodia, a Preexisting Astrocytic Template and Specific R-Cadherin Adhesion. *Investigative Ophthalmology & Visual Science*, *43*(11), 3500–3510. Retrieved from http://dx.doi.org/

Dougher-Vermazen, M., Hulmes, J. D., Bohlen, P., & Terman, B. I. (1994). Biological Activity and Phosphorylation Sites of the Bacterially Expressed Cytosolic Domain of the KDR VEGF-Receptor. *Biochemical and Biophysical Research Communications*, *205*(1), 728–738. https://doi.org/10.1006/BBRC.1994.2726

Dragoni, S., Reforgiato, M., Zuccolo, E., Poletto, V., Lodola, F., Ruffinatti, F. A., … Moccia, F. (2015). Dysregulation of VEGF-induced proangiogenic Ca^{2+} oscillations in primary myelofibrosis-derived endothelial colony-forming cells. *Experimental Hematology*, *43*(12), 1019–1030.e3. https://doi.org/10.1016/j.exphem.2015.09.002

Du, J., Ma, X., Shen, B., Huang, Y., Birnbaumer, L., & Yao, X. (2014). TRPV4, TRPC1, and TRPP2 assemble to form a flow-sensitive heteromeric channel. *The FASEB Journal*, *28*(11), 4677–4685. https://doi.org/10.1096/fj.14-251652

Dumont, D. J., Jussila, L., Taipale, J., Lymboussaki, A., Mustonen, T., Pajusola, K., … Alitalo, K. (1998). Cardiovascular Failure in Mouse Embryos Deficient in VEGF Receptor-3. *Science*, *282*(5390), 946 LP-949. Retrieved from http://science.sciencemag.org/content/282/5390/946.abstract

Dunn, K. M., Hill-Eubanks, D. C., Liedtke, W., & Nelson, M. T. (2013). TRPV4 channels stimulate Ca2+-induced Ca2+ release in astrocytic endfeet and amplify neurovascular coupling responses.

Eagle, K., Lim, M., & Dabbous, O. (2004). A validated prediction model for all forms of acute coronary syndrome: Estimating the risk of 6-month postdischarge death in an international registry. *JAMA*, *291*(22), 2727–2733. Retrieved from http://dx.doi.org/10.1001/jama.291.22.2727

Eijkelkamp, N., Quick, K., & Wood, J. N. (2013). Transient Receptor Potential Channels and Mechanosensation. https://doi.org/10.1146/annurev-neuro-062012-170412

Eisenberg, C. A., & Eisenberg, L. M. (1999). WNT11 promotes cardiac tissue formation of early mesoderm. *Developmental Dynamics*, *216*(1), 45–58.

https://doi.org/10.1002/(SICI)1097-0177(199909)216:1<45::AID-DVDY7>3.0.CO;2-L

Ellertsdottir, E., Lenard, A., Blum, Y., Krudewig, A., Herwig, L., Affolter, M., & Belting, H. G. (2010). Vascular morphogenesis in the zebrafish embryo. *Dev Biol*, *341*(1), 56–65. https://doi.org/10.1016/j.ydbio.2009.10.035

Emerson, G. G., Segal, S. S., Geoffrey, G., & Electrical, S. S. S. (2001). Electrical activation of endothelium evokes vasodilation and hyperpolarization along hamster feed arteries. *Am J Physiol Heart Circ Physiol*, *06519*(1), 160–167. Retrieved from http://ajpheart.physiology.org/content/280/1/H160

Fantl, W. J., Escobedo, J. A., Martin, G. A., Turck, C. W., del Rosario, M., McCormick, F., & Williams, L. T. (1992). Distinct phosphotyrosines on a growth factor receptor bind to specific molecules that mediate different signaling pathways. *Cell*, *69*(3), 413–423. https://doi.org/10.1016/0092-8674(92)90444-H

Fearnley, G. W., Bruns, A. F., Wheatcroft, S. B., & Ponnambalam, S. (2015). VEGF-A isoform-specific regulation of calcium ion flux , transcriptional activation and endothelial cell migration, 731–742. https://doi.org/10.1242/bio.201410884

Félétou, M., Köhler, R., & Vanhoutte, P. M. (2010). Endothelium-derived Vasoactive Factors and Hypertension: Possible Roles in Pathogenesis and as Treatment Targets. *Current Hypertension Reports*, *12*(4), 267–275. https://doi.org/10.1007/s11906-010-0118-2

Ferrara, N., Carver-Moore, K., Chen, H., Dowd, M., Lu, L., O'Shea, K. S., … Moore, M. W. (1996). Heterozygous embryonic lethality induced by targeted inactivation of the VEGF gene. *Nature*, *380*(6573), 439–442. Retrieved from http://dx.doi.org/10.1038/380439a0

Ferrara, N., & Kerbel, R. S. (2005). Angiogenesis as a therapeutic target. *Nature*, *438*(7070), 967–974. https://doi.org/10.1038/nature04483

Filosa, J. A., Yao, X., & Rath, G. (2013). TRPV4 and the regulation of vascular tone. *Journal of Cardiovascular Pharmacology*, *61*(2), 113–119. https://doi.org/10.1097/FJC.0b013e318279ba42

Fisher, S., Grice, E. A., Vinton, R. M., Bessling, S. L., & McCallion, A. S. (2006). Conservation of RET Regulatory Function from Human to Zebrafish Without Sequence Similarity. *Science*, *312*(5771), 276 LP-279. https://doi.org/10.1126/science.1124070

Flaherty, M. P., & Dawn, B. (2008, October). Non canonical Wnt11Signaling and Cardiomiyogenenic Differentiation. https://doi.org/10.1016/j.tcm.2008.12.001

Flavell, S. W., & Greenberg, M. E. (2008). Signaling Mechanisms Linking Neuronal Activity to Gene Expression and Plasticity of the Nervous System. *Annual Review of Neuroscience*, *31*(1), 563–590. https://doi.org/10.1146/annurev.neuro.31.060407.125631

Folkman, J. (2007). Angiogenesis: an organizing principle for drug discovery? *Nature Reviews. Drug Discovery*, *6*, 273–286. https://doi.org/10.1016/j.jpedsurg.2006.09.048

Fong, G.-H., Rossant, J., Gertsenstein, M., & Breitman, M. L. (1995). Role of the Flt-1 receptor tyrosine kinase in regulating the assembly of vascular endothelium. *Nature*, *376*, 66. Retrieved from https://doi.org/10.1038/376066a0

Fraisl, P., Mazzone, M., Schmidt, T., & Carmeliet, P. (2009). Regulation of Angiogenesis by Oxygen and Metabolism. *Developmental Cell*, *16*(2), 167–179. https://doi.org/http://dx.doi.org/10.1016/j.devcel.2009.01.003

Franco, C. A., Jones, M. L., Bernabeu, M. O., Geudens, I., Mathivet, T., Rosa, A.,

… Gerhardt, H. (2015). Dynamic endothelial cell rearrangements drive developmental vessel regression. *PLoS Biol*, *13*(4), e1002125. https://doi.org/10.1371/journal.pbio.1002125

Franzini-Armstrong, C., Protasi, F., & Ramesh, V. (1999). Shape, Size, and Distribution of Ca2+ Release Units and Couplons in Skeletal and Cardiac Muscles. *Biophysical Journal*, *77*(3), 1528–1539. https://doi.org/10.1016/S0006-3495(99)77000-1

Fuh, G., Garcia, K. C., & de Vos, A. M. (2000). The interaction of Neuropilin-1 with Vascular Endothelial Growth Factor and its receptor Flt-1. *Journal of Biological Chemistry* . https://doi.org/10.1074/jbc.M003955200

Fukumura, D., Salehi, H. A., Witwer, B., Tuma, R. F., Melder, R. J., & Jain, R. K. (1995). Tumor Necrosis Factor α-induced Leukocyte Adhesion in Normal and Tumor Vessels: Effect of Tumor Type, Transplantation Site, and Host Strain. *Cancer Research*, *55*(21), 4824 LP-4829. Retrieved from http://cancerres.aacrjournals.org/content/55/21/4824.abstract

Fukumura, D., Yuan, F., Endo, M., & Jain, R. K. (1997). Role of nitric oxide in tumor microcirculation. Blood flow, vascular permeability, and leukocyte-endothelial interactions. *The American Journal of Pathology*, *150*(2), 713–725. Retrieved from https://www.ncbi.nlm.nih.gov/pubmed/9033284

Funahashi, Y., Shawber, C. J., Vorontchikhina, M., Sharma, A., Outtz, H. H., & Kitajewski, J. (2010). Notch regulates the angiogenic response via induction of VEGFR-1. *Journal of Angiogenesis Research*, *2*(1), 3. https://doi.org/10.1186/2040-2384-2-3

Gariano, R. F., & Gardner, T. W. (2005). Retinal angiogenesis in development and disease. *Nature*, *438*(7070), 960–966. https://doi.org/10.1038/nature04482

Garland, C. J., Bagher, P., Powell, C., Ye, X., Lemmey, H. A. L., Borysova, L., & Dora, K. A. (2017). Voltage-dependent Ca 2 + entry into smooth muscle during contraction promotes endothelium-mediated feedback vasodilation in arterioles. *Sci. Signal.*, *10*.

Gasperini, R. J., Pavez, M., Thompson, A. C., Mitchell, C. B., Hardy, H., Young, K. M., … Foa, L. (2017). How does calcium interact with the cytoskeleton to regulate growth cone motility during axon pathfinding? *Molecular and Cellular Neuroscience*, *84*(July), 29–35. https://doi.org/10.1016/j.mcn.2017.07.006

Ge, R., Tai, Y., Sun, Y., Zhou, K., Yang, S., Cheng, T., … Wang, Y. (2009). Critical role of TRPC6 channels in VEGF-mediated angiogenesis. *Cancer Letters*, *283*(1), 43–51. https://doi.org/10.1016/j.canlet.2009.03.023

Gebala, V., Collins, R., Geudens, I., Phng, L., & Gerhardt, H. (2016). Blood flow drives lumen formation by inverse membrane blebbing during angiogenesis in vivo. *Nat Cell Biol*, *18*(4). https://doi.org/10.1038/ncb3320

Gerhardt, H., Golding, M., Fruttiger, M., Ruhrberg, C., Lundkvist, A., Abramsson, A., … Betsholtz, C. (2003). VEGF guides angiogenic sprouting utilizing endothelial tip cell filopodia. *J Cell Biol*, *161*(6), 1163–1177. https://doi.org/10.1083/jcb.200302047

Geudens, I., Herpers, R., Hermans, K., Segura, I., Ruiz de Almodovar, C., Bussmann, J., … Dewerchin, M. (2010). Role of delta-like-4/Notch in the formation and wiring of the lymphatic network in zebrafish. *Arterioscler Thromb Vasc Biol*, *30*(9), 1695–1702. https://doi.org/10.1161/ATVBAHA.110.203034

Ghigo, A., Laffargue, M., Li, M., & Hirsch, E. (2017). PI3K and Calcium Signaling in Cardiovascular Disease. *Circulation Research*, *121*(3), 282–292. https://doi.org/10.1161/CIRCRESAHA.117.310183

Giacca, M., & Zacchigna, S. (2012). VEGF gene therapy: therapeutic angiogenesis in the clinic and beyond. *Gene Therapy*, *19*, 622. Retrieved from https://doi.org/10.1038/gt.2012.17

Gluzman-Poltorak, Z., Cohen, T., Shibuya, M., & Neufeld, G. (2001). Vascular Endothelial Growth Factor Receptor-1 and Neuropilin-2 Form Complexes. *Journal of Biological Chemistry* , *276*(22), 18688–18694. Retrieved from http://www.jbc.org/content/276/22/18688.abstract

Goel, S., Duda, D. G., Xu, L., Munn, L. L., Boucher, Y., Fukumura, D., & Jain, R. K. (2011). Normalization of the vasculature for treatment of cancer and other diseases. *Physiological Reviews*, *91*(3), 1071–1121. https://doi.org/10.1152/physrev.00038.2010

Goetz, J. G., Steed, E., Ferreira, R. R., Roth, S., Ramspacher, C., Boselli, F., … Vermot, J. (2014). Endothelial cilia mediate low flow sensing during zebrafish vascular development. *Cell Rep*, *6*(5), 799–808. https://doi.org/10.1016/j.celrep.2014.01.032

Gomez-Ospina, N., Panagiotakos, G., Portmann, T., Pasca, S. P., Rabah, D., Budzillo, A., … Dolmetsch, R. E. (2013). A promoter in the coding region of the calcium channel gene CACNA1C generates the transcription factor CCAT. *PLoS One*, *8*(4), e60526. https://doi.org/10.1371/journal.pone.0060526

Gomez-Ospina, N., Tsuruta, F., Barreto-Chang, O., Hu, L., & Dolmetsch, R. (2006). The C terminus of the L-type voltage-gated calcium channel Ca(V)1.2 encodes a transcription factor. *Cell*, *127*(3), 591–606. https://doi.org/10.1016/j.cell.2006.10.017

Gore, A. V, Monzo, K., Cha, Y. R., Pan, W., & Weinstein, B. M. (2012). Vascular Development in the Zebrafish, 1–21.

Griendling, K. K., Schmidt, A., Brixius, K., & Bloch, W. (2007). Endothelial Precursor Cell Migration During Vasculogenesis. https://doi.org/10.1161/CIRCRESAHA.107.148932

Harrington, L. S., Sainson, R. C. A., Williams, C. K., Taylor, J. M., Shi, W., Li, J.-L., & Harris, A. L. (2008). Regulation of multiple angiogenic pathways by Dll4 and Notch in human umbilical vein endothelial cells. *Microvascular Research*, *75*(2), 144–154. https://doi.org/http://dx.doi.org/10.1016/j.mvr.2007.06.006

Hell, J. W., Westenbroek, R. E., Warner, C., Ahlijanian, M. K., Prystay, W., Gilbert, M. M., … Catterall, W. A. (1993). Identification and differential subcellular localization of the neuronal class C and class D L-type calcium channel alpha 1 subunits. *The Journal of Cell Biology*, *123*(4), 949–962. https://doi.org/10.1083/jcb.123.4.949

Hellstrom, M., Kal n, M., Lindahl, P., Abramsson, A., & Betsholtz, C. (1999). Role of PDGF-B and PDGFR-beta in recruitment of vascular smooth muscle cells and pericytes during embryonic blood vessel formation in the mouse. *Development*, *126*(14), 3047 LP-3055. Retrieved from http://dev.biologists.org/content/126/14/3047.abstract

Hellstrom, M., Phng, L. K., Hofmann, J. J., Wallgard, E., Coultas, L., Lindblom, P., … Betsholtz, C. (2007). Dll4 signalling through Notch1 regulates formation of tip cells during angiogenesis. *Nature*, *445*(7129), 776–780. https://doi.org/10.1038/nature05571

Hendrickx, M., & Leyns, L. (2008). Non-conventional Frizzled ligands and Wnt receptors. *Development Growth and Differentiation*. https://doi.org/10.1111/j.1440-169X.2008.01016.x

Hierck, B. P., Heiden, K. Van Der, Alkemade, F. E., Pas, S. Van De, Thienen, J. V.

Van, Groenendijk, B. C. W., … Poelmann, R. E. (2008). Primary Cilia Sensitize Endothelial Cells for Fluid Shear Stress, (February), 725–735. https://doi.org/10.1002/dvdy.21472

Hofmann, J. J., & Iruela-Arispe, M. L. (2007). Notch signaling in blood vessels: Who is talking to whom about what? *Circulation Research*, *100*(11), 1556–1568. https://doi.org/10.1161/01.RES.0000266408.42939.e4

Hofmann, T., Schaefer, M., Schultz, G., & Gudermann, T. (2002). Subunit composition of mammalian transient receptor potential channels in living cells. *Proceedings of the National Academy of Sciences of the United States of America*, *99*(11), 7461–7466. https://doi.org/10.1073/pnas.102596199

Holmqvist, K., Cross, M., Riley, D., & Welsh, M. (2003). The Shb adaptor protein causes Src-dependent cell spreading and activation of focal adhesion kinase in murine brain endothelial cells. *Cellular Signalling*, *15*(2), 171–179. https://doi.org/http://dx.doi.org/10.1016/S0898-6568(02)00076-1

Hong, K., Nishiyama, M., Henley, J., Tessier-Lavigne, M., & Poo, M. (2000). Calcium signalling in the guidance of nerve growth by netrin-1. *Nature*, *403*, 93. Retrieved from http://dx.doi.org/10.1038/47507

Hughes, S., Yang, H., & Chan-Ling, T. (2000). Vascularization of the Human Fetal Retina: Roles of Vasculogenesis and Angiogenesis. *Investigative Ophthalmology & Visual Science*, *41*(5), 1217–1228. Retrieved from http://dx.doi.org/

Hulme, J. T., Ahn, M., Hauschka, S. D., Scheuer, T., & Catterall, W. A. (2002). A novel leucine zipper targets AKAP15 and cyclic AMP-dependent protein kinase to the C terminus of the skeletal muscle Ca2+ channel and modulates its function. *Journal of Biological Chemistry*, *277*(6), 4079–4087. https://doi.org/10.1074/jbc.M109814200

Hulme, J. T., Lin, T. W., Westenbroek, R. E., Scheuer, T., & Catterall, W. A. (2003). b-adrenergic regulation requires direct anchoring of PKA to cardiac CaV1.2 channels via a leucine zipper interaction with A kinase-anchoring protein 15. *Proc Natl Acad Sci U S A*, *100*(22), 13093–13098. https://doi.org/10.1073/pnas.2135335100

Hulme, J. T., Westenbroek, R. E., Scheuer, T., & Catterall, W. A. (2006). Phosphorylation of serine 1928 in the distal C-terminal domain of cardiac CaV1.2 channels during b1-adrenergic regulation. *Proc Natl Acad Sci U S A*, *103*(44), 16574–16579. https://doi.org/10.1073/pnas.0607294103

Hulme, Yarov Yarovoy, V., Lin, T. W., Scheuer, T., & Catterall, W. A. (2006). Autoinhibitory control of the CaV1.2 channel by its proteolytically processed distal C-terminal domain. *J Physiol*, *576*(Pt 1), 87–102. https://doi.org/10.1113/jphysiol.2006.111799

Isogai, S., Lawson, N. D., Torrealday, S., Horiguchi, M., & Weinstein, B. M. (2003). Angiogenic network formation in the developing vertebrate trunk. *Development (Cambridge, England)*, *130*(21), 5281–5290. https://doi.org/10.1242/dev.00733

Jaffe, E. A., Grulich, J., Weksler, B. B., Hampel, G., & Watanabe, K. (1987). Correlation between thrombin-induced prostacyclin production and inositol trisphosphate and cytosolic free calcium levels in cultured human endothelial cells. *Journal of Biological Chemistry* , *262*(18), 8557–8565. Retrieved from http://www.jbc.org/content/262/18/8557.abstract

Jain, R. K. (2005). Normalization of tumor vasculature: an emerging concept in antiangiogenic therapy. *Science*, *307*(5706), 58–62. https://doi.org/10.1126/science.1104819

Jain, R. K., Munn, L. L., & Fukumura, D. (2002). Dissecting tumour pathophysiology

using intravital microscopy. *Nature Reviews Cancer*, *2*, 266. Retrieved from https://doi.org/10.1038/nrc778

Jakobsson, L., Franco, C. A., Bentley, K., Collins, R. T., Ponsioen, B., Aspalter, I. M., … Gerhardt, H. (2010). Endothelial cells dynamically compete for the tip cell position during angiogenic sprouting. https://doi.org/10.1038/ncb2103

Jho, D., Mehta, D., Ahmmed, G., Gao, X. P., Tiruppathi, C., Broman, M., & Malik, A. B. (2005). Angiopoietin-1 opposes VEGF-induced increase in endothelial permeability by inhibiting TRPC1-dependent Ca 2+ influx. *Circulation Research*, *96*(12), 1282–1290. https://doi.org/10.1161/01.RES.0000171894.03801.03

Johnson, B. D., Brousal, J. P., Peterson, B. Z., Gallombardo, P. A., Hockerman, G. H., Lai, Y., … Catterall, W. A. (1997). Modulation of the cloned skeletal muscle L-type Ca2+ channel by anchored cAMP-dependent protein kinase. *The Journal of Neuroscience : The Official Journal of the Society for Neuroscience*, *17*(4), 1243–1255.

Kallakuri, S., Yu, J. A., Li, J., Li, Y., Weinstein, B. M., Nicoli, S., & Sun, Z. (2015). Endothelial Cilia Are Essential for Developmental Vascular Integrity in Zebra fish, 864–875. https://doi.org/10.1681/ASN.2013121314

Kamei, M., Brian Saunders, W., Bayless, K. J., Dye, L., Davis, G. E., & Weinstein, B. M. (2006). Endothelial tubes assemble from intracellular vacuoles in vivo. *Nature*, *442*, 453. Retrieved from https://doi.org/10.1038/nature04923

Kamp, T. J., & Hell, J. W. (2000). Regulation of cardiac L-type calcium channels by protein kinase A and protein kinase C. *Circ Res*, *87*(12), 1095–1102. Retrieved from http://www.ncbi.nlm.nih.gov/pubmed/11110765%5Cnhttp://circres.ahajournals.org/content/87/12/1095.full.pdf

Kaplun, L., Fridman, A. L., Chen, W., Levin, N. K., Ahsan, S., Petrucelli, N., … Tainsky, M. A. (2012). Variants in the Signaling Protein TSAd are Associated with Susceptibility to Ovarian Cancer in BRCA1/2 Negative High Risk Families. *Biomarker Insights*, *7*, 151–157. https://doi.org/10.4137/BMI.S10815

Karthik, S., Djukic, T., Kim, J.-D., Zuber, B., Makanya, A., Odriozola, A., … Djonov, V. (2018). Synergistic interaction of sprouting and intussusceptive angiogenesis during zebrafish caudal vein plexus development. *Scientific Reports*, *8*(1), 9840. https://doi.org/10.1038/s41598-018-27791-6

Kaufman, C. K., White, R. M., & Zon, L. (2009). Chemical genetic screening in the zebrafish embryo. *Nature Protocols*, *4*(10), 1422–1432. https://doi.org/10.1038/nprot.2009.144

Kawamura, H., Li, X., Goishi, K., Van Meeteren, L. A., Jakobsson, L., Cébe-Suarez, S., … Claesson-Welsh, L. (2008). Neuropilin-1 in regulation of VEGF-induced activation of p38MAPK and endothelial cell organization. *Blood*, *112*(9), 3638–3649. https://doi.org/10.1182/blood-2007-12-125856

Kawamura, H., Li, X., Harper, S. J., Bates, D. O., & Claesson-Welsh, L. (2008). Vascular Endothelial Growth Factor (VEGF)-A165b Is a Weak In vitro Agonist for VEGF Receptor-2 Due to Lack of Coreceptor Binding and Deficient Regulation of Kinase Activity. *Cancer Research*, *68*(12), 4683 LP-4692. Retrieved from http://cancerres.aacrjournals.org/content/68/12/4683.abstract

Kendall, R. L., Rutledge, R. Z., Mao, X., Tebben, A. J., Hungate, R. W., & Thomas, K. A. (1999). Vascular Endothelial Growth Factor Receptor KDR Tyrosine Kinase Activity Is Increased by Autophosphorylation of Two Activation Loop Tyrosine Residues. *Journal of Biological Chemistry* , *274*(10), 6453–6460.

https://doi.org/10.1074/jbc.274.10.6453

Khan, M., Dhammu, T. S., Matsuda, F., Baarine, M., Dhindsa, T. S., Singh, I., & Singh, A. K. (2015). Promoting endothelial function by S-nitrosoglutathione through the HIF-1α/VEGF pathway stimulates neurorepair and functional recovery following experimental stroke in rats. *Drug Design, Development and Therapy*, *9*, 2233–2247. https://doi.org/10.2147/DDDT.S77115

Kim, A. D., Melick, C. H., Clements, W. K., Stachura, D. L., Distel, M., Panáková, D., … Kim, A. D. (2014). Discrete Notch signaling requirements in the specification of hematopoietic stem cells, *33*(20), 2363–2373.

Kim, J. D., Kang, Y., Kim, J., Papangeli, I., Kang, H., Wu, J., … Jin, S. W. (2014). Essential role of apelin signaling during lymphatic development in Zebrafish. *Arteriosclerosis, Thrombosis, and Vascular Biology*, *34*(2), 338–345. https://doi.org/10.1161/ATVBAHA.113.302785

Kim, J. M., Lee, M., Kim, N., & Do, W. (2016). Optogenetic toolkit reveals the role of Ca 2 + sparklets in coordinated cell migration. *PNAS*, *113*(21), 5952–5957. https://doi.org/10.1073/pnas.1518412113

Kimmes, C. (2004). Stages of Embryonic Development of the Zebrafish.

Koch, S., & Claesson-Welsh, L. (2012). Signal transduction by vascular endothelial growth factor receptors. *Cold Spring Harbor Perspectives in Medicine*, *2*(7), 1–21. https://doi.org/10.1101/cshperspect.a006502

Kochhan, E., Lenard, A., Ellertsdottir, E., Herwig, L., Affolter, M., Belting, H., & Siekmann, A. F. (2013). Blood Flow Changes Coincide with Cellular Rearrangements during Blood Vessel Pruning in Zebrafish Embryos, *8*(10), 1–7. https://doi.org/10.1371/journal.pone.0075060

Kohn, A. D., & Moon, R. T. (2005). Wnt and calcium signaling: β-Catenin-independent pathways. *Cell Calcium*, *38*(3), 439–446. https://doi.org/https://doi.org/10.1016/j.ceca.2005.06.022

Kok, F. O., Shin, M., Ni, C.-W., Gupta, A., Grosse, A. S., van Impel, A., … Lawson, N. D. (2015). Reverse Genetic Screening Reveals Poor Correlation between Morpholino-Induced and Mutant Phenotypes in Zebrafish. *Developmental Cell*, *32*(1), 97–108. https://doi.org/10.1016/j.devcel.2014.11.018

Komiya, Y., & Habas, R. (2008). Wnt signal transduction pathways. *Organogenesis*, *4*(2), 68–75. https://doi.org/10.4161/org.4.2.5851

Kopan, R., & Ilagan, M. X. (2009). The canonical Notch signaling pathway: unfolding the activation mechanism. *Cell*, *137*(2), 216–233. https://doi.org/10.1016/j.cell.2009.03.045

Krueger, J., Liu, D., Scholz, K., Zimmer, A., Shi, Y., Klein, C., … le Noble, F. (2011). Flt1 acts as a negative regulator of tip cell formation and branching morphogenesis in the zebrafish embryo. *Development*, *138*(10), 2111–2120. https://doi.org/10.1242/dev.063933

Kühl, M., Sheldahl, L. C., Malbon, C. C., & Moon, R. T. (2000). Ca2+/calmodulin-dependent protein kinase II is stimulated by Wnt and Frizzled homologs and promotes ventral cell fates in Xenopus. *Journal of Biological Chemistry*, *275*(17), 12701–12711. https://doi.org/10.1074/jbc.275.17.12701

Kumar, B., Dreja, K., Shah, S. S., Cheong, A., Xu, S., Sukumar, P., … Beech, D. J. (2006). Upregulated TRPC1 Channel in Vascular Injury In Vivo and Its Role in Human Neointimal Hyperplasia. https://doi.org/10.1161/01.RES.0000204724.29685.db

Kume, T. (2009). Novel insights into the differential functions of Notch ligands in

vascular formation. *J Angiogenes Res*, *1*, 8. https://doi.org/10.1186/2040-2384-1-8

Kuo, I. Y.-T., Wölfle, S. E., & Hill, C. E. (2011). T-type calcium channels and vascular function: the new kid on the block? *The Journal of Physiology*, *589*(4), 783–795. https://doi.org/10.1113/jphysiol.2010.199497

Lacerda, A. E., Rampe, D., & Brown, A. M. (1988). Effects of protein kinase C activators on cardiac Ca2+ channels. *Nature*, *335*, 249. Retrieved from https://doi.org/10.1038/335249a0

Lafaurie-janvore, J., Antoine, E. E., Perkins, S. J., Babataheri, A., & Barakat, A. I. (2016). A simple microfluidic device to study cell-scale endothelial mechanotransduction. *Biomedical Microdevices*. https://doi.org/10.1007/s10544-016-0090-y

Lam, S. H., Wu, Y. L., Vega, V. B., Miller, L. D., Spitsbergen, J., Tong, Y., … Gong, Z. (2005). Conservation of gene expression signatures between zebrafish and human liver tumors and tumor progression. *Nature Biotechnology*, *24*, 73. Retrieved from https://doi.org/10.1038/nbt1169

Lamalice, L., Houle, F., & Huot, J. (2006). Phosphorylation of Tyr1214 within VEGFR-2 Triggers the Recruitment of Nck and Activation of Fyn Leading to SAPK2/p38 Activation and Endothelial Cell Migration in Response to VEGF. *Journal of Biological Chemistry* , *281*(45), 34009–34020. https://doi.org/10.1074/jbc.M603928200

Lamalice, L., Houle, F., Jourdan, G., & Huot, J. (2004). Phosphorylation of tyrosine 1214 on VEGFR2 is required for VEGF-induced activation of Cdc42 upstream of SAPK2//p38. *Oncogene*, *23*(2), 434–445. Retrieved from http://dx.doi.org/10.1038/sj.onc.1207034

Lemmon, M. A., & Schlessinger, J. (2010). Cell signaling by receptor tyrosine kinases. *Cell*, *141*(7), 1117–1134. https://doi.org/10.1016/j.cell.2010.06.011

Leslie, J. D., Ariza-McNaughton, L., Bermange, A. L., McAdow, R., Johnson, S. L., & Lewis, J. (2007). Endothelial signalling by the Notch ligand Delta-like 4 restricts angiogenesis. *Development*, *134*(5), 839–844. https://doi.org/10.1242/dev.003244

Li, J., Cubbon, R. M., Wilson, L. A., Amer, M. S., Mckeown, L., Hou, B., … Crac, O. (2011). Orai1 and CRAC Channel Dependence of VEGF-Activated Ca 2 ⁺ Entry and Endothelial Tube Formation. https://doi.org/10.1161/CIRCRESAHA.111.243352

Li, X., Zhao, X., Fang, Y., Duong, T., Fan, C., Huang, C., … Jiang, X. (1998). Generation of Destabilized Green Fluorescent Protein as a Transcription Reporter Generation of Destabilized Green Fluorescent Protein as a Transcription Reporter. *The Journal of Biological Chemistry*, *273*(52), 34970–34975. https://doi.org/10.1074/jbc.273.52.34970

Liu, Z.-J., Shirakawa, T., Li, Y., Soma, A., Oka, M., Dotto, G. P., … Herlyn, M. (2003). Regulation of Notch1 and Dll4 by vascular endothelial growth factor in arterial endothelial cells: implications for modulating arteriogenesis and angiogenesis. *Molecular and Cellular Biology*, *23*(1), 14–25. https://doi.org/10.1128/MCB.23.1.14-25.2003

Liu, Z., Xiao, M., Balint, K., Soma, A., Pinnix, C. C., Capobianco, A. J., … Herlyn, M. (2006). Inhibition of endothelial cell proliferation by Notch1 signaling is mediated by repressing MAPK and PI3K / Akt pathways and requires MAML1. *FASEB J*, *20*, 1009–1011. https://doi.org/10.1096/fj.05-4880fje

Livak, K. J., & Schmittgen, T. D. (2001). Analysis of Relative Gene Expression Data Using Real-Time Quantitative PCR and the 2−ΔΔCT Method. *Methods*, *25*(4), 402–408. https://doi.org/https://doi.org/10.1006/meth.2001.1262

Lobov, I. B., Renard, R. A., & Papadopoulos, N. (2007). Delta-like ligand 4 (Dll4) is induced by VEGF as a negative regulator of angiogenic sprouting.

Ma, X., Cao, J., Luo, J., Nilius, B., Huang, Y., Ambudkar, I. S., & Yao, X. (2010). Depletion of Intracellular Ca(2+) Stores Stimulates the Translocation of Vanilloid Transient Receptor Potential 4-C1 Heteromeric Channels to the Plasma Membrane. *Arteriosclerosis, Thrombosis, and Vascular Biology*, *30*(11), 2249–2255. https://doi.org/10.1161/ATVBAHA.110.212084

Mac Gabhann, F., & Popel, A. S. (2007). Dimerization of VEGF receptors and implications for signal transduction: a computational study. *Biophysical Chemistry*, *128*(2–3), 125–139. https://doi.org/10.1016/j.bpc.2007.03.010

MacRae, C. A., & Peterson, R. T. (2003). Zebrafish-Based Small Molecule Discovery. *Chemistry & Biology*, *10*(10), 901–908. https://doi.org/10.1016/j.chembiol.2003.10.003

Majmundar, A. J., Wong, W. J., & Simon, M. C. (2010). Hypoxia-Inducible Factors and the Response to Hypoxic Stress. *Molecular Cell*, *40*(2), 294–309. https://doi.org/http://dx.doi.org/10.1016/j.molcel.2010.09.022

Malli, R., Frieden, M., Trenker, M., & Graier, W. F. (2005). The Role of Mitochondria for Ca2+ Refilling of the Endoplasmic Reticulum. *Journal of Biological Chemistry* , *280*(13), 12114–12122. https://doi.org/10.1074/jbc.M409353200

Marin-Padilla, M. (1985). Early vascularization of the embryonic cerebral cortex: Golgi and electron microscopic studies. *Journal of Comparative Neurology*, *241*(2), 237–249. https://doi.org/10.1002/cne.902410210

Marlow, F., Topczewski, J., Sepich, D., & Solnica-Krezel, L. (2002). Zebrafish Rho kinase 2 acts downstream of Wnt11 to mediate cell polarity and effective convergence and extension movements. *Current Biology*, *12*(11), 876–884. https://doi.org/10.1016/S0960-9822(02)00864-3

Matsui, T., Raya, Á., Kawakami, Y., Callol-Massot, C., Capdevila, J., Rodríguez-Esteban, C., & Izpisúa Belmonte, J. C. (2005). Noncanonical Wnt signaling regulates midline convergence of organ primordia during zebrafish development. *Genes & Development*, *19*(1), 164–175. https://doi.org/10.1101/gad.1253605

Matsumoto, T., Bohman, S., Dixelius, J., Berge, T., Dimberg, A., Magnusson, P., … Claesson-Welsh, L. (2005). VEGF receptor-2 Y951 signaling and a role for the adapter molecule TSAd in tumor angiogenesis. *The EMBO Journal*, *24*(13), 2342–2353. https://doi.org/10.1038/sj.emboj.7600709

Mazzone, M., Dettori, D., Leite de Oliveira, R., Loges, S., Schmidt, T., Jonckx, B., … Carmeliet, P. (2009). Heterozygous Deficiency of PHD2 Restores Tumor Oxygenation and Inhibits Metastasis via Endothelial Normalization. *Cell*, *136*(5), 839–851. https://doi.org/10.1016/J.CELL.2009.01.020

McColl, B. K., Baldwin, M. E., Roufail, S., Freeman, C., Moritz, R. L., Simpson, R. J., … Achen, M. G. (2003). Plasmin Activates the Lymphangiogenic Growth Factors VEGF-C and VEGF-D. *The Journal of Experimental Medicine*, *198*(6), 863–868. https://doi.org/10.1084/jem.20030361

McGrath, J., Somlo, S., Makova, S., Tian, X., & Brueckner, M. (2003). Two Populations of Node Monocilia Initiate Left-Right Asymmetry in the Mouse. *Cell*, *114*(1), 61–73. https://doi.org/http://doi.org/10.1016/S0092-8674(03)00511-7

McHugh, D., Sharp, E. M., Scheuer, T., & Catterall, W. A. (2000). Inhibition of cardiac L-type calcium channels by protein kinase C phosphorylation of two sites in the N-terminal domain. *Proc Natl Acad Sci U S A*, *97*(22), 12334–12338. https://doi.org/10.1073/pnas.210384297\r210384297 [pii]

McMullen, M. E., Bryant, P. W., Glembotski, C. C., Vincent, P. A., & Pumiglia, K. M. (2005). Activation of p38 has opposing effects on the proliferation and migration of endothelial cells. *Journal of Biological Chemistry*, *280*(22), 20995–21003. https://doi.org/10.1074/jbc.M407060200

Mederos y Schnitzler, M., Storch, U., Meibers, S., Nurwakagari, P., Breit, A., Essin, K., … Gudermann, T. (2008). G(q)-coupled receptors as mechanosensors mediating myogenic vasoconstriction. *The EMBO Journal*, *27*(23), 3092–3103. https://doi.org/10.1038/emboj.2008.233

Melani, M., & Weinstein, B. M. (2010). Common factors regulating patterning of the nervous and vascular systems. *Annu Rev Cell Dev Biol*, *26*, 639–665. https://doi.org/10.1146/annurev.cellbio.093008.093324

Merks, A. M., Swinarski, M., Meyer, A. M., Müller, N. V., Özcan, I., Donat, S., … Panáková, D. (2018). Planar cell polarity signalling coordinates heart tube remodelling through tissue-scale polarisation of actomyosin activity. *Nature Communications*, *9*(1). https://doi.org/10.1038/s41467-018-04566-1

Miyazaki, T., Honda, K., & Ohata, H. (2007). Requirement of Ca2+ influx- and phosphatidylinositol 3-kinase-mediated m-calpain activity for shear stress-induced endothelial cell polarity. *American Journal of Physiology Cell Physiology*, *293*(4), C1216–C1225. https://doi.org/10.1152/ajpcell.00083.2007

Moccia, F. (2018). Endothelial Ca 2 + Signaling and the Resistance to Anticancer Treatments : Partners in Crime. *International Journal of Molecular Sciences*, *19*. https://doi.org/10.3390/ijms19010217

Moccia, F., Berra-romani, R., & Tanzi, F. (2012). Update on vascular endothelial Ca2+ signalling: A tale of ion channels, pumps and transporters, *3*(7), 127–158. https://doi.org/10.4331/wjbc.v3.i7.127

Moccia, F., & Guerra, G. (2016). Ca2+ Signalling in Endothelial Progenitor Cells: Friend or Foe? *Journal of Cellular Physiology*, *231*(2), 314–327. https://doi.org/10.1002/jcp.25126

Moccia, F., & Poletto, V. (2015). May the remodeling of the Ca2+ toolkit in endothelial progenitor cells derived from cancer patients suggest alternative targets for anti-angiogenic treatment? *Biochimica et Biophysica Acta - Molecular Cell Research*, *1853*(9), 1958–1973. https://doi.org/10.1016/j.bbamcr.2014.10.024

Morera, F. J., Saravia, J., Pontigo, J. P., Vargas-Chacoff, L., Contreras, G. F., Pupo, A., … Gonzalez, C. (2015). Voltage-dependent BK and Hv1 channels expressed in non-excitable tissues: New therapeutics opportunities as targets in human diseases. *Pharmacological Research*, *101*, 56–64. https://doi.org/10.1016/j.phrs.2015.08.011

Mosimann, C., Panáková, D., Werdich, A. A., Musso, G., Burger, A., Lawson, K. L., … Zon, L. I. (2015). Chamber identity programs drive early functional partitioning of the heart. *Nature Communications*, *6*, 8146. https://doi.org/10.1038/ncomms9146

Mulligan, T. S., & Weinstein, B. M. (2014). Emerging from the PAC: Studying zebrafish lymphatic development. *Microvascular Research*, *96*, 23–30. https://doi.org/10.1016/j.mvr.2014.06.001

Munaron, L. (2006). Intracellular calcium, endothelial cells and angiogenesis. *Recent Patents on Anti-Cancer Drug Discovery*, *1*(1), 105–119. https://doi.org/10.2174/157489206775246502

Nagasawa, T., Hirota, S., Tachibana, K., Takakura, N., Nishikawa, S., Kitamura, Y., … Kishimoto, T. (1996). Defects of B-cell lymphopoiesis and bone-marrow myelopoiesis in mice lacking the CXC chemokine PBSF/SDF-1. *Nature*,

382(6592), 635–638. Retrieved from http://dx.doi.org/10.1038/382635a0

Nauli, S. M., Alenghat, F. J., Luo, Y., Williams, E., Vassilev, P., Li, X., … Zhou, J. (2003). Polycystins 1 and 2 mediate mechanosensation in the primary cilium of kidney cells. *Nat Genet*, *33*(2), 129–137. Retrieved from http://dx.doi.org/10.1038/ng1076

Nauli, S. M., Kawanabe, Y., Kaminski, J. J., Pearce, W. J., Ingber, D. E., & Zhou, J. (2008). Endothelial Cilia Are Fluid Shear Sensors That Regulate Calcium Signaling and Nitric Oxide Production Through Polycystin-1, 1161–1172. https://doi.org/10.1161/CIRCULATIONAHA.107.710111

Navedo, M. F., & Santana, L. F. (2013). CaV 1.2 sparklets in heart and vascular smooth muscle. *J Mol Cell Cardiol.*, *58*(10), 67–76. https://doi.org/10.3174/ajnr.A1256.Functional

Nezu, M., Souma, T., Yu, L., Sekine, H., Takahashi, N., Wei, A. Z.-S., … Yamamoto, M. (2017). Nrf2 inactivation enhances placental angiogenesis in a preeclampsia mouse model and improves maternal and fetal outcomes. *Science Signaling*, *10*(479), eaam5711. https://doi.org/10.1126/scisignal.aam5711

Nicoli, S., Standley, C., Walker, P., Hurlstone, A., Fogarty, K. E., & Lawson, N. D. (2010). microRNA-mediated integration of haemodynamics and Vegf signaling during angiogenesis. *Nature*, *464*(7292), 1196–1200. https://doi.org/10.1038/nature08889.microRNA-mediated

Nilius, B., & Droogmans, G. U. Y. (2001). Ion Channels and Their Functional Role in Vascular Endothelium II, *81*(4).

Ninov, N., Borius, M., & Stainier, D. Y. (2012). Different levels of Notch signaling regulate quiescence, renewal and differentiation in pancreatic endocrine progenitors. *Development*, *139*(9), 1557–1567. https://doi.org/10.1242/dev.076000

Nishiyama, M., Hoshino, A., Tsai, L., Henley, J. R., Goshima, Y., Tessier-Lavigne, M., … Hong, K. (2003). Cyclic AMP/GMP-dependent modulation of Ca2+ channels sets the polarity of nerve growth-cone turning. *Nature*, *423*, 990. Retrieved from http://dx.doi.org/10.1038/nature01751

Noren, D. P., Chou, W. H., Sung, H. L., Qutub, A. A., Wagner, D. S., Popel, A. S., & Levchenko, A. (2016). Endothelial cells decode VEGF-mediated Ca2+ signaling patterns to produce distinct functional responses. *Sci Signal.*, *9*(416), 1–27. https://doi.org/10.1126/scisignal.aad3188.Endothelial

Olesen, S.-P., Claphamt, D., & Davies, P. (1988). Haemodynamic shear stress activates a K+ current in vascular endothelial cells. *Nature*, *331*(6152), 168–170. Retrieved from http://dx.doi.org/10.1038/331168a0

Oliveria, S. F., Dell'Acqua, M. L., & Sather, W. A. (2007). AKAP79/150 Anchoring of Calcineurin Controls Neuronal L-Type Ca2+ Channel Activity and Nuclear Signaling. *Neuron*, *55*(2), 261–275. https://doi.org/10.1016/j.neuron.2007.06.032

Olsson, A. K., Dimberg, A., Kreuger, J., & Claesson-Welsh, L. (2006). VEGF receptor signalling - in control of vascular function. *Nat Rev Mol Cell Biol*, *7*(5), 359–371. https://doi.org/10.1038/nrm1911

Panakova, D., Werdich, A. A., & MacRae, C. A. (2010). Wnt11 patterns a myocardial electrical gradient via regulation of the L-type Ca2+ channel. *Nature*, *466*(7308), 874–878. https://doi.org/10.1038/nature09249.Wnt11

Pandur, P., Lasche, M., Eisenberg, L. M., & Kuhl, M. (2002). Wnt-11 activation of a non-canonical Wnt signalling pathway is required for cardiogenesis. *Nature*, *418*(6898), 636–641. Retrieved from http://dx.doi.org/10.1038/nature00921

Parsons, J. T. (2003). Focal adhesion kinase: the first ten years. *Journal of Cell Science*, *116*(8), 1409 LP-1416. Retrieved from http://jcs.biologists.org/content/116/8/1409.abstract

Pelster, B., & Burggren, W. W. (1996). Disruption of Hemoglobin Oxygen Transport Does Not Impact Oxygen-Dependent Physiological Processes in Developing Embryos of Zebra Fish (Danio rerio). *Circulation Research*, *79*(2), 358 LP-362. Retrieved from http://circres.ahajournals.org/content/79/2/358.abstract

Phng, L. K., & Gerhardt, H. (2009). Angiogenesis: a team effort coordinated by notch. *Dev Cell*, *16*(2), 196–208. https://doi.org/10.1016/j.devcel.2009.01.015

Phng, L. K., Potente, M., Leslie, J. D., Babbage, J., Nyqvist, D., Lobov, I., … Gerhardt, H. (2009). Nrarp coordinates endothelial Notch and Wnt signaling to control vessel density in angiogenesis. *Dev Cell*, *16*(1), 70–82. https://doi.org/10.1016/j.devcel.2008.12.009

Pollock, D. M., Keith, T. L., & Highsmith, R. F. (1995). Endothelin receptors and calcium signaling. *FASEB J.*

Postlethwait, J. H., Yan, Y.-L., Gates, M. A., Horne, S., Amores, A., Brownlie, A., … Talbot, W. S. (1998). Vertebrate genome evolution and the zebrafish gene map. *Nature Genetics*, *18*, 345. Retrieved from https://doi.org/10.1038/ng0498-345

Potente, M., Gerhardt, H., & Carmeliet, P. (2011). Basic and therapeutic aspects of angiogenesis. *Cell*, *146*(6), 873–887. https://doi.org/10.1016/j.cell.2011.08.039

Pouysségur, J., Dayan, F., & Mazure, N. M. (2006). Hypoxia signalling in cancer and approaches to enforce tumour regression. *Nature*, *441*, 437. Retrieved from http://dx.doi.org/10.1038/nature04871

Powers, M., Greven, M., Kleinman, R., Nguyen, Q. D., & Do, D. (2017). Recent advances in the management and understanding of diabetic retinopathy. *F1000Research*, *6*(2063). https://doi.org/10.12688/f1000research.12662.1

Prakriya, M. (2013). Store-Operated Orai Channels: Structure and Function. *Current Topics in Membranes*, *71*, 1–32. https://doi.org/10.1016/B978-0-12-407870-3.00001-9

Prakriya, M., Feske, S., Gwack, Y., Srikanth, S., Rao, A., & Hogan, P. G. (2006). Orai1 is an essential pore subunit of the CRAC channel. *Nature*, *443*, 230. Retrieved from http://dx.doi.org/10.1038/nature05122

Qu, Y. Y., Wang, L. A. M. E. I., Zhong, H. U. A., & Liu, Y. M. I. N. (2017). TRPC1 stimulates calcium - sensing receptor - induced store - operated Ca 2 + entry and nitric oxide production in endothelial cells, 4613–4619. https://doi.org/10.3892/mmr.2017.7164

Rajanayagam, M. A. S., Shou, M., Thirumurti, V., Lazarous, D. F., Quyyumi, A. A., Goncalves, L., … Unger, E. F. (2000). Intracoronary Basic Fibroblast Growth Factor Enhances Myocardial Collateral Perfusion in Dogs, *35*(2). https://doi.org/10.1016/S0735-1097(99)00550-1

Ramachandran, K. V, Hennessey, J. A., Barnett, A. S., Yin, X., Stadt, H. A., Foster, E., … Pitt, G. S. (2013). Calcium influx through L-type CaV1.2 Ca2+ channels regulates mandibular development. *J Clin Invest*, *123*(4), 1638–1646. https://doi.org/10.1172/JCI66903

Rebbeck, R. T., Karunasekara, Y., Board, P. G., Beard, N. A., Casarotto, M. G., & Dulhunty, A. F. (2014). Skeletal muscle excitation-contraction coupling: Who are the dancing partners? *International Journal of Biochemistry and Cell Biology*. https://doi.org/10.1016/j.biocel.2013.12.001

Rissanen, T. T., & Ylä-Herttuala, S. (2007). Current Status of Cardiovascular Gene Therapy. *Molecular Therapy*, *15*(7), 1233–1247. https://doi.org/10.1038/SJ.MT.6300175

Roman, B. L., Pham, V. N., Lawson, N. D., Kulik, M., Childs, S., Lekven, A. C., … Weinstein, B. M. (2002). Disruption of acvrl1 increases endothelial cell number in zebrafish cranial vessels. *Development*, *129*(12), 3009 LP-3019. Retrieved from http://dev.biologists.org/content/129/12/3009.abstract

Rossi, A., Kontarakis, Z., Gerri, C., Nolte, H., Hölper, S., Krüger, M., & Stainier, D. Y. R. (2015). Genetic compensation induced by deleterious mutations but not gene knockdowns. *Nature*, *524*, 230. Retrieved from http://dx.doi.org/10.1038/nature14580

Ruan, L., Wang, B., ZhuGe, Q., & Jin, K. (2015). Coupling of Neurogenesis and Angiogenesis After Ischemic Stroke. *Brain Research*, *1623*, 166–173. https://doi.org/10.1016/j.brainres.2015.02.042.Coupling

Rubanyi, G. M. (2013). Mechanistic, technical, and clinical perspectives in therapeutic stimulation of coronary collateral development by angiogenic growth factors. *Molecular Therapy*, *21*(4), 725–738. https://doi.org/10.1038/mt.2013.13

Ruhrberg, C., Gerhardt, H., Golding, M., Watson, R., Ioannidou, S., Fujisawa, H., … Shima, D. T. (2002). Spatially restricted patterning cues provided by heparin-binding VEGF-A control blood vessel branching morphogenesis. *Genes & Development*, *16*(20), 2684–2698. https://doi.org/10.1101/gad.242002

Saint-Geniez, M., & D'Amore, P. A. (2004). Development and pathology of the hyaloid, choroidal and retinal vasculature. *International Journal of Developmental Biology*, *48*(8–9), 1045–1058. https://doi.org/10.1387/ijdb.041895ms

Sandoo, A., Veldhuijzen van Zanten, J. J. C. S., Metsios, G. S., Carroll, D., & Kitas, G. D. (2010). The Endothelium and Its Role in Regulating Vascular Tone. *The Open Cardiovascular Medicine Journal*, *4*(1), 302–312. https://doi.org/10.2174/1874192401004010302

Santoro, M. M., Pesce, G., & Stainier, D. Y. (2009). Specification of arterial, venous, and lymphatic endothelial cells during embryonic development. *Mechanisms of Development*, *126*(6–8), 637–646. https://doi.org/10.1016/j.mod.2009.06.1080.Characterization

Satin, J., Schroder, E. A., & Crump, S. M. (2011). L-type calcium channel auto-regulation of transcription. *Cell Calcium*, *49*(5), 306–313. https://doi.org/10.1016/j.ceca.2011.01.001

Sato, K., Laham, R. J., Pearlman, J. D., Novicki, D., Sellke, F. W., Simons, M., & Post, M. J. (2000). Efficacy of intracoronary versus intravenous FGF-2 in a pig model of chronic myocardial ischemia. *The Annals of Thoracic Surgery*, *70*(6), 2113–2118. https://doi.org/10.1016/S0003-4975(00)02018-X

Saunders, W. B., Bohnsack, B. L., Faske, J. B., Anthis, N. J., Bayless, K. J., Hirschi, K. K., & Davis, G. E. (2006). Coregulation of vascular tube stabilization by endothelial cell TIMP-2 and pericyte TIMP-3. *The Journal of Cell Biology*, *175*(1), 179–191. https://doi.org/10.1083/jcb.200603176

Schroder, E., Byse, M., & Satin, J. (2009). L-type calcium channel C terminus autoregulates transcription. *Circ Res*, *104*(12), 1373–1381. https://doi.org/10.1161/CIRCRESAHA.108.191387

Schuermann, A., Helker, C. S. M., & Herzog, W. (2014). Seminars in Cell & Developmental Biology Angiogenesis in zebrafish. *Seminars in Cell and Developmental Biology*, *31*, 106–114. https://doi.org/10.1016/j.semcdb.2014.04.037

Sculptoreanu, A., Scheuer, T., & Catterall, W. A. (1993). Voltage-dependent potentiation of L-type Ca2+ channels due to phosphorylation by cAMP-dependent protein kinase. *Nature*, *364*(6434), 240–243. https://doi.org/10.1038/364240a0

Sehnert, A. J., Huq, A., Weinstein, B. M., Walker, C., Fishman, M., & Stainier, D. Y. R. (2002). Cardiac troponin T is essential in sarcomere assembly and cardiac contractility. *Nature Genetics*, *31*, 106. Retrieved from http://dx.doi.org/10.1038/ng875

Seiler, C., Stoller, M., Pitt, B., & Meier, P. (2013). Clinical update The human coronary collateral circulation : development and clinical importance, 2674–2682. https://doi.org/10.1093/eurheartj/eht195

Shalaby, F., Rossant, J., Yamaguchi, T. P., Gertsenstein, M., Wu, X.-F., Breitman, M. L., & Schuh, A. C. (1995). Failure of blood-island formation and vasculogenesis in Flk-1-deficient mice. *Nature*, *376*(6535), 62–66. Retrieved from http://dx.doi.org/10.1038/376062a0

Sheldahl, L. C., Slusarski, D. C., Pandur, P., Miller, J. R., Kühl, M., & Moon, R. T. (2003). Dishevelled activates Ca2+ flux, PKC, and CamKII in vertebrate embryos. *Journal of Cell Biology*, *161*(4), 769–777. https://doi.org/10.1083/jcb.200211094

Shi, J., Gu, P., Zhu, Z., Liu, J., Chen, Z., Sun, X., … Zhang, Z. (2012). Protein phosphatase 2A effectively modulates basal L-type Ca2+current by dephosphorylating Cav1.2 at serine 1866 in mouse cardiac myocytes. *Biochemical and Biophysical Research Communications*, *418*(4), 792–798. https://doi.org/10.1016/j.bbrc.2012.01.105

Shi, J., Miralles, F., Birnbaumer, L., Large, W. A., & Albert, A. P. (2017). Store-operated interactions between plasmalemmal STIM1 and TRPC1 proteins stimulate PLC β 1 to induce TRPC1 channel activation in vascular smooth muscle cells, *4*(595), 1039–1058. https://doi.org/10.1113/JP273302

Siekmann, A. F., Covassin, L., & Lawson, N. D. (2008). Modulation of VEGF signalling output by the Notch pathway. *Bioessays*, *30*(4), 303–313. https://doi.org/10.1002/bies.20736

Siekmann, A. F., Standley, C., Fogarty, K. E., Wolfe, S. A., & Lawson, N. D. (2009). Chemokine signaling guides regional patterning of the first embryonic artery. *Genes and Development*, *23*(19), 2272–2277. https://doi.org/10.1101/gad.1813509

Siekmann, & Lawson, N. D. (2007). Notch signalling limits angiogenic cell behaviour in developing zebrafish arteries. *Nature*, *445*(7129), 781–784. https://doi.org/10.1038/nature05577

Simons, M., Gordon, E., & Claesson-welsh, L. (2016). Mechanisms and regulation of endothelial VEGF receptor signalling. *Nature Publishing Group*, *17*(10), 611–625. https://doi.org/10.1038/nrm.2016.87

Slusarski, D. C., & Pelegri, F. (2007). Calcium signaling in vertebrate embryonic patterning and morphogenesis. *Developmental Biology*. https://doi.org/10.1016/j.ydbio.2007.04.043

Solowiej, J., Bergqvist, S., McTigue, M. A., Marrone, T., Quenzer, T., Cobbs, M., … Murray, B. W. (2009). Characterizing the Effects of the Juxtamembrane Domain on Vascular Endothelial Growth Factor Receptor-2 Enzymatic Activity, Autophosphorylation, and Inhibition by Axitinib. *Biochemistry*, *48*(29), 7019–7031. https://doi.org/10.1021/bi900522y

Sonkusare, S. K., Bonev, A. D., Ledoux, J., Liedtke, W., Kotlikoff, M. I., Heppner, T. J., … Nelson, M. T. (2012). Elementary Ca2+ Signals Through Endothelial TRPV4 Channels Regulate Vascular Function. *Science*, *336*, 597–601.

https://doi.org/10.1016/j.fertnstert.2010.09.017.Development

Spiegelman, V. S., Slaga, T. J., Pagano, M., Minamoto, T., Ronai, Z., & Fuchs, S. Y. (2000). Wnt/β-Catenin Signaling Induces the Expression and Activity of βTrCP Ubiquitin Ligase Receptor. *Molecular Cell*, *5*(5), 877–882. https://doi.org/https://doi.org/10.1016/S1097-2765(00)80327-5

Stahl, A., Connor, K. M., Sapieha, P., Chen, J., Dennison, R. J., Krah, N. M., … Smith, L. E. H. (2010). The Mouse Retina as an Angiogenesis Model. *Investigative Ophthalmology & Visual Science*, *51*(6), 2813–2826. Retrieved from http://dx.doi.org/10.1167/iovs.10-5176

Stainier, D. Y. R., Raz, E., Lawson, N. D., Ekker, S. C., Burdine, R. D., Eisen, J. S., … Moens, C. B. (2017). Guidelines for morpholino use in zebrafish. *PLOS Genetics*, *13*(10), e1007000. https://doi.org/10.1371/journal.pgen.1007000

Stamos, J. L., & Weis, W. I. (2013). The β-catenin destruction complex. *Cold Spring Harbor Perspectives in Biology*. https://doi.org/10.1101/cshperspect.a007898

Stone, J., Itin, A., Alon, T., Pe'er, J., Gnessin, H., Chan-Ling, T., & Keshet, E. (1995). Development of retinal vasculature is mediated by hypoxia-induced vascular endothelial growth factor (VEGF) expression by neuroglia. *The Journal of Neuroscience*, *15*(7), 4738 LP-4747. https://doi.org/10.1523/JNEUROSCI.15-07-04738.1995

Streisinger, G., Walker, C., Dower, N., Knauber, D., & Singer, F. (1981). Production of clones of homozygous diploid zebra fish (Brachydanio rerio). *Nature*, *291*(5813), 293–296. Retrieved from http://dx.doi.org/10.1038/291293a0

Striessnig, J., Koschak, A., Sinnegger-Brauns, M. J., Hetzenauer, A., Nguyen, N. K., Busquet, P., … Singewald, N. (2006). Role of voltage-gated L-type Ca2+ channel isoforms for brain function. *Biochem Soc Trans*, *34*(Pt 5), 903–909. https://doi.org/10.1042/BST0340903

Suchting, S., & Eichmann, A. (2009). Jagged gives endothelial tip cells an edge. *Cell*, *137*(6), 988–990. https://doi.org/10.1016/j.cell.2009.05.024

Suchting, S., Freitas, C., le Noble, F., Benedito, R., Bréant, C., Duarte, A., & Eichmann, A. (2007). The Notch ligand Delta-like 4 negatively regulates endothelial tip cell formation and vessel branching. *Proceedings of the National Academy of Sciences of the United States of America*, *104*(9), 3225–3230. https://doi.org/10.1073/pnas.0611177104

Sutherland, D. J., Pujic, Z., & Goodhill, G. J. (2014). Calcium signaling in axon guidance. *Trends Neurosci*, *37*(8), 424–432. https://doi.org/10.1016/j.tins.2014.05.008

Tachibana, K., Hirota, S., Iizasa, H., Yoshida, H., Kawabata, K., Kataoka, Y., … Nagasawa, T. (1998). The chemokine receptor CXCR4 is essential for vascularization of the gastrointestinal tract. *Nature*, *393*(6685), 591–594. Retrieved from http://dx.doi.org/10.1038/31261

Takahashi, M., Seagar, M. J., Jones, J. F., Reber, B. F., & Catterall, W. A. (1987). Subunit structure of dihydropyridine-sensitive calcium channels from skeletal muscle. *Proceedings of the National Academy of Sciences of the United States of America*, *84*(15), 5478–5482. https://doi.org/10.1073/pnas.84.15.5478

Takahashi, T., Yamaguchi, S., Chida, K., & Shibuya, M. (2001). A single autophosphorylation site on KDR/Flk-1 is essential for VEGF-A-dependent activation of PLC-γ and DNA synthesis in vascular endothelial cells. *The EMBO Journal*, *20*(11), 2768–2778. https://doi.org/10.1093/emboj/20.11.2768

Tamagnone, L., Artigiani, S., Chen, H., He, Z., Ming, G. L., Song, H. J., …

Comoglio, P. M. (1999). Plexins are a large family of receptors for transmembrane, secreted, and GPI-anchored semaphorins in vertebrates. *Cell*, *99*(1), 71–80. https://doi.org/10.1016/S0092-8674(00)80063-X

Tamagnone, L., & Mazzone, M. (2011). Semaphorin signals on the road of endothelial tip cells. *Dev Cell*, *21*(2), 189–190. https://doi.org/10.1016/j.devcel.2011.07.017

Tamanini, C., & De Ambrogi, M. (2004). Angiogenesis in Developing Follicle and Corpus Luteum. *Reproduction in Domestic Animals*, *39*(4), 206–216. https://doi.org/10.1111/j.1439-0531.2004.00505.x

Taylor, M. S., Bonev, A. D., Gross, T. P., Eckman, D. M., Brayden, J. E., Bond, C. T., … Nelson, M. T. (2003). Altered Expression of Small-Conductance Ca²⁺-Activated K⁺ (SK3) Channels Modulates Arterial Tone and Blood Pressure. *Circulation Research*, *93*(2), 124 LP-131. Retrieved from http://circres.ahajournals.org/content/93/2/124.abstract

Taylor, M. S., Francis, M., Qian, X., & Solodushko, V. (2012). Dynamic Ca2+ signal modalities in the vascular endothelium. *Microcirculation*, *19*(5), 423–429. https://doi.org/10.1111/j.1549-8719.2012.00180.x.Dynamic

Tchaikovski, V., Fellbrich, G., & Waltenberger, J. (2008). The Molecular Basis of VEGFR-1 Signal Transduction Pathways in Primary Human Monocytes. *Arteriosclerosis, Thrombosis, and Vascular Biology*, *28*(2), 322–328. https://doi.org/10.1161/ATVBAHA.107.158022

Torregroza, I., Holtzinger, A., Mendelson, K., Liu, T. C., Hla, T., & Evans, T. (2012). Regulation of a Vascular Plexus by gata4 Is Mediated in Zebrafish through the Chemokine sdf1a. *PLoS ONE*, *7*(10). https://doi.org/10.1371/journal.pone.0046844

Torres-Vázquez, J., Gitler, A. D., Fraser, S. D., Berk, J. D., Pham, V. N., Fishman, M. C., … Weinstein, B. M. (2004). Semaphorin-plexin signaling guides patterning of the developing vasculature. *Developmental Cell*, *7*(1), 117–123. https://doi.org/10.1016/j.devcel.2004.06.008

Tran, Q. K., Ohashi, K., & Watanabe, H. (2000). Calcium signalling in endothelial cells. *Cardiovascular Research*, *48*(1), 13–22. https://doi.org/10.1016/S0008-6363(00)00172-3

Tsai, F., Kuo, G., Chang, S., & Tsai, P. (2015). Ca 2 + Signaling in Cytoskeletal Reorganization , Cell Migration , and Cancer Metastasis, *2015*.

Tsai, F., Seki, A., Yang, H. W., Hayer, A., Carrasco, S., & Meyer, T. (2014). A polarized Ca2+ , diacylglycerol, and STIM1 signaling system regulates directed cell migration. *Nat Cell Biol*, *16*(2), 133–144. https://doi.org/10.1038/ncb2906.A

Tseng, G. N., & Boyden, P. A. (1991). Different effects of intracellular Ca and protein kinase C on cardiac T and L Ca currents. *American Journal of Physiology-Heart and Circulatory Physiology*, *261*(2), H364–H379. https://doi.org/10.1152/ajpheart.1991.261.2.H364

Tyson, J. R., & Snutch, T. P. (2013). Molecular nature of voltage-gated calcium channels: Structure and species comparison. *Wiley Interdisciplinary Reviews: Membrane Transport and Signaling*, *2*(5), 181–206. https://doi.org/10.1002/wmts.91

Venna, V. R., Li, J., Hammond, M. D., Mancini, N. S., & McCullough, L. D. (2014). Chronic metformin treatment improves post-stroke angiogenesis and recovery after experimental stroke. *The European Journal of Neuroscience*, *39*(12), 2129–2138. https://doi.org/10.1111/ejn.12556

Villa, N., Walker, L., Lindsell, C. E., Gasson, J., Iruela-Arispe, M. L., & Weinmaster,

G. (2001). Vascular expression of Notch pathway receptors and ligands is restricted to arterial vessels. *Mechanisms of Development*, *108*(1–2), 161–164. https://doi.org/10.1016/S0925-4773(01)00469-5

Villalta, P. C., & Townsley, M. I. (2014). Transient receptor potential channels and regulation of lung endothelial permeability. *Pulmonary Circulation*, *3*(4), 802–815. https://doi.org/10.1086/674765.I

Vinet, R., & Vargas, F. F. (1999). L- and T-type voltage-gated Ca2+ currents in adrenal medulla endothelial cells. *The American Journal of Physiology*, *276*(4 Pt 2), H1313–H1322.

Vogeli, K. M., Jin, S.-W., Martin, G. R., & Stainier, D. Y. R. (2006). A common progenitor for haematopoietic and endothelial lineages in the zebrafish gastrula. *Nature*, *443*, 337. Retrieved from https://doi.org/10.1038/nature05045

Wälchli, T., Wacker, A., Frei, K., Regli, L., Schwab, M. E., & Hoerstrup, S. P. (2015). Review Wiring the Vascular Network with Neural Cues : A CNS Perspective, *4*, 271–296. https://doi.org/10.1016/j.neuron.2015.06.038

Walker, C., & Streisinger, G. (1983). Induction of Mutations by γ-Rays in Pregonial Germ Cells of Zebrafish Embryos. *Genetics*, *103*(1), 125–136. Retrieved from http://www.ncbi.nlm.nih.gov/pmc/articles/PMC1202017/

Wang, G. X., & Poo, M. (2005). Requirement of TRPC channels in netrin-1-induced chemotropic turning of nerve growth cones. *Nature*, *434*, 898. Retrieved from http://dx.doi.org/10.1038/nature03478

Watanabe, T., Delbridge, L. M., Bustamante, J. O., & Mcdonald, T. F. (1981). Heterogeneity of the Action Potential in Isolated Rat Ventricular Myocytes and Tissue, *2*, 280–291.

Waxman, J. S., Hocking, A. M., Stoick, C. L., & Moon, R. T. (2004). Zebrafish Dapper1 and Dapper2 play distinct roles in Wnt-mediated developmental processes. *Development*, *131*(23), 5909 LP-5921. Retrieved from http://dev.biologists.org/content/131/23/5909.abstract

Weiser, D. C., Pyati, U. J., & Kimelman, D. (2007). Gravin regulates mesodermal cell behavior changes required for axis elongation during zebrafish gastrulation. *Genes and Development*, *21*(12), 1559–1571. https://doi.org/10.1101/gad.1535007

Weiss, S., Oz, S., Benmocha, A., & Dascal, N. (2013). Regulation of cardiac L-Type Ca2+ channel CaV1.2 via the β-adrenergic-cAMP-protein kinase a pathway: Old dogmas, advances, and new uncertainties. *Circulation Research*, *113*(5), 617–631. https://doi.org/10.1161/CIRCRESAHA.113.301781

Weissmann, N., Sydykov, A., Kalwa, H., Storch, U., Fuchs, B., Mederos, M., … Dietrich, A. (2012). Activation of TRPC6 channels is essential for lung ischaemia–reperfusion induced oedema in mice. *Nature Communications*, *3*, 610–649. https://doi.org/10.1038/ncomms1660

Wen, Z., Guirland, C., Ming, G., & Zheng, J. Q. (2004). A CaMKII/Calcineurin Switch Controls the Direction of Ca2+-Dependent Growth Cone Guidance. *Neuron*, *43*(6), 835–846. https://doi.org/https://doi.org/10.1016/j.neuron.2004.08.037

Westerfield, M. (2007). The zebrafish book. A guide for the laboratory use of zebrafish (Danio rerio). *5th Ed., Univ. of Oregon Press, Eugene.*

Wheeler, D. G., Barrett, C. F., Groth, R. D., Safa, P., & Tsien, R. W. (2008). CaMKII locally encodes L-type channel activity to signal to nuclear CREB in excitation - transcription coupling. *Journal of Cell Biology*, *183*(5), 849–863. https://doi.org/10.1083/jcb.200805048

Williams, C. K., Li, J.-L., Murga, M., Harris, A. L., & Tosato, G. (2006). Up-regulation of the Notch ligand Delta-like 4 inhibits VEGF-induced endothelial cell function. *Blood*, *107*(3), 931–939. https://doi.org/10.1182/blood-2005-03-1000

Wong, A. Y. K., & Klassen, G. A. (1995). A model of electrical activity and cytosolic calcium dynamics in vascular endothelial cells in response to fluid shear stress. *Annals of Biomedical Engineering*, *23*(6), 822–832. https://doi.org/10.1007/BF02584481

Wood, P. G., & Gillespie, J. I. (1998). Evidence for Mitochondrial Ca 2/ -Induced Ca 2/ Release in Permeabilised Endothelial Cells, *246*(246), 543–548. Retrieved from https://ac.els-cdn.com/S0006291X98986612/1-s2.0-S0006291X98986612-main.pdf?_tid=40c75ffc-9fa4-11e7-a638-00000aab0f27&acdnat=1506091527_1ecfe101c0d098fef738fd90984f682f

Yamamoto, K., Sokabe, T., Ohura, N., Nakatsuka, H., Kamiya, A., & Ando, J. (2003). Endogenously released ATP mediates shear stress-induced Ca2+ influx into pulmonary artery endothelial cells. *American Journal of Physiology - Heart and Circulatory Physiology*, *285*(2), H793 LP-H803. Retrieved from http://ajpheart.physiology.org/content/285/2/H793.abstract

Yanagisawa, M., Kurihara, H., Kimura, S., Goto, K., & Masaki, T. (1989). *A novel peptide vasoconstrictor, endothelin, is produced by vascular endothelium and modulates smooth muscle Ca2+ channels*. *Journal of hypertension. Supplement : official journal of the International Society of Hypertension* (Vol. 6). https://doi.org/10.1097/00004872-198812040-00056

Yao, S., Xie, L., Qian, M., Yang, H., Zhou, L., Zhou, Q., … Mo, X. (2008). Pnas4 is a novel regulator for convergence and extension during vertebrate gastrulation. *FEBS Letters*, *582*(15), 2325–2332. https://doi.org/10.1016/j.febslet.2008.05.036

Yokota, Y., Nakajima, H., Wakayama, Y., Muto, A., Kawakami, K., Fukuhara, S., & Mochizuki, N. (2015). Endothelial Ca2+ oscillations reflect VEGFR signaling-regulated angiogenic capacity in vivo. *ELife*, *2015*, 409245. https://doi.org/10.1155/2015/409245

Yoshiba, S., Shiratori, H., Kuo, I. Y., Kawasumi, A., Shinohara, K., Nonaka, S., … Hamada, H. (2012). Cilia at the node of mouse embryos sense fluid flow for left-right determination via Pkd2. *Science (New York, N.Y.)*, *338*(6104), 226–231. https://doi.org/10.1126/science.1222538

Yu, P. C., Gu, S. Y., Bu, J. W., & Du, J. L. (2010). TRPC1 is essential for in vivo angiogenesis in zebrafish. *Circ Res*, *106*(7), 1221–1232. https://doi.org/10.1161/CIRCRESAHA.109.207670

Zacchigna, S., Almodovar, C. R. de, & Carmeliet, P. (2007). Similarities Between Angiogenesis and Neural Development: What Small Animal Models Can Tell Us. *Current Topics in Developmental Biology*, *80*(07), 1–55. https://doi.org/10.1016/S0070-2153(07)80001-9

Zhang, A. Y. (2006). Vascular physiology of a Ca 2+ mobilizing second messenger - cyclic ADP - ribose, (804).

Zhang, H.-T., Scott, P. A. E., Morbidelli, L., Peak, S., Moore, J., Turley, H., … Bicknell, R. (2000). The 121 amino acid isoform of vascular endothelial growth factor is more strongly tumorigenic than other splice variants in vivo. *British Journal of Cancer*, *83*(1), 63–68. https://doi.org/10.1054/bjoc.2000.1279

Zheng, J. Q. (2000). Turning of nerve growth cones induced by localized increases in intracellular calcium ions. *Nature*, *403*(6765), 89–93. https://doi.org/10.1038/47501

Zhu, M. X., Ma, J., Parrington, J., Galione, A., & Evans, A. M. (2010). TPCs:

Endolysosomal channels for Ca(2+) mobilization from acidic organelles triggered by NAADP. *FEBS Letters*, *584*(10), 1966–1974. https://doi.org/10.1016/j.febslet.2010.02.028

Zlotnik, A., Yoshie, O., & Nomiyama, H. (2006). The chemokine and chemokine receptor superfamilies and their molecular evolution. *Genome Biology*, *7*(12), 243. https://doi.org/10.1186/gb-2006-7-12-243

Zygmunt, T., Gay, C. M., Blondelle, J., Singh, M. K., Flaherty, K. M., Means, P. C., … Torres-Vazquez, J. (2011). Semaphorin-PlexinD1 signaling limits angiogenic potential via the VEGF decoy receptor sFlt1. *Dev Cell*, *21*(2), 301–314. https://doi.org/10.1016/j.devcel.2011.06.033

7 Abbreviations

Table 9: List of Abbreviations

Abbreviation	Name
bp	base pair(s)
Cdc42	cell division cycle 42
cDNA	complementary DNA
C_T	cycle threshold
ctl	control
CV	cardinal vein
DA	dorsal aorta
DAG	diacylglycerol
DLAV	dorsal longitudinal anastomotic vessel
Dll4	delta-like 4
DMSO	dimethylsulfoxide
DNA	2-deoxyribonucleic acid
DNase	deoxyribonuclease
dNTP	2'-deoxynucleoside 5'-triphosphate
dpf	days post fertilization
EC	endothelial cell
EGF	epidermal growth factor
EGFP	enhanced green fluorescent protein
ER	endoplasmic reticulum
ERK	extracellular signal-regulated kinase
ex	exon
FACS	fluorescence-activated cell sorting
FAK	focal adhesion kinase
FC	fold change
fw	forward
Fyn	cytoplasmic tyrosine kinase
h	hour(s)
hpf	hour(s) post fertilization
HS	heparan sulfate
Hsp27	heat-shock protein-27

Ig	immunoglobulin
ISV	intersegmental vessels
kDa	Kilo Dalton
LPM	lateral plate mesoderm
M	molar
MAML	mastermind-like proteins
MAPK	mitogen-activated protein kinase
MAPKAPK2	MAPK-activated protein kinase 2
MEK	mitogen-activated protein kinase kinase
mg	milligram
min	minute(s)
ml	milliliter
mM	millimolar
MO	morpholino oligonucleotide
mRNA	messenger RNA
ng	nanogram
NICD	notch intracellular domain
Nrarp	notch-regulated ankyrin repeat protein
NRP	neuropilin
p38MAPK	p38 mitogen-activated protein kinase
PAK2	activated protein kinase-2
PCR	polymerase chain reaction
PCV	posterior cardinal vein
PI3K	phosphatidylinositol-3 kinase
PlGF	placental growth factor
PKB	AKT/protein kinase B
PKC	Protein kinase C
PTU	1-Phenyl-2-thiourea
RAF	ras-activated serine/threonine kinase
RNA	ribonucleic acid
RNase	ribonuclease
RT	room temperature
RT qPCR	Real time quantitative PCR
rv	reverse
s	second(s)

SD	standard deviation
SHB	SH2 domain containing adaptor protein B
SOCE	store operated calcium entry
SRC	cytosolic tyrosine kinase
Tg	transgenic
TM	transmembrane
UNG	uracil-N-glycosylase
VEGF	vascular endothelial growth factor
VEGFR	vascular endothelial growth factor receptor
VGCC	voltage-gated ion channel
vSMC	Vascular smoth muscle cell
ZIRC	Zebrafish International Resource Center
µg	microgram
µl	microliter
µmol	micromole

8 List of Figures

9 List of Tables

10 Acknowledgment

Most importantly, I want to express my sincere gratitude to my supervisor Dr. Daniela Panáková, for her continuous support, guidance, and patience; not only for my PhD research but also outside the lab. I was very lucky to have her as supervisor, who is caring towards her students, with a great enthusiasms and positiveness, and brilliant scientific ideas, which were a constant source of inspiration.

I would like to thank Prof. Dr. Petra Knaus for her supervision at the Freie Universität Berlin and for accepting to review this work with short notice.

I would like also to thank the rest of my MDC PhD committee: Dr. Annette Hammes-Lewin, Prof. Dr. Fritz Rathjen, Prof. Dr. Carmen Birchmeier, and Prof. Dr. Holger Gerhardt for the discussions and helpful suggestion.

Many thanks to MDC TransCard Research School for giving me numerous opportunities to attend courses and conferences where I was able to gain as well as share knowledge. Thanks in particular to Inka Gotthardt for her personal help and support.

I would like to acknowledge the MDC Fish Facility, MDC Advanced Light Microscopy Facility, and MDC Flow Cytometry Facility for excellent expert support.

Special thanks go to all the current and former members of the Panáková team. Alex, Marie and Tareck for helping me in the first years and get started. Bahar, Mikie, Sara, and Kevin for their support in the final sprint. I'm very thankful in particular to Anne, Mariana, Nicola and Kitti to share with me the good and bad days of this adventure, for their constant support, critical thinking, helpful input and above all for their true friendship.

A profound gratitude go to Rebecca, Charlotte, Angélica, Caro, and Andreia, for their precious friendship, for the babysitting, catsitting, and for being always there when I needed. I thank Sara and Matthias, for their support, help and endless translations. A second special thanks go to Rebecca and Angélica for their incredible help, feedback and input for this work.

From the bottom of my heart I want to thank my family, especially my "mama" for her unconditional love, wisdom and practical help. I wouldn't be able to do this without her.